Corkscrew Watershed Initiative

Deliverable 5.1.3: Final Refined Model Report

Prepared for

South Florida Water Management District

July 11, 2025

Prepared by

Collective Water Resources

With

J-Tech, an Alliance between Jacobs Engineering and Tetra Tech, Inc.

Table of Contents

List of Figures

List of Tables

Abbreviations and Acronyms

APT	aquifer performance test
Ac-ft	acre-feet
AHED	Arc Hydro Enhanced Database
BCB	Big Cypress Basin
CFD	Computational Fluid Dynamics
cfs	cubic feet per second
CREW	Corkscrew Regional Ecosystem Watershed
CSS	Corkscrew Swamp Sanctuary
CWI	Corkscrew Watershed Initiative
DEM	digital elevation model
ERP	Environmental Resource Permit
ET	evapotranspiration
ft	foot/feet
LiDAR	light detection and ranging
LWCSIM	Lower West Coast MODFLOW
NAVD88	North American Vertical Datum of 1988
NGVD29	National Geodetic Vertical Datum of 1929
SFWMD	South Florida Water Management District
SLCWP	South Lee County Watershed Plan
USGS	U.S. Geological Survey
1D	one-dimensional
2D	two-dimensional
3D	three-dimensional

1.0 Background/Introduction

1.1 Project Purpose

J-Tech was selected for the completion and delivery of the Corkscrew Watershed Initiative (CWI) Project. The Notice to Proceed was established for this project on March 1, 2024. The objective of the CWI Project is to develop a comprehensive strategy to achieve ecological restoration of the Corkscrew Watershed by improving wetland hydroperiods and natural flows, while reducing flood risk in nearby flood-prone areas without adversely impacting the water supply and water management needs of the Corkscrew Watershed. The objective will be accomplished through a public planning process that engages and involves key partners, stakeholders, and the public. The project will identify viable short-term and long-term strategies to achieve the CWI Project goals. The proposed restoration alternatives will be cost-effective, feasible, and resilient. The CWI Project will consider population growth, land development, and climate change, including sea level rise and future rainfall. This project aligns with the mission of the South Florida Water Management District's (SFWMD) Big Cypress Basin (BCB) 2023–2028 Strategic Plan and will contribute to the resiliency of the Big Cypress Watershed.

1.2 Project Background and Scope of Work

The CWI Project boundary encompasses southern Hendry County, northern Collier County, and southern Lee County as shown in Figure 1-1. The project area is comprised of rivers (Imperial and Estero), creeks (Halfway and Spring), and wetland sloughs/swamps (Flint Pen Strand and Upper Corkscrew Swamp) within the Estero Bay Basin Watershed in southern Lee County and the Cocohatchee Canal/River Basin and Golden Gate/Naples Bay Watershed in northern Collier County. The initial project planning area was broadened beyond what may be considered an effective area to ensure thorough consideration of vulnerable communities and ecosystems. The initial project planning area will be refined, as necessary, to support developing and evaluating projects within targeted areas.

Previous studies and monitoring have documented reduced hydroperiods and increased water level recession rates in Audubon's Corkscrew Swamp Sanctuary (CSS; owned and managed by National Audubon Society), a critically important ecosystem, within the past 60 years. This three-year planning CWI Project (2024–2027) is funded by the BCB and builds upon previous efforts to determine potential causes of the shortened hydroperiod documented at the CSS. The project will develop and evaluate restoration alternatives that address the purpose and needs of the project. The Technical Working Group (TWG) will be the project planning team, and is comprised of SFWMD staff, representatives of local governments in the region, and others with responsibility for the management of the Corkscrew Watershed. TWG participants are those with expertise in the Corkscrew Watershed and the ability to fund and implement projects in the CWI Project area. Collectively, representatives of the City of Bonita Springs, Collier County, CSS, Corkscrew Regional Ecosystem Watershed (CREW) Land & Water Trust, Lee County, SFWMD staff, and Village of Estero make up the TWG. The TWG will provide guidance to the SFWMD Project Manager responsible for administering the contract and acting as the liaison between the TWG, the CWI Project Consultant (J-Tech), and the SFWMD Project Development Team (PDT).

The CWI Project work plan was finalized on July 1, 2024, and includes a detailed history of work on the project that has been completed to date by the SFWMD and TWG member organizations (J-Tech 2024).

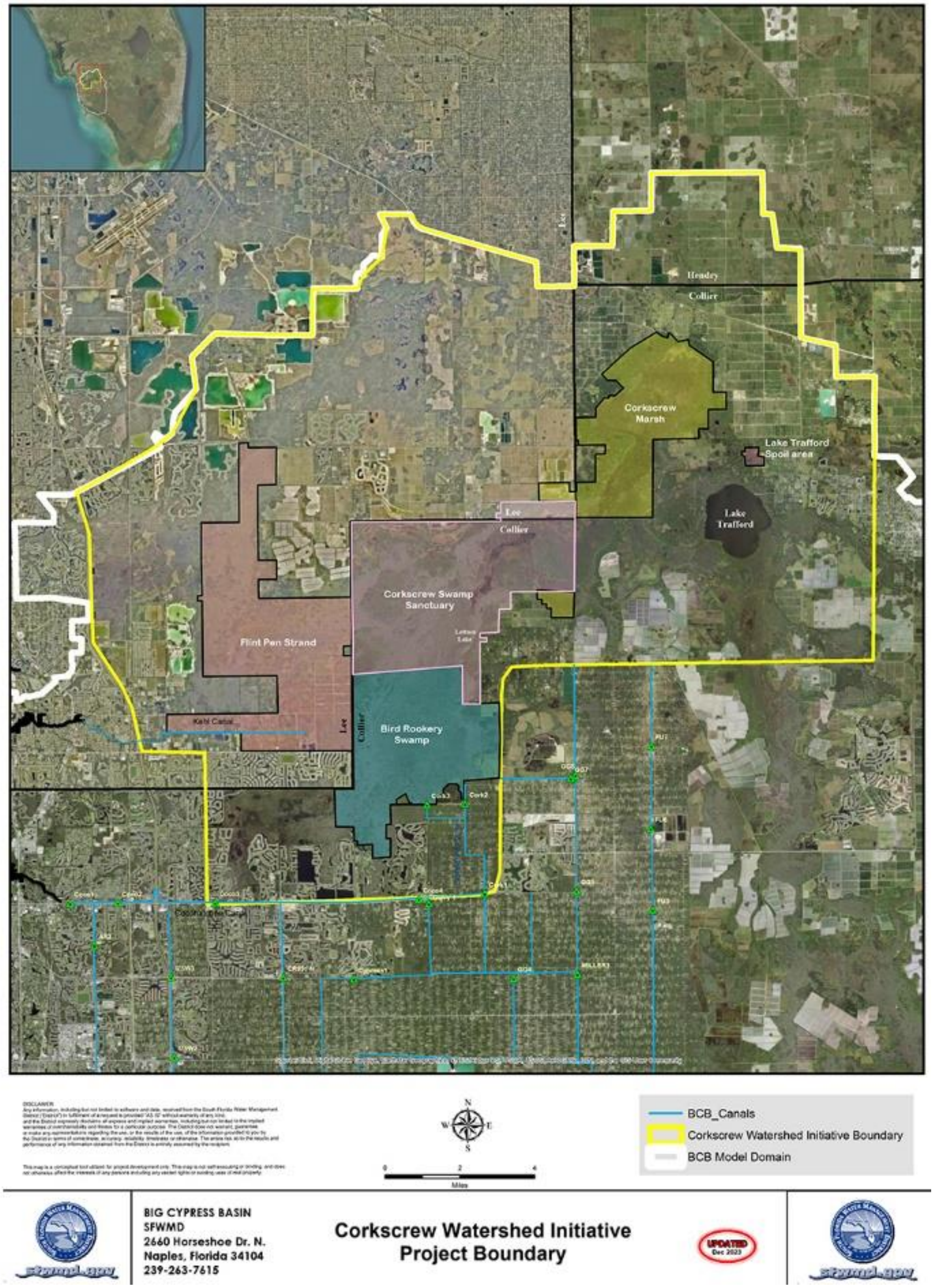

Figure 1-1. Corkscrew Watershed Initiative Project Area

The work plan also identifies the various tasks and deliverables that will be completed as part of the CWI Project. In summary, the CWI Project tasks include the following:

Task 1 – Project Coordination

Task 2 – Information Collection and Review and Site Reconnaissance

Task 3 – Develop Performance Measures and Metrics

Task 4 – Refine Project Area

Task 5 – BCB Model Refinement and Existing Conditions Simulation

Task 6 – Develop Initial List of Potential Ecologic and Hydrologic Restoration Projects

Task 7 – Future Baseline and Alternative Conditions Models Development/Evaluation

Task 8 – Develop Final Project Matrix Including Project Goals, Cost and Regulatory Requirements

Task 9 – CWI Public Planning Project Report, Conceptual Plan(s) and Funding Summary Memo

1.3 Document Structure

This Final Refined BCB Model Report meets the deliverable requirements of Task 5.1. This document includes the following technical sections related to the CWI project area:

2.0 – Objective and Summary of Model Refinements.

3.0 – LiDAR Modification in the Corkscrew Wetland Area.

4.0 – Development of Corkscrew Wetland Flow Ways.

5.0 – Structure Verifications and Operations

6.0 – Hydraulic Connections and Constrictions

7.0 – Corkscrew-Adjacent Basin Drainage

8.0 – Revision of Hydrogeological Layers

9.0 – Review of Water Use Abstractions (Groundwater Pumping)

10.0 – Revision of Boundary and Initial Conditions

11.0 – Focus Model Areas for CWI, Optimization, and Results

12.0 – Model Limitations and Recommendations

13.0 – References

2.0 Objective and Summary of Model Refinements

2.1 BCB Model

The BCB updated and calibrated model (Hazen and Sawyer, 2025), from here on referred to as BCB UM, is the latest BCB model prior to the CWI model refinement (CWI RM). The BCB UM is a coupled MIKE SHE/MIKE HYDRO model that includes the western watersheds of Collier County (including the Cocohatchee, Golden Gate Main, Faka Union, Henderson-Belle Meade, and Fakahatchee watersheds), the southeastern portion of Lee County that includes portions of Corkscrew, Flint Pen, and the Imperial River Basin sub-watersheds, and a small portion of Hendry County that is part of the Corkscrew East sub-watershed.

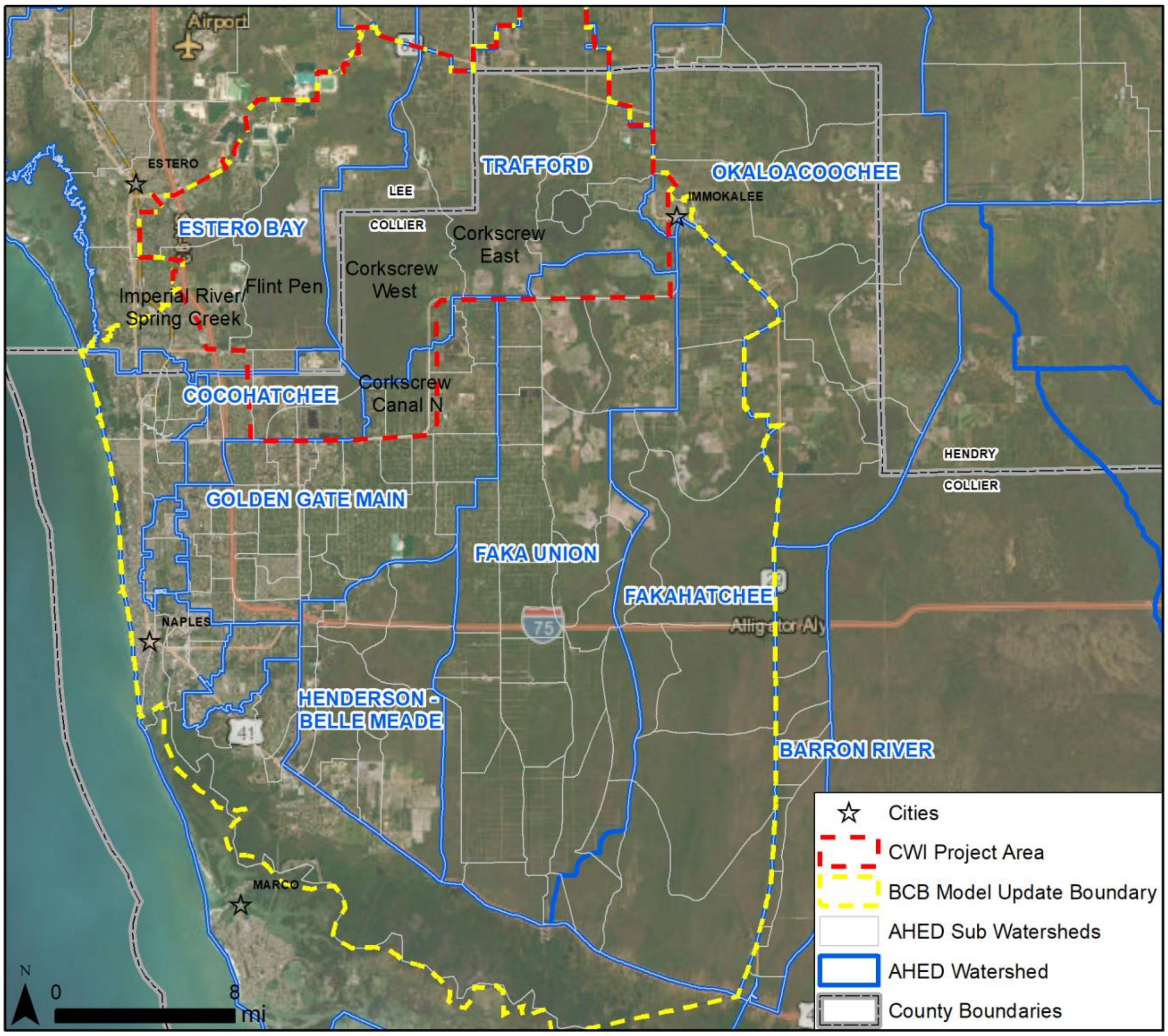

Figure 2-1. BCB Updated Model Domain, Counties, AHED Watersheds and Sub-Watersheds

MIKE SHE is an integrated model that simulates 3D saturated groundwater flow, 2D overland flow, 1D unsaturated flow and hydrological and water use processes (i.e., rainfall, land use based ET, drainage, irrigation, pumping). MIKE HYDRO is a 1D surface water model that simulates open channel flow dynamics and hydraulic operable and non-operable structures. The BCB UM has a grid cell size of 500 feet, which is applied to all components in MIKE SHE and includes a 5-layer groundwater model that includes the Surficial Aquifer System (SAS) and the upper portion of the Intermediate Aquifer System (IAS). The model layers are the hydrogeologic units shown in Table 2-1, with the three Sandstone Aquifer units represented as one layer. The BCB UM used as a starting point the BCB FPLOS model (Parsons and Interflow Engineering, 2017) and incorporated data from other previous model efforts, such as the South Lee County Watershed Initiative (SLCWI) model (CHNEP and Lago, 2021) for the surface water model and the LWC model (Bandara et al., 2020) for the groundwater model. The BCB UM was calibrated for the period of January 1, 2017 to December 31, 2020.

Table 2-1. Hydrogeologic Units included in the BCB Updated Model (Adapted from Zumbro et al., 2023)

System	Hydrogeologic Unit		Lithographic Unit	
Surficial Aquifer	Water Table Aquifer (WTA)		Undifferentiated Sediments Holocene / Pleistocene	
	Tamiami Confining Unit (TCU)		Tamiami Formation	Bonita Springs Marl / Caloosahatchee Clay Member
	Lower Tamiami Aquifer (LTA)			Ochopee Limestone Member
Intermediate Aquifer	Upper Hawthorn Confining Unit (H1)		Hawthorn Group	Peace River Formation
	Sandstone Aquifer	Clastic Zone (S2)		
		Interconfining Unit (SC)		
		Carbonate Zone (S1)		

The CWI RM uses the same model boundary and resolution as the BCB UM model. Prior models used for Corkscrew studies, such as the Audubon's Corkscrew Swamp Sanctuary study (WSA, 2021) and the SLCWI models, are much smaller than the BCB model, which have the benefit of faster running times and a lower level of complexity and uncertainty (i.e., degrees of freedom) due to boundary conditions that are fixed closer to the area of interest. However, the SFWMD project team considered it important to have a tool that would shift the effect of the southern boundary away from the project area and that could also be used to evaluate the impacts of the proposed projects south of the project area. It should be noted that the CWI scope of work did not provide for a recalibration of the BCB model but a refinement of key components to serve the needs of the project. Nevertheless, limited parameter adjustments were included in the refinement effort to optimize the calibration in some key areas of the model. The calibration period for CWI RM was kept the same as the BCB UM (January 1, 2017 to December 31, 2020).

2.2 Objectives of Model Refinements

The main objective of the model refinements is to improve the prediction of performance measures (PM) for proposed project alternatives impacting Corkscrew and adjacent basins. Model output for development of PMs will involve:

- Hydroperiods and depth targets in the Corkscrew wetland areas
- Dry season groundwater levels and recession rates
- Wetland sheet flow across barriers
- Flood risk measures – stages and flows in the primary system and flood depth mapping
- Flows to estuaries, which will be tied to potential impacts in salinity
- Predicting impacts on water supply

The details added to the model considered these types of outputs as well as potential types of projects that would be evaluated with the model. For example, to evaluate the potential benefit of removing flow barriers and uncontrolled drainages, features that represent blockages and drainage under existing conditions need to be included in the baseline model.

2.3 Summary of Refinements

A summary of the refinements incorporated into the CWI RM is listed below.

- Corkscrew DEM adjustment
- Redefinition of wetland flow ways based on a high-resolution overland flow model
- Primary system structure verifications and change of structure operations from targeting measured stages to operate using the measured gate levels in the Corkscrew and Cocohatchee Canals
- Addition of hydraulic connections to Corkscrew and to the downstream drainage system
- Addition of flow blockages in Corkscrew
- Hydraulic modifications along Kehl Canal and tributaries, Corkscrew and Cocohatchee Canals – structures corrections, cross sections revisions, parameter optimization
- Agriculture and urban basin drainage revisions
- Groundwater use data / pumping model input checks
- Boundary and initial conditions
- Optimization surface water stages, flows and groundwater levels by model parameter adjustments.

3.0 LiDAR Modification in the Corkscrew Wetland Area

3.1 Topographic Data Sources

Various data sources were compiled and processed to develop a digital elevation model (DEM) for the CWI RM. The main source used to develop the project DEM is the Southwest Florida Digital Elevation Model 2018-2019. This dataset was processed by SFWMD at a 1.6-foot resolution from the 2018 U.S. Geological Survey (USGS) light detection and ranging (LiDAR) developed by Digital Aerial Solutions, LLC (Digital Aerial Solutions, 2018). Survey transects were collected by AIM Engineering in 2022 (AIM

Engineering, 2022) at various locations in the CREW wetland areas. This data was used to check the accuracy of the LiDAR at the survey locations. The wetland areas within the project area were delineated and the LiDAR topography was adjusted within this boundary to reduce the difference between the LiDAR and the survey, as described below. The resulting adjusted DEM was used as input in the CWI RM. Figure 3-1 shows the wetland area delineation, the survey locations and elevations and the USGS 2018 LiDAR elevations. Note that to illustrate the difference in elevations, the survey and LiDAR elevations are shown in similar intervals and colors, with survey points slightly darker tone and an offset outline. The figure shows that when mapped using similar scales, the survey point elevations are substantially lower than the LiDAR in most locations, particularly in the central portions of the southern transects. Other LiDAR-based DEM sources were reviewed and processed in the development of the adjusted DEM. The spatial extent of all LiDAR-based DEM sources that were utilized are shown in Figure 3-2. These additional sources are the 5-foot FDEM 2007 LiDAR for Lee County and Collier County(Lee/Charlotte 2007 FDEM 5-ft | South Florida Water Management District Open Data [arcgis.com]) and the 2018 USGS LiDAR processed by Lee County (LiDAR Data [leegov.com]) at a 1-meter resolution.

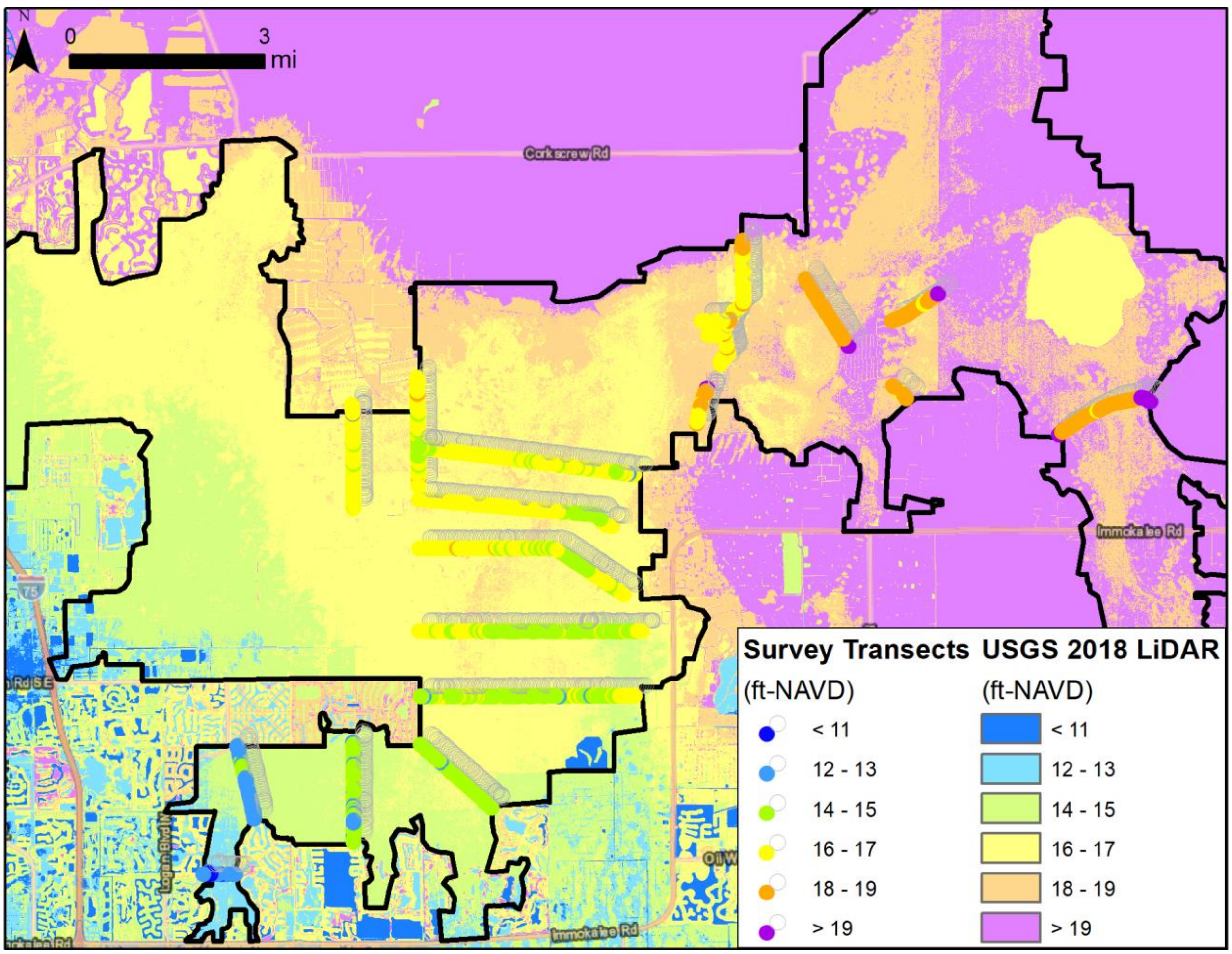

Figure 3-1. Corkscrew Delineated Wetland Areas (Black Outline), 2018 USGS LiDAR and Survey Transects

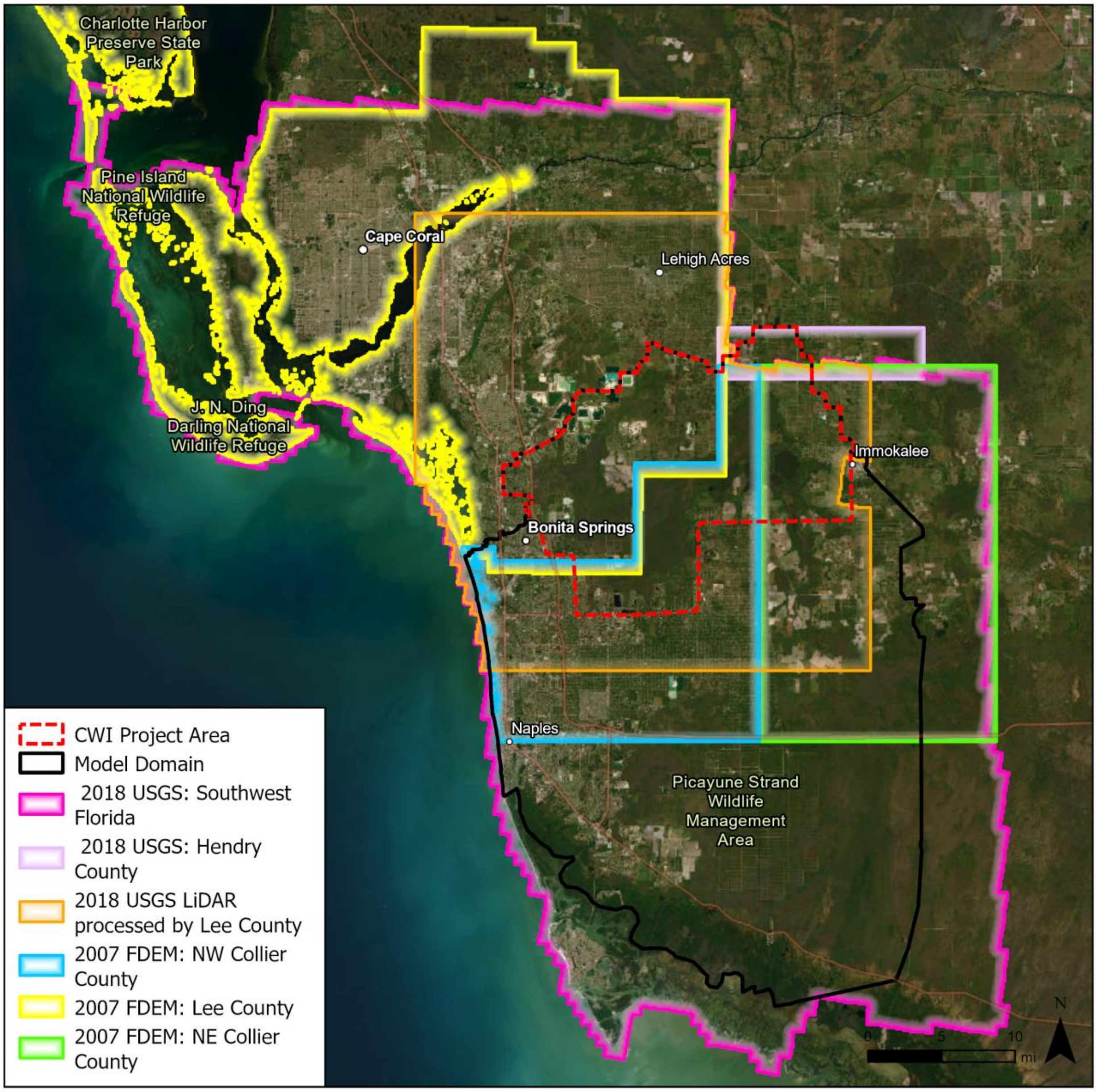

Figure 3-2. Spatial Extent of all LiDAR Based Topographic Data Sources Utilized in the Development of the Adjusted DEM.

3.2 Topographic Adjustments for Model Use

A comparison between the USGS 2018 LiDAR and the survey transects was conducted revealing large discrepancies in elevation. In most locations surveyed, the LiDAR elevations are higher than the survey elevations, up to 4.6 feet, with an average error of 0.9 foot. This is due to the inability of the LiDAR to penetrate through dense vegetation and water ponding. In contrast, survey data available in other nearby areas shows that the LiDAR is much more accurate in non-water and non-wetland areas, such as roadways (Figure 3-3). Producing a more accurate ground topography in Corkscrew is critical not only for establishing gradients and flow patterns, but to determine accurate water depths and hydroperiods. Thus, a multi-step methodology to reduce the LiDAR error in Corkscrew was implemented.

The review and comparison of the other LiDAR sources mentioned above with the survey showed that, in some areas, the error is lower than in the USGS 2018 LiDAR. This could be due to a combination of the wet/dry conditions when the LiDAR datasets were flown and the processing techniques implemented to correct for dense vegetation. Thus, a process to combine the LiDAR data sources to calculate the minimum elevation where these datasets intersect was implemented. This processed reduced the average error (i.e., combined minimum LiDAR minus survey elevations) to 0.6 foot.

Figure 3-3. Shady Hollow survey points showing differences between LiDAR and survey elevations

Another issue with processed LiDAR datasets is that in some areas, artificial changes in elevation occur along straight lines without any real physical meaning. This is likely due to data tiles being pieced together for which data collection was conducted (flown) at different times for the development of the LiDAR raster grids. Three areas in Corkscrew were identified having this issue and were smoothed by applying a correction factor representative of the average change in elevation along the straight lines. Applying this smoothing correction reduced the average error in the survey points to 0.3 foot. Figure 3-4 shows two of areas with the LiDAR artifacts and the applied correction to the DEM.

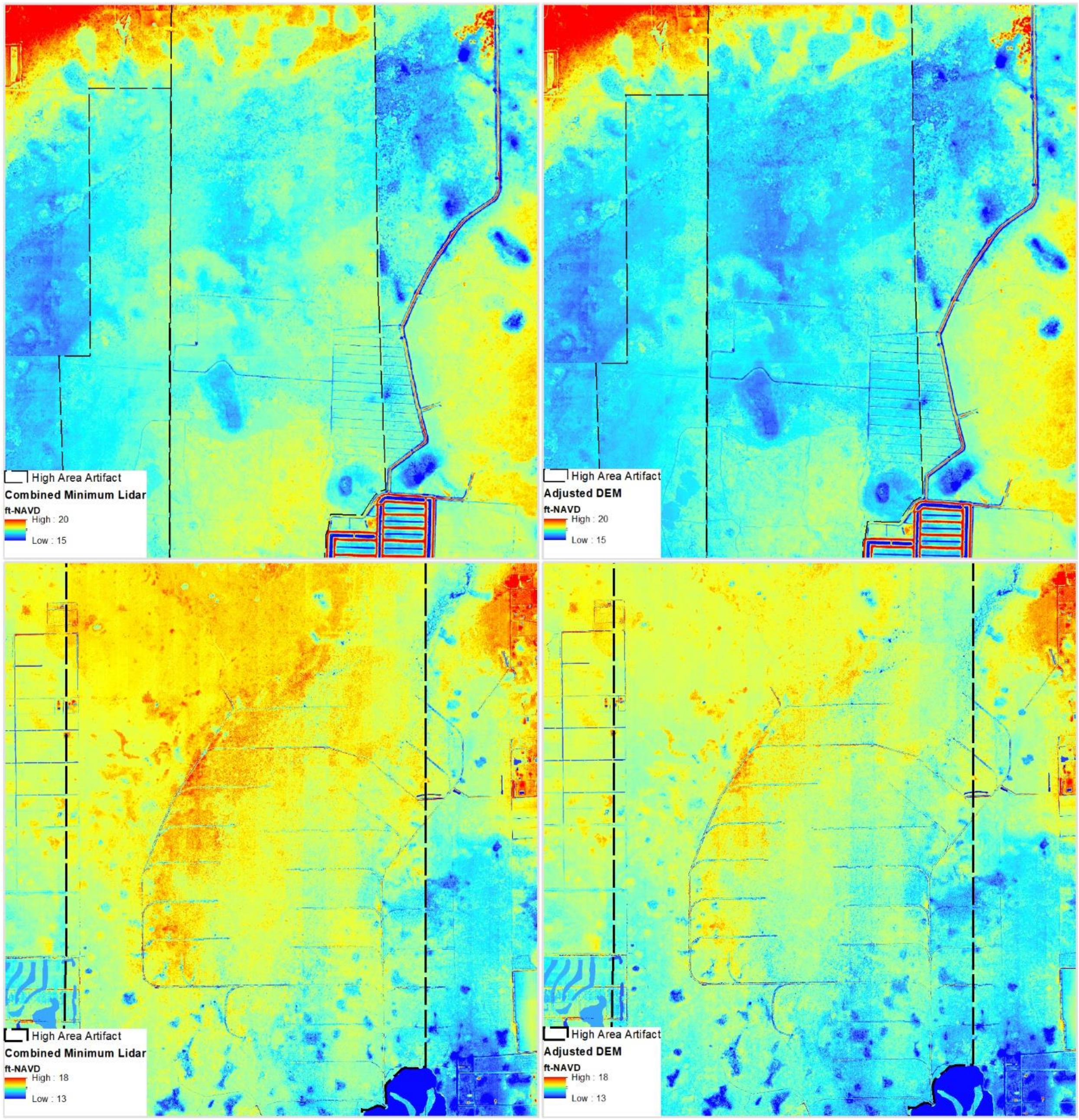

Figure 3-4. LiDAR Artifacts' Close Views (left) and Adjustments to the DEM (right)

The final step in the DEM adjustment process was to create an association with the wetland vegetation communities in the SFWMD land use map and the error in the survey locations. This association is based on the average difference for the vegetation types with the highest frequencies in the survey transect points. The vegetation types, survey point count for each, and the average difference between the LiDAR (after processing in the previous step) and the survey elevations are shown in Table 3-1. Figure 3-5 depicts the reduction in elevation error related to the processing of the data as described above.

Table 3-1. Vegetation-LiDAR Error Association and DEM Adjustment

FLUCCS Code	Description	Point Count	Average Difference in Adjusted DEM and Survey (ft)
6170	Mixed Wetland Hardwoods	55	0.9
6172	Mixed Shrubs	131	0.6
6210	Cypress	196	0.5
6215	Cypress- Domes/Heads	11	1.0
6216	Cypress - Mixed Hardwoods	69	0.7
6250	Wet Pinelands Hydric Pine	42	0.5

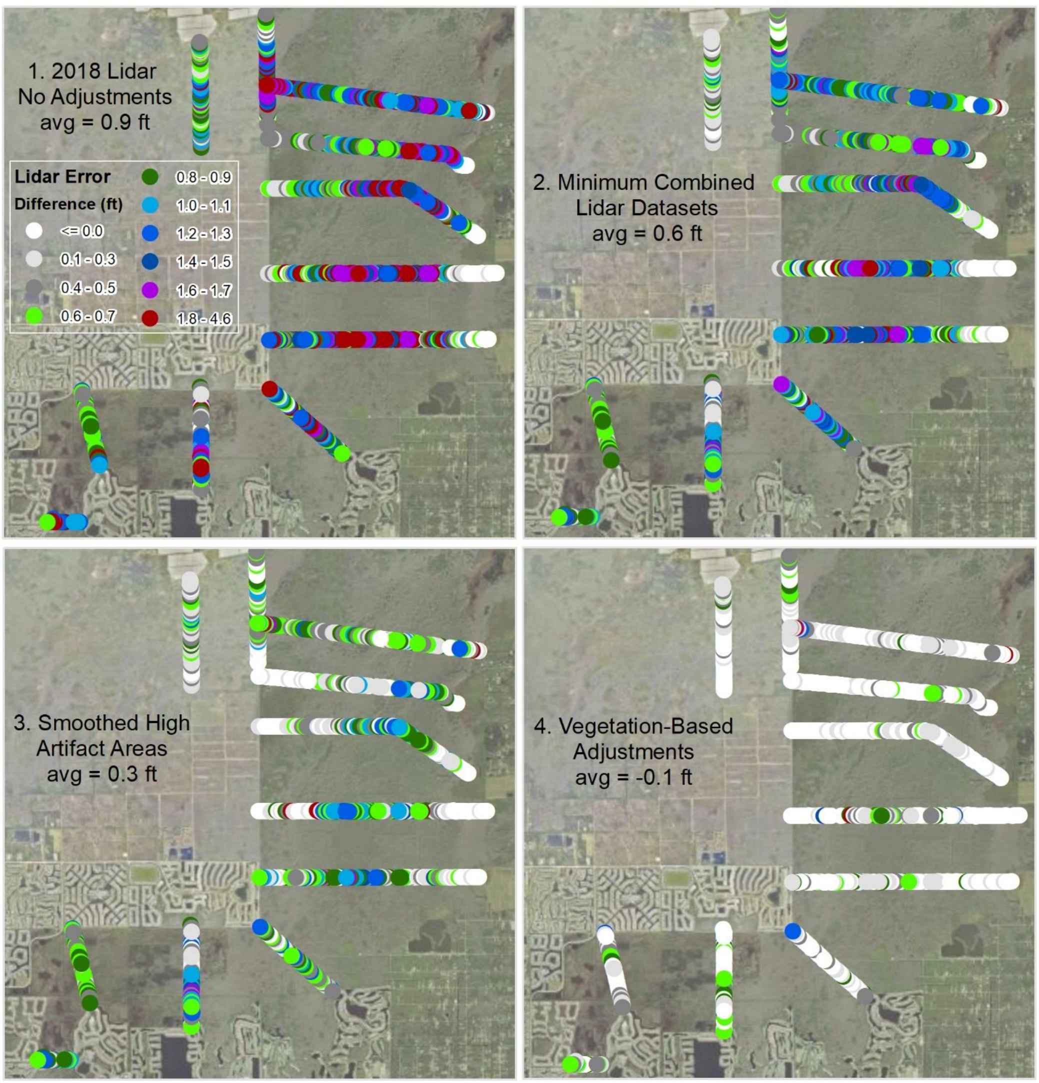

Figure 3-5. Reduction in Elevation Error during DEM Adjustment Processing Steps

3.3 Interpolation of the Revised DEM for Model Input

The adjusted DEM for the Corkscrew area was combined with the original 2018 LiDAR for the rest of the BCB model area. The original resolution of 1.6-ft grid was resampled to a 2-ft grid for averaging using integer multiples at lower resolutions. This 2-ft resolution LiDAR was used to extract cross sections for flow ways and for added and refined canals. Note that for canals with survey data, a combination of LiDAR (banks and floodplains) and survey (water portion) was used.

The 2-ft corrected LiDAR was averaged over 50-ft (Section 4.1) and 500-ft grid resolutions using the Aggregate tool ArcGIS Spatial Analyst for MIKE SHE model input. Section 11.2.3 describes how the MIKE SHE model topography in Corkscrew was adjusted during the optimization process.

4.0 Development of Corkscrew Wetland Flow Ways

4.1 Flow Way Alignments

In theory, a 2D overland flow model can be used to simulate the above ground surface sheet flow in a wetland system. The overland flow component in MIKE SHE uses a finite difference formulation to approximate the diffusive wave form of the St. Venant equations. Flow moves from cell to cell according to the topographic gradient at a rate based on the 2D Manning's equation. However, this model component is limited by the 500-ft model resolution, which is insufficient to effectively capture the local high elevations that impede flow and depressions and short-circuiting pathways where flow accumulates. Moreover, the overland flow component is numerically expensive and running times tend to increase the more overland flow volume is accumulated. Thus, the longer the travel times to receiving canals, the more flow volume may accumulate in the overland flow component, which likely increases model running times. Figure 4-1 shows a comparison of 2-ft, 50-ft, and 500-ft DEM resolutions at a location in southern Corkscrew that discharges into the Cocohatchee Canal upstream of the COCO3 structure. Note that high areas that are a part of a golf course that constrain flow towards the downstream outfall weir, as well as the local depressions within the higher topographic areas that may act to slow down and detain flow downstream, are maintained in the 50-ft resolution DEM but not defined in the 500-ft resolution DEM. Thus, a representation of wetland flow via flow ways in the 1D surface water component is beneficial in order to: 1) represent a higher resolution topography in the 1D cross sections, 2) reduce travel times in the overland flow component to the relatively low topographic areas, 3) represent short circuiting pathways in the wetland system, 4) connect wetlands to discharging and receiving canals in the surface water model, and 5) serve as hydraulic connections between sheet flow obstructions, such as roads and berms, through which flow may occur via overtopping over model weirs and through culverts.

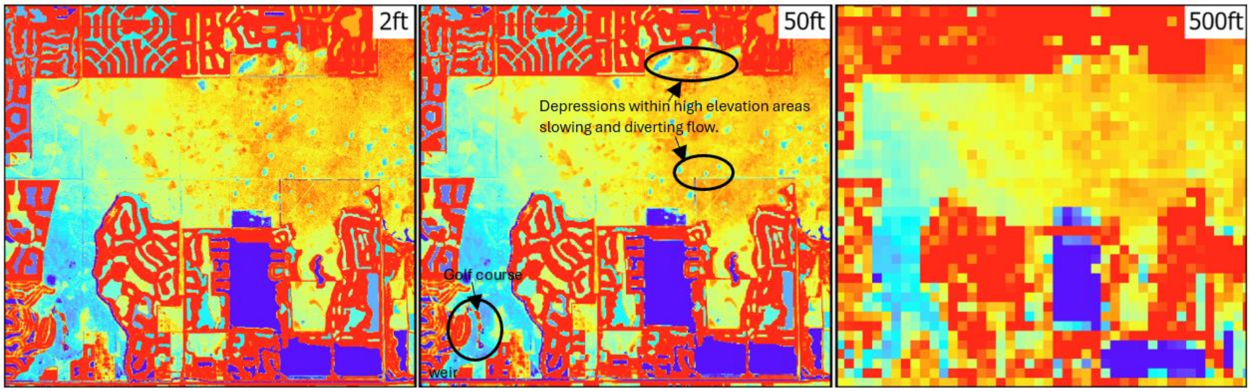

Figure 4-1. Snapshot of DEM resolutions (from darker blue below 10 to darker red above 15, ft-NAVD).

Previous models that include the Corkscrew wetland area have used the 1D surface water component to represent general wetland flow ways. However, these previous definitions simplify the 2D aspect of wetland flow. Portions of Corkscrew in the BCB UM are represented with a single flow way traveling in one direction. A 1D cross section in MIKE HYDRO can only simulate a single stage hydrograph for that location. Some of the BCB UM cross sections are over 5,000 ft wide. This introduces a bias that may approximate how flow occurs during high flow/wet periods but not the more complex dry period flow. This simplification may impact flow routing, travel times and hydroperiods. Thus, a redefinition of the flow ways based on a separate higher resolution (50-ft) overland flow model (HROFM) was conducted. The domain of the HROFM includes only the Corkscrew wetland areas. In this model, overland flow component of the model is linked to a simple 1D (MIKE HYDRO) component that contains only connecting structures through obstructions and downstream outfalls.

The flow ways were aligned to capture the middle or lower portions of the resulting HROFM vectors along a given direction. Inspection of constrictions and pathways in the topography were also taken into account in defining the flow ways. The intent was to add the major pathways as previous models of Corkscrew have done, but also represent more localized flow patterns in the 1D model in a way that approximates the 2D nature of wetland flow. Only pathways of lengths above 1,000 ft, which is the minimum length needed to link a branch (i.e., the MIKE HYDRO 1D element) to the 500-ft MIKE SHE grid, were included in the 1D network. Note that in areas where there are no flow ways defined, the 2D overland flow component in MIKE SHE can move water above the surface and the 3D saturated groundwater flow can move the water below the water table. Figure 4-2 shows screenshots of the resulting HROFM vectors (gray lines) and flow ways (blue lines).

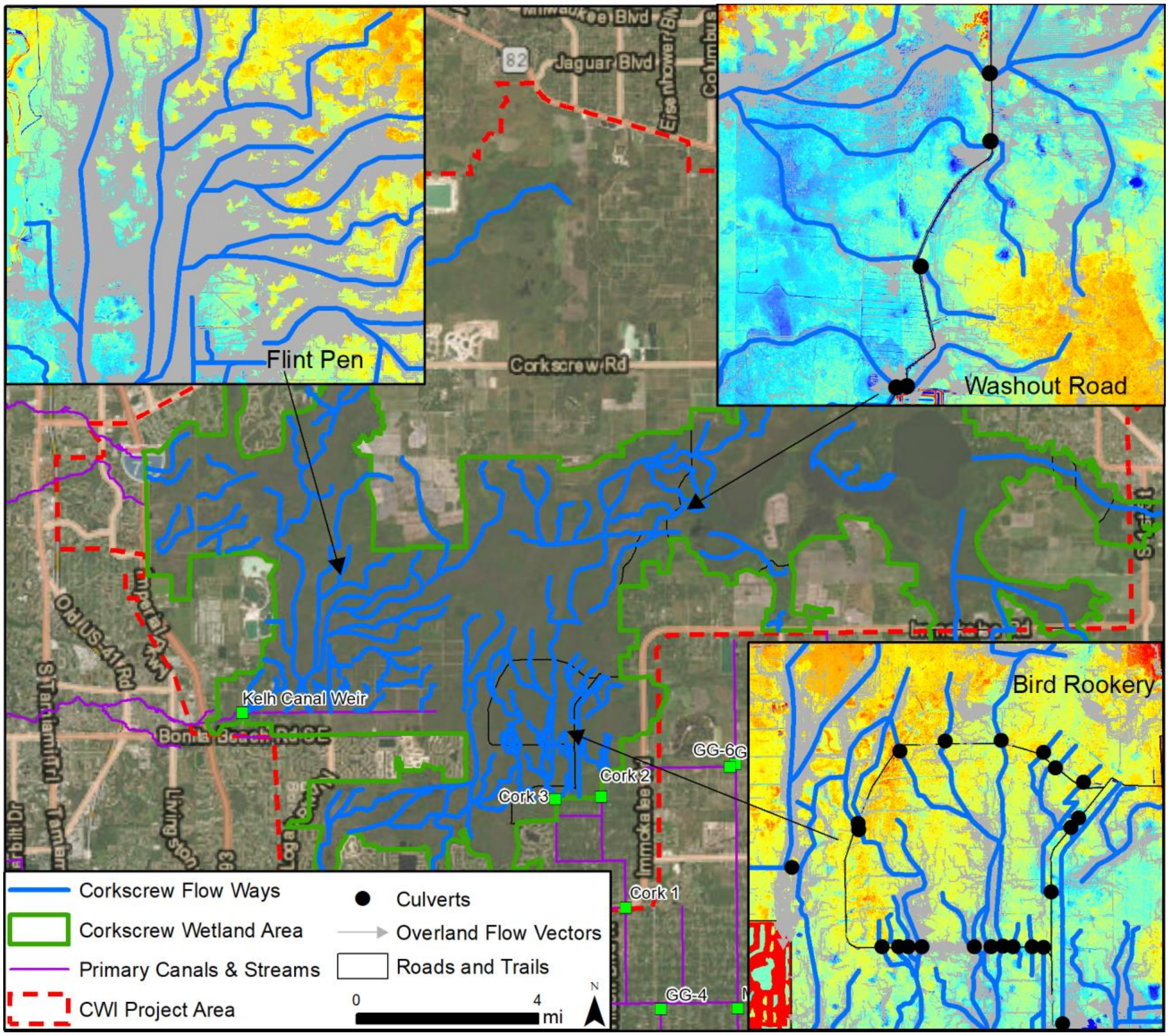

Figure 4-2. Screenshots of Overland Flow Vectors and Flow-ways

4.2 Flow way cross sections

Cross sections for the 1D flow ways were extracted with ArcGIS 3D Analyst from the adjusted Corkscrew DEM at distances of every 1,000 feet. Most cross sections were cut at widths of 500 feet, the same as the MIKE SHE cell size, except in some of the areas where a relatively large accumulation of flow along the flow way direction resulted in the overland flow model. In these areas wider cross sections, up to 2,000 feet, were used.

4.3 Flow Way Exchange with MIKE SHE

MIKE HYDRO flow ways (i.e., branches) can dynamically and bidirectionally exchange flow with the MIKE SHE overland flow and groundwater flow components. The overland flow component will discharge into a flow way if ponded water level in the adjacent MIKE SHE cell is above the nearest stage in the flow way.

This overland-to-flow way is the dominant flow direction that is expected to occur in most cases because the flow ways are generally delineated along the lower elevation pathways and connect to the downstream canals. However, flood codes are a mechanism that allow flow to occur from the MIKE HYDRO branches to the overland flow component in MIKE SHE. During periods of high flow conditions, water levels in the flow ways may exceed the microtopography storage specified in the 1D cross section and thus are allowed to overflow into the 2D overland flow system when flood codes are specified. Most flow ways are connected similar to river tributaries that flow towards a downstream canal or culvert connection. Some, however, are not directly connected to a downstream portion of the canal network and instead serve as overland flow connectors between areas blocked by roads or berms represented by Separated Flow Areas (which act as infinite walls along the boundaries). These connector flow ways rely on flood codes to communicate overland flow areas. The flow exchange between cells with flood codes and MIKE HYDRO or with the overland flow component depends on whether the cell is flooded or not flooded. To determine whether these cells are flooded, the stages in the nearest MIKE HYDRO water level nodes (or h-points) have to be above the adjacent MIKE SHE topography. In this case, the stage in the flooded cell(s) is set to the stage in MIKE HYDRO and the water budget and routing of the flooded cell(s) becomes part of MIKE HYDRO. No overland flow occurs within flooded cells but overland flow from flooded cells to other non-flooded cells can occur. If the cells with flood codes are not flooded, i.e., when stage in MIKE HYDRO is below the topography, then overland flow to and from that cell and the water budget is part of the overland flow component. To maintain storage volume consistency, it is considered good practice to match the MIKE HYDRO cross section width with the flooded cell area. Thus, flood codes were specified along most flow way segments generally following this practice.

Groundwater flow exchange with the flow ways is a function of the head difference between the adjacent water table and the flow way stages and the conductance specified in the MIKE SHE coupling links menu in MIKE HYDRO. The conductance type and leakage coefficients were adjusted during the optimization process. For most of the eastern and central flow way couplings, the Aquifer Only option was used, which means that the exchange rate is only limited by the hydraulic conductivity of the top aquifer layer since flow ways are relatively shallow. For the western flow ways in Flint Pen Strand, either the Aquifer + River or River Only options were used. For these options a leakage coefficient is specified, which acts as an additional resistance to flow.

Figure 4-3 shows a schematic of the flow exchanges scenarios representing average or drier conditions and flood conditions. During the dry season smaller rainfall events cause flow to start accumulating in the flow ways as the water table begins to increase. If water levels in the MIKE SHE cells are below the topography, no overland flow will occur. If water levels in the flow ways are below the MIKE SHE topography, no flooding from the flow way to the overland flow component will occur. During wetter conditions, larger rainfall events will exceed the flow way storage and will flood to the adjacent cells when the stage exceeds the MIKE SHE topography. As more flow accumulates in the flooded cells and the MIKE SHE water levels are above ground, 2D overland flow can occur to other cells that are not directly linked to flow ways. Head dependent groundwater flow also occurs between the cells and flow ways.

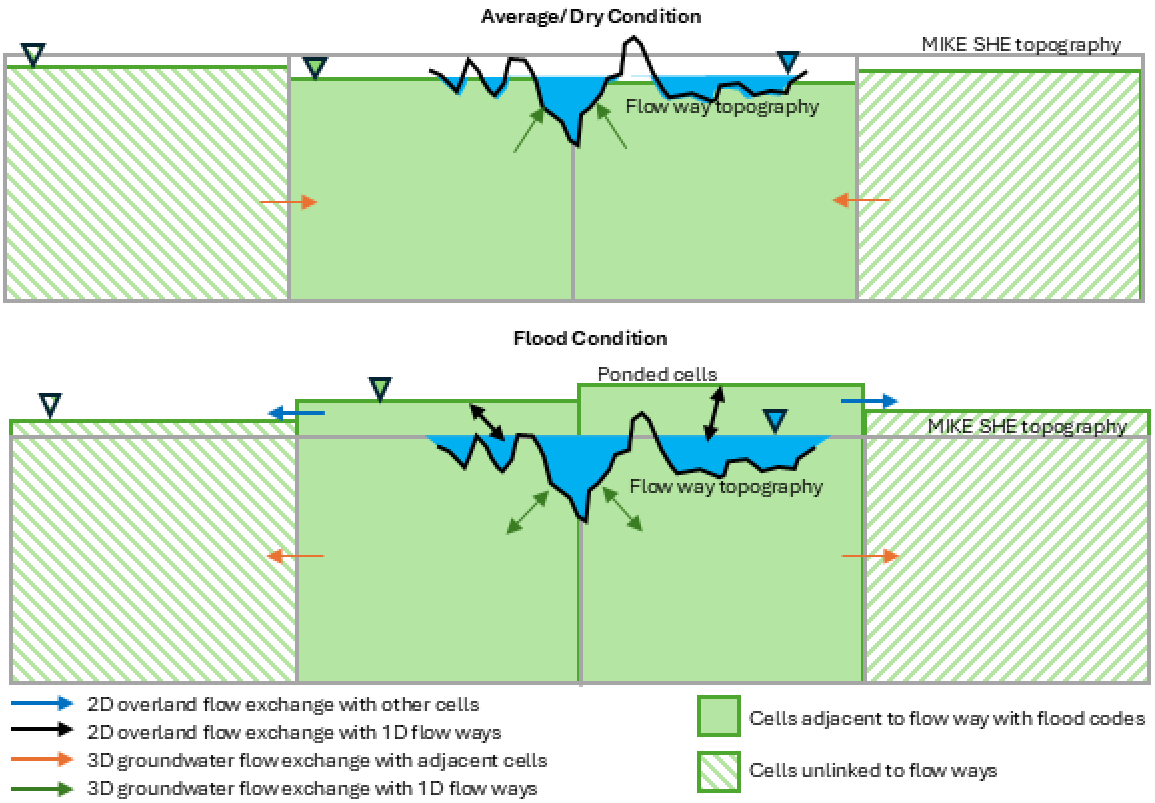

Figure 4-3. Conceptual Graphic of Flow Exchanges between 1D Flow Ways and Adjacent Cells

5.0 Structure Operations and Flow Verification

The operations of structures in the BCB UM (Hazen and Sawyer, 2023) used observed water level to control the gates in order to match stages, that is, if the simulated headwater is above the observed, the gate opens, otherwise, the gate closes. This was a way to mitigate potential errors in gate opening data. For the CWI RM this approach was revised to operate the structures that more directly impact the project area with the historic gate levels. Although, this would likely introduce some stage error into the calibration, it was considered important to do so in order to understand potential water budget and head loss deficiencies in the model. The structures for which the operations were modified are: Cork1, Cork2, Cork3, COCO1, COCO2, COCO3, COCO4, Curry1, CR951N, and the Kehl Canal gates (Figure 5-1).

The following sections describe the flow verification that was conducted at Cork3, Cork2, Cork1, COCO3, COCO4, Curry1, and the Kehl Canal Weir. The flow verification was conducted at these structures because of their proximity to Corkscrew.

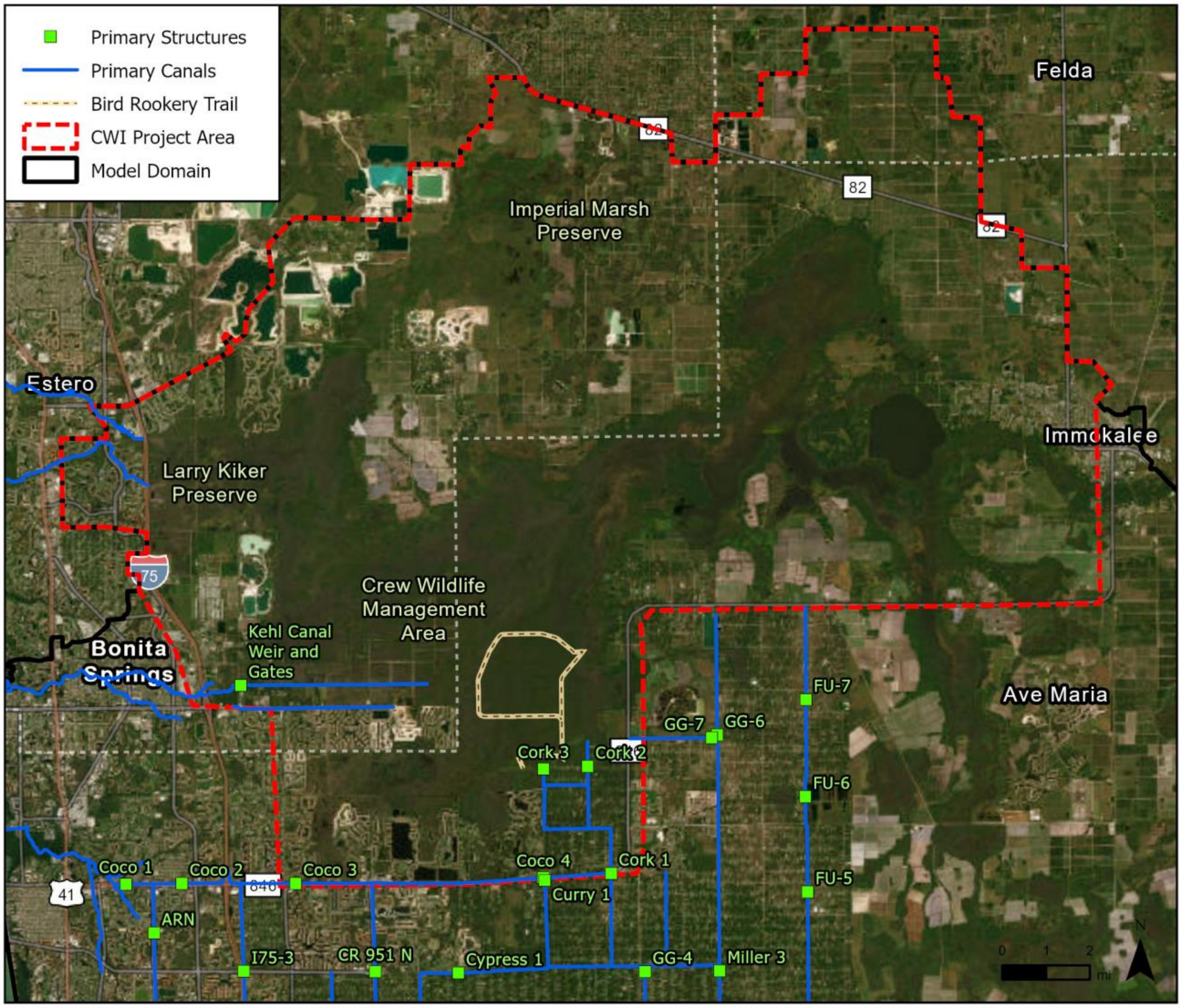

Figure 5-1. Primary Structures Downstream of Corkscrew

Structure verifications were conducted to ensure that flow is properly simulated by the key primary structures in the model. The flow verifications were conducted by developing small models of the structures and comparing the simulated flow to the flow time series in DBHYDRO, if available, and/or to flow calculations. The structure verification models use stage boundaries upstream and downstream of the structure based on the measured headwater and tailwater and the measured gate levels are used to operate the individual gates for each structure. For structures that do not have flow data in DBHYDRO for the calibration period, flow estimates were developed using the flow rating parameters calibrated by SFWMD (Rakib and Zeng, 2019, 2020a, 2020b, 2020c, 2020d, and 2020e) based on CFD models to fit the structure flow equations in the SFWMD Atlas of Flow Computation (SFWMD, 2015). These flow rating reports are available for most of the BCB primary structures. Some of the structures, such as Cork2 and Cork3, do not have tailwater data available for the calibration period. For these structures, the tailwater values were approximated based on the closest available station unrestricted by a structure in between.

For example, the measured stages at Gold846 (this station is now known as Cork1_H since 2023) was used to approximate the tailwater stages for Cork2 and Cork3. To support this assumption, recent data collected in Cork2_T, starting in 2022, indicates that the stages are similar to the Cork1_H and COCO4_T stages, except for the period of higher flow when the COCO4 gates are opened (Figure 5-2). During the calibration period, however, COCO4_T and Gold846 (now known as Cork1_H) show higher differences, and in conversations with District staff, it was recommended using the Gold846 headwater stages over COCO4_T, thus Gold846 was used to approximate the tailwater at Cork2 and 3. The structure verifications and changes to the structure in the model based the verification are described below.

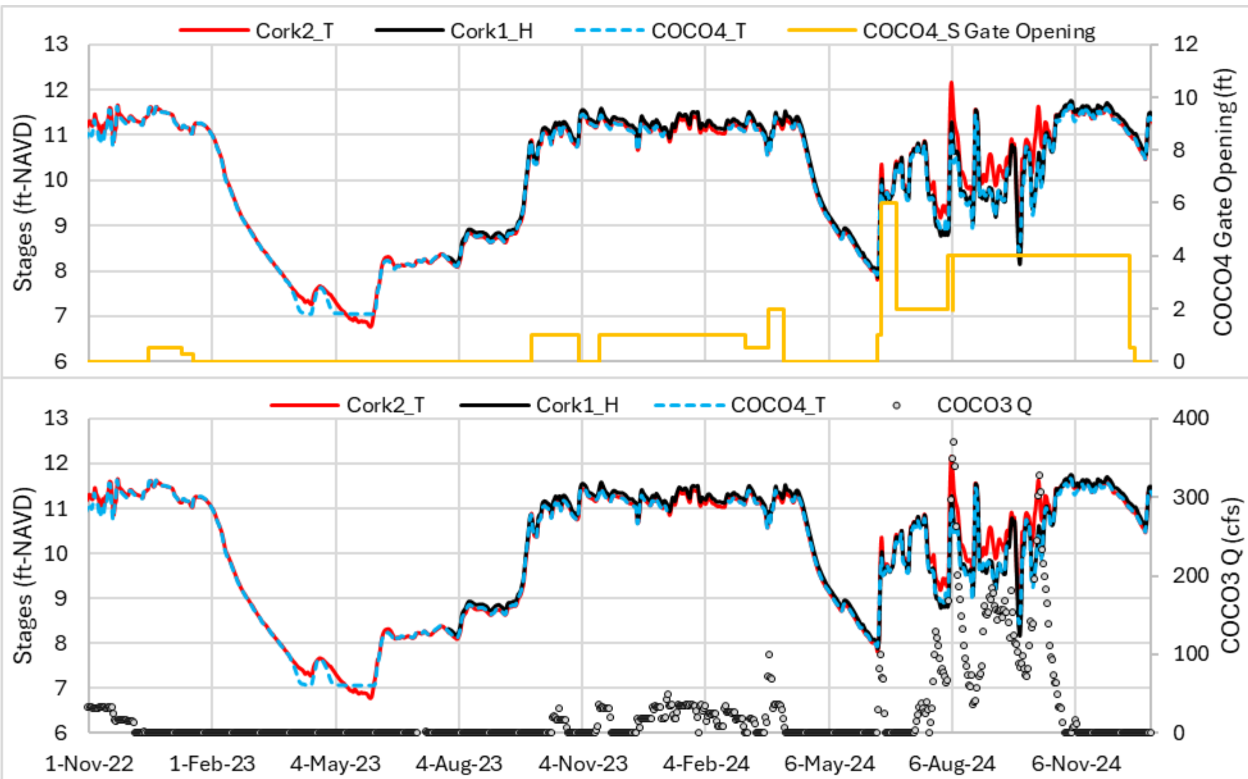

Figure 5-2. Recent Measurements in Cork2_T versus COCO_4_T

5.1 Cork3

Cork3 is a one-bay gated culvert with a box drainage grate inlet located at the western upstream end of the Corkscrew Canal. Cork3, along with Cork2, controls the flow from the Bird Rookery Swamp south to the Corkscrew Canal basin. Headwater levels are available in DBHYDRO starting in 2004 and manual gate openings records are available from DBHYDRO starting in 2018. Manual gate records openings previous to 2018 were provided by SFWMD for the BCB UM effort. There is no flow or tailwater measurements available for this structure and thus, these were estimated for the calibration period. The flow calculations were checked to ensure that the flow matched the ratings report (Rakib and Zeng, 2019) for the same boundary conditions. As previously mentioned, the tailwater stages for these calculations were approximated with the measured stages at Gold846.

The BCB UM used an overflow gate, a fixed weir and a culvert to represent this structure. Since the gate that controls the flow below the inlet is a vertical lift gate, the gate in the model was changed to an underflow gate. A fixed weir that represents the box grate inlet overtopping in the channel was kept in the model. The BCB UM included a culvert specified in the same location as the gate (thus, in parallel), if kept it should be specified downstream of the gate but this would add numerical complexity to that location in the model. Thus, the culvert was removed.

The Cork3 structure verification model shows that the underflow gate with the default parameters reduces the original gate volume error from the BCB UM (overflow gate) but it is still much higher than the calculated volume from flow rating equations. Thus the underflow contraction coefficient (CC) was reduced from the default value of 0.63 to 0.3 (unitless). This reduces the total volume error (i.e., |simulated – calculated| / calculated) for the four-year calibration period to 1% (Figure 5-3).

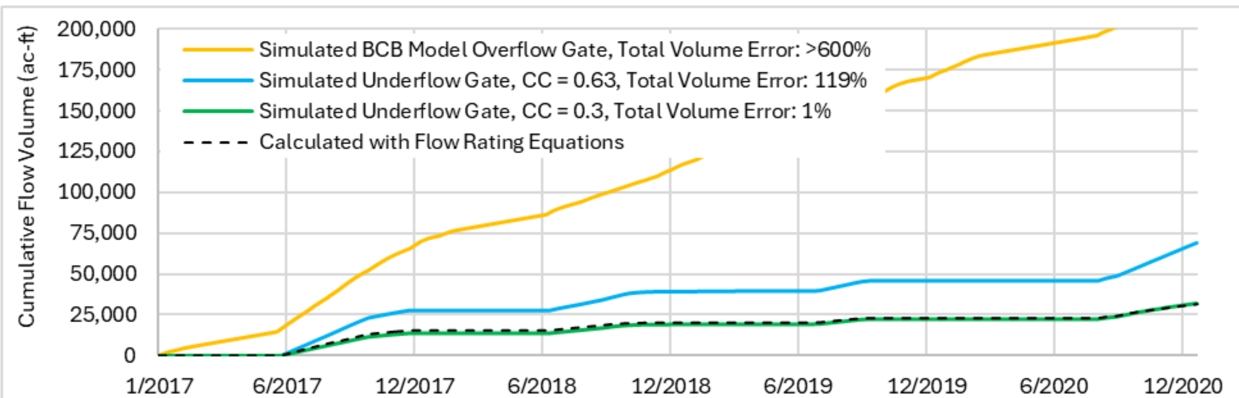

Figure 5-3. Cork3 Cumulative Flow Volume, Simulated Structure Models versus Calculated Based on Rating Equations

Although the lower calibrated CC underpredicts the peak flows (as calculated from the flow equations) in 2017 by approximately 10 cfs, the model is able to match the lower flows well (Figure 5-4). The CWI RM was updated with the Cork3 structure set-up and parameters as included in the structure verification model.

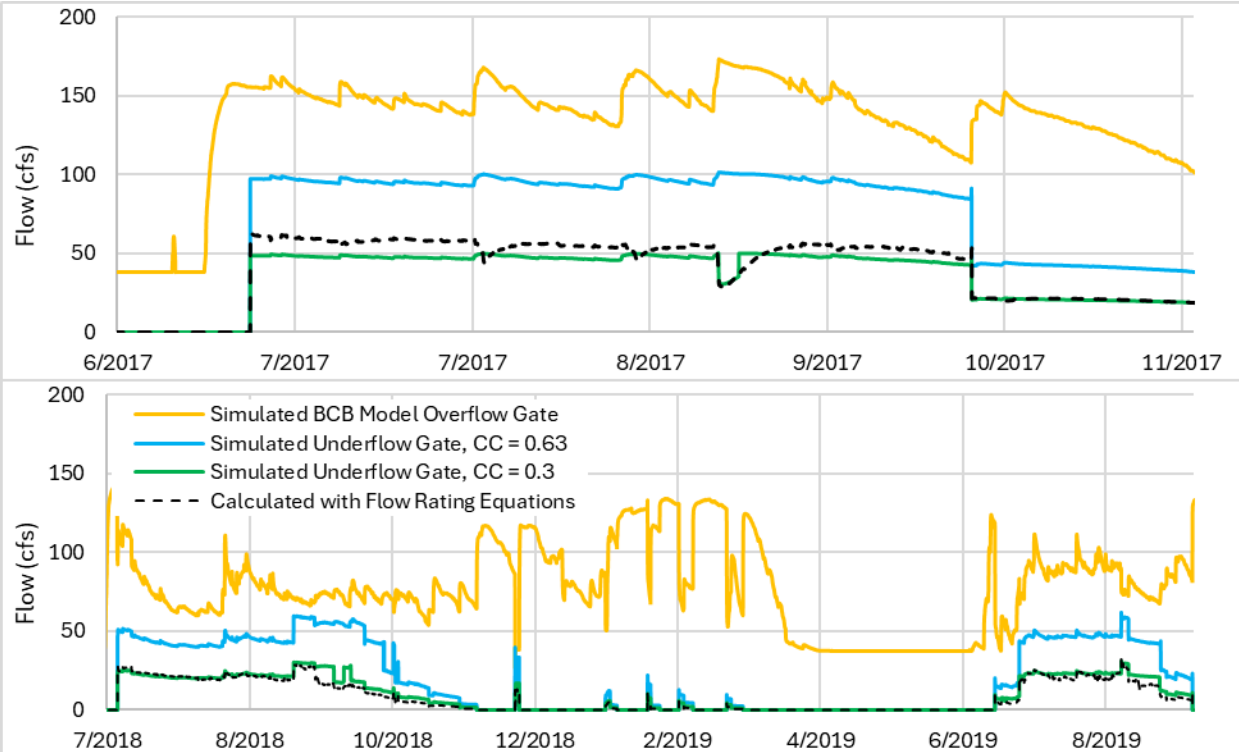

Figure 5-4. Cork3 Simulated Flow in Structure Verification Models versus Calculated Based on Rating Equations

5.2 Cork2

Cork2 is a double barrel box culvert with underflow gates located at the eastern upstream end of the Corkscrew Canal. Cork2, along with Cork3, controls the flow from the Bird Rookery Swamp south to the Corkscrew Canal basin. Measured headwater stages are available, but tailwater stages and flow were estimated, as previously mentioned. The rating report (Rakib and Zeng, 2020a) for this structure calibrated the parameters are used for Type 3 and Type 5 culvert flow in the Atlas of Flow (SFWMD, 2015) to match the flow calculated by a CFD model. The equations and parameters provided by the rating report were used to generate a flow time series for the calibration period. Checks were made to make sure that the flow calculations match the rating report using similar boundary conditions. The BCB UM model used a single sluice type gate in MIKE HYDRO, which calculates the dimensional analysis equations Atlas of Flow for spillway. Since Cork2 is not a spillway structure, it was changed to an underflow type gate in MIKE HYDRO, which produced a better match in the structure verification model (Figure 5-5 and Figure 5-6). The largest deviation of the simulated flow in the structure verification model when using the underflow gate with default parameters is during the peak flow. However, when the CC is lowered to better match the peak flow, the simulated model flow is underestimated during lower flow (based on the flow equations) leading to a higher volume error. An additional verification exercise was conducted using the observed data for 2024 for which measured tailwater values are available and thus do not need to be approximated. This led to a higher CC to better match the observed flow, however, when applied to the large CWI RM model, it led to instabilities and did not improve calibration. Thus, the underflow gate was kept in the model with the default CC of 0.63. The CWI RM was updated with the Cork2 structure set-up and parameters as included in the structure verification model.

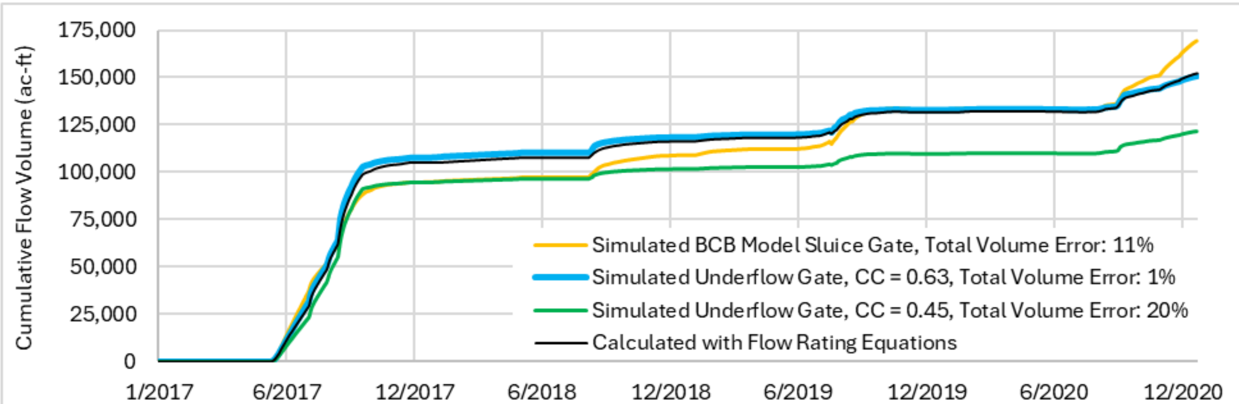

Figure 5-5. Cork2 Cumulative Flow Volume, Simulated Structure Models versus Calculated Based on Rating Equations

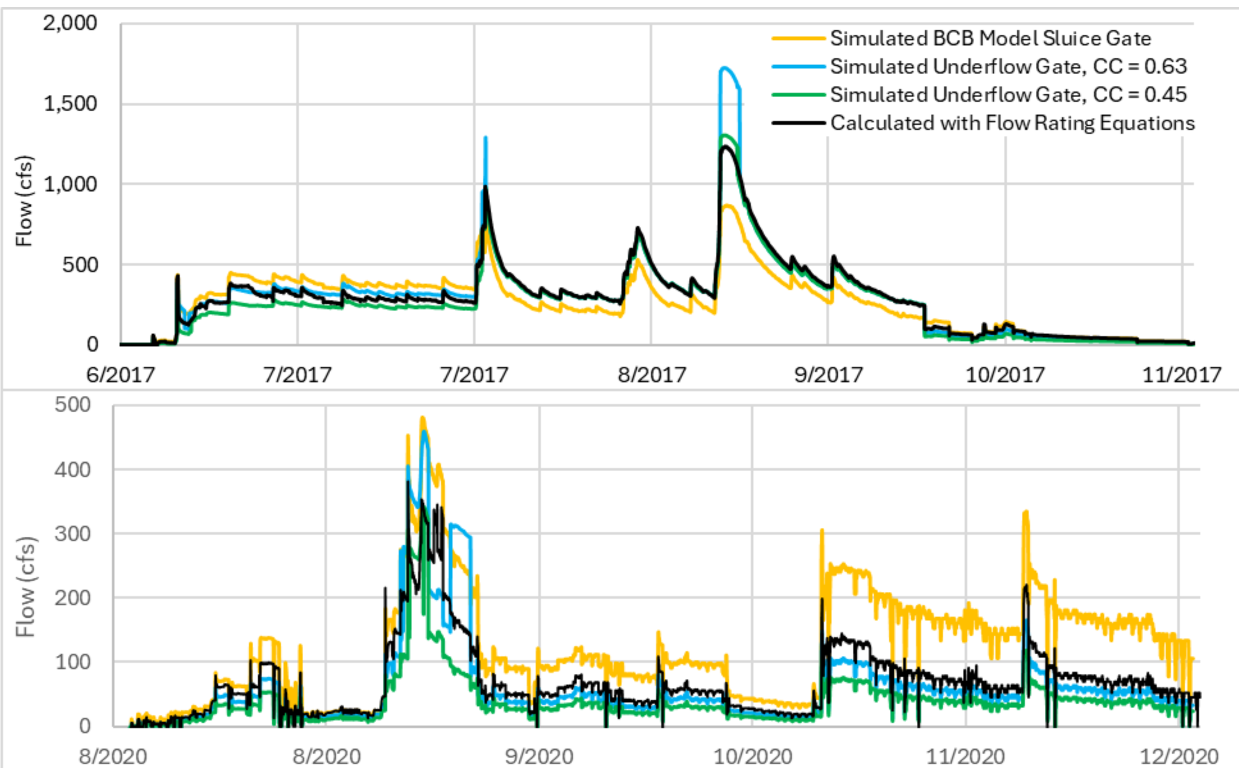

Figure 5-6. Cork2 Simulated Flow in Structure Models versus Calculated Based on Rating Equations

5.3 Cork1

Cork1 is a two-bay gated culvert located at the intersection of the Corkscrew Canal with the Cocohatchee Canal. It controls the flow from the northern Corkscrew Canal south towards Cypress Canal in the Golden Gate basin. Measured headwater stages are available for Gold846 (now known as Cork1_H), but tailwater stages and flow were not available before 2022 and were estimated for the calibration period. To approximate the stages in Cork1_T, the recently collected stages at the tailwater station were compared with the measured stages in Gold846 (Cork1_H) and GG4_H (Figure 5-7). As shown in the plot below, when the gates are closed, the Cork1_T stages are almost identical to GG4_H, but when the gates are opened, the higher the opening, the more the Cork_T stages deviate from GG4_H and are closer to Gold846 (Cork1_H). Thus, a gate opening versus dH (Gold846 – Cork1_T) equation was generated and used to approximate the Cork_T stages when the gates are open. This approach was tested for the summer of 2022 period and resulted in a maximum and average errors of 9% and 0.1%, respectively.

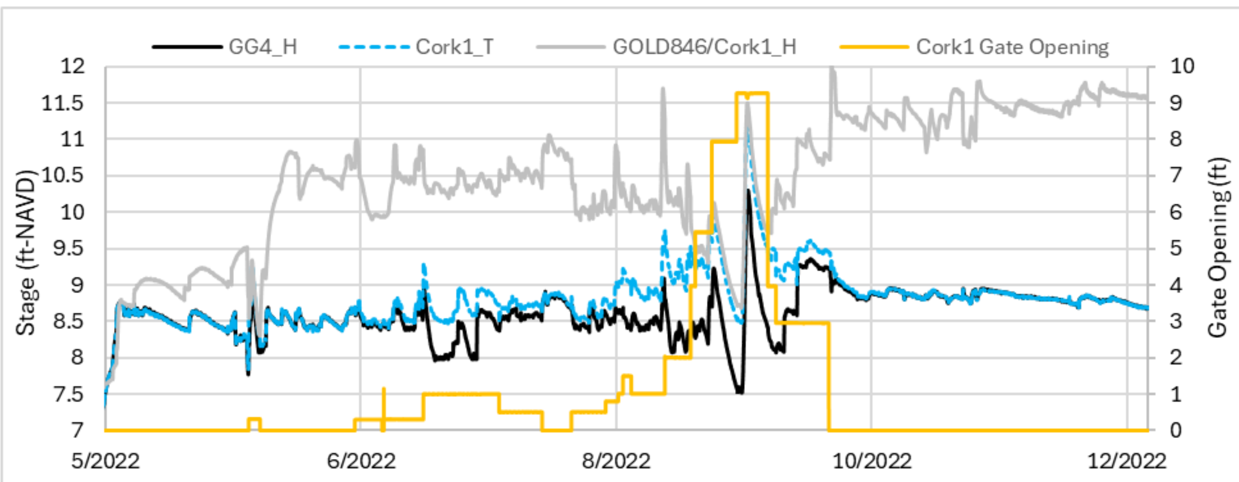

Figure 5-7. Comparison of Cork1_T versus GG4_H and Cork1_H observed stages

The rating report (Rakib and Zeng, 2020b) for this structure calibrated the parameters for Type 3 and Type 5 culvert flow in the Atlas of Flow (SFWMD, 2015) to match the flow calculated by a CFD model. The equations and parameters provided by the rating report were used to generate a flow time series for the calibration period. Checks were made to make sure that the flow calculations match the rating report using similar boundary conditions. The BCB UM represented the structure with a MIKE HYDRO sluice gate which calculates the dimensional analysis equations for spillways. Since the structure is a gated culvert with vertical lift gates, it was changed to an underflow gate. A structure verification model was developed and tested with various structure setups and parameters, including the original BCB sluice gate setup, the underflow gate type with the default CC, the underflow gate with a lower CC value of 0.43, and the addition of a culvert downstream of the default underflow type gate.

Figure 5-8 and Figure 5-9 show the cumulative flow volume and flow, respectively for the four cases tested versus the calculated flow. In terms of the total flow volume error, the underflow gate with default parameters (CC=0.63) performed the closest to the calculated flow than the other cases. However, the peak flows during the summer of 2017 were better approximated when a culvert downstream of the gate was added. Lowering the CC did not have any effect on the 2017 peaks. The BCB sluice gate in general had a worst performance with flows generally too low, except for the Hurricane Irma peak, which better matches the calculated flow. This peak period coincides with the stages above the top of the gate opening when the gates are fully open. The CWI RM was updated with the Cork1 structure with the underflow type gate. In addition, the BCB Water Control Operations Atlas (SFWMD, 2020) indicates that flow over the top of the gate is possible when the gates are fully closed. To account for this possible over top flow, operable overflow gates were added to the model. The use of operable overflow gates instead of a fixed weir is to avoid an overestimate of flow through the fixed weir when the gates are operating, since multiple structures at one location act in parallel. Thus, when the underflow gates are open, the overflow gates are also lifted above the overtop weir elevation (i.e., the top of the gate when fully closed).

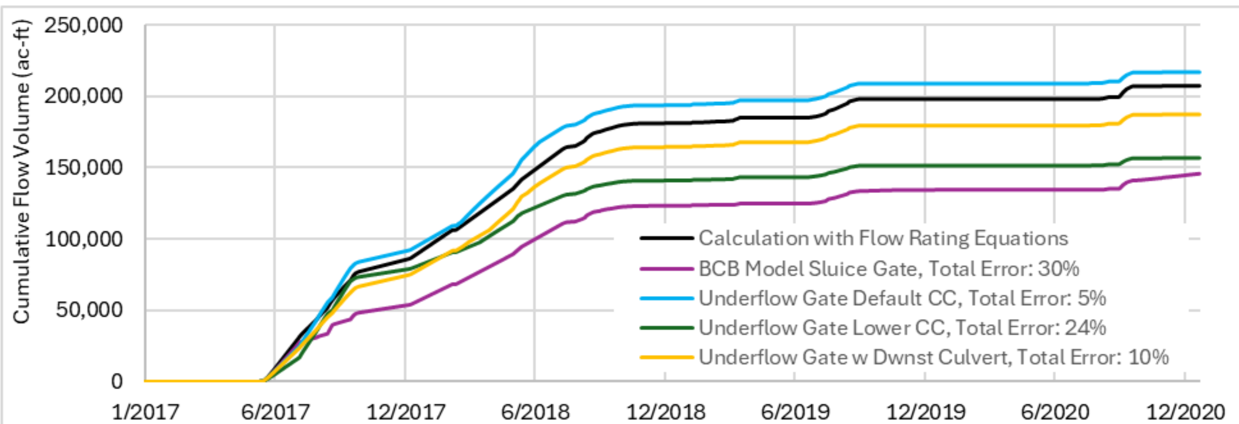

Figure 5-8. Cork1 Cumulative Flow Volume, Simulated Structure Models versus Calculated Based on Rating Equation

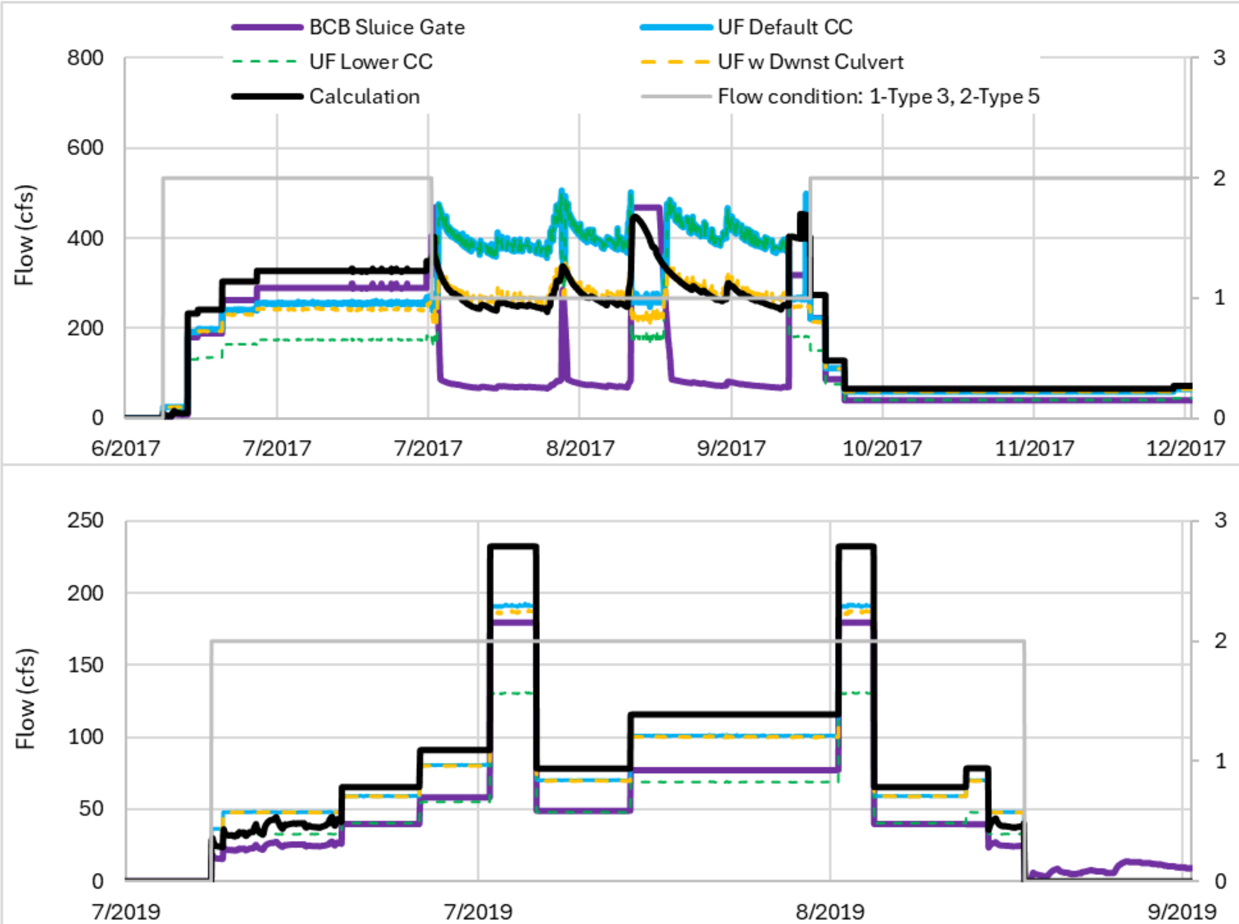

Figure 5-9. Cork 1 Simulated Flow in Structure Models versus Calculated Based on Rating Equations

5.4 COCO3

COCO3, located approximately 5.6 miles east of COCO4 and 2.6 miles west of COCO2, is a two-gated spillway structure with a fixed weir. It controls the flow coming from the southern portions of Corkscrew and the Corkscrew Canal North Basin to the east towards the Gulf of Mexico. In the BCB UM this structure was represented as an underflow gate. Since the structure is a spillway and parameters for the dimensional analysis equations (Case 5 for spillways in the Atlas of Flow, SFWMD, 2015) have been calibrated by Rakib and Zeng, 2020c, for the CWI RM it was changed to a sluice gate type in MIKE HYDRO.

High frequency headwater, tailwater and flow are available in DBHDRO for COCO3. Spreadsheet calculations and a structure verification model were developed to compare to the DBHYDRO flow for COCO3. The spreadsheet flow calculations with the calibrated flow rating parameters were checked against the reported values in Rakib and Zeng, 2020c to confirm the spreadsheet calculations were accurate. In comparing the calculations to the DBHYDRO spillway flow, it was found that they matched flow for control submerged (CS) condition, but were off during uncontrol submerged (US) conditions. Other flow regimes (control free or uncontrol free) are not common for this structure. The deviation in flow between the spreadsheet flow calculation and the DBHYDRO flow seems to occur at the beginning of the transition from CS to US and is better matched when the US "a" parameter is changed from the calibrated value of 1.08 to 1.36 in the spreadsheet calculations.

The COCO3 structure verification model was ran with the calibrated flow rating parameters and it matched the spreadsheet calculations for both flow conditions (Figure 5-10 and Figure 5-11). The simulated peak flow differences in the structure model compared to the flow equations are as high as 150 cfs. However, the total cumulative volume error for the four-year calibration period between DBHYDRO and the flow calculations is relatively small (5%), since the US condition mostly occurred during the summer of 2017. As a result of this structure verification, it was determined that the CWI RM model should use the calibrated flow rating parameters. However, because of the discrepancy between the DBHYDRO flow and the flow calculations, the CWI RM simulated flow should be compared to a revised flow time series based on the calculated spillway flow instead of the DBHYDRO time series flow at the COCO3 location.

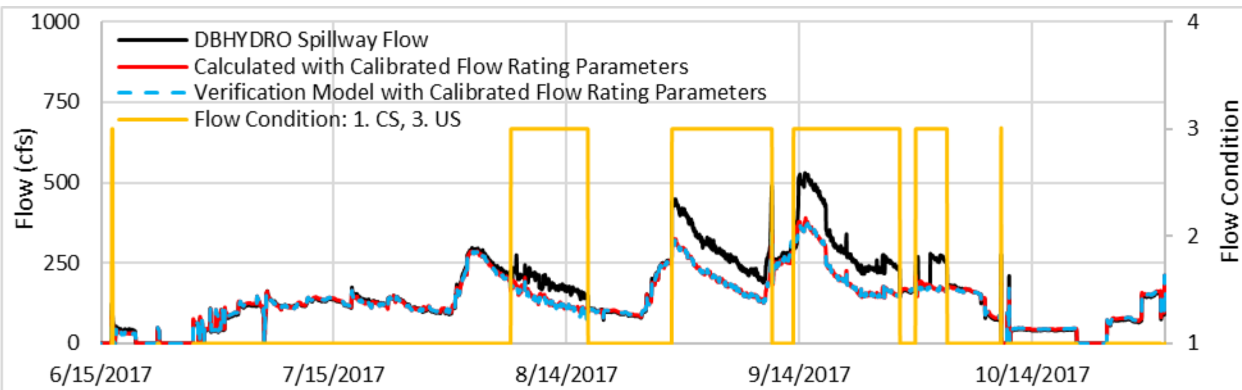

Figure 5-10. COCO3 Calculated Flow and Structure Verification Model Flow versus DBHYDRO Flow

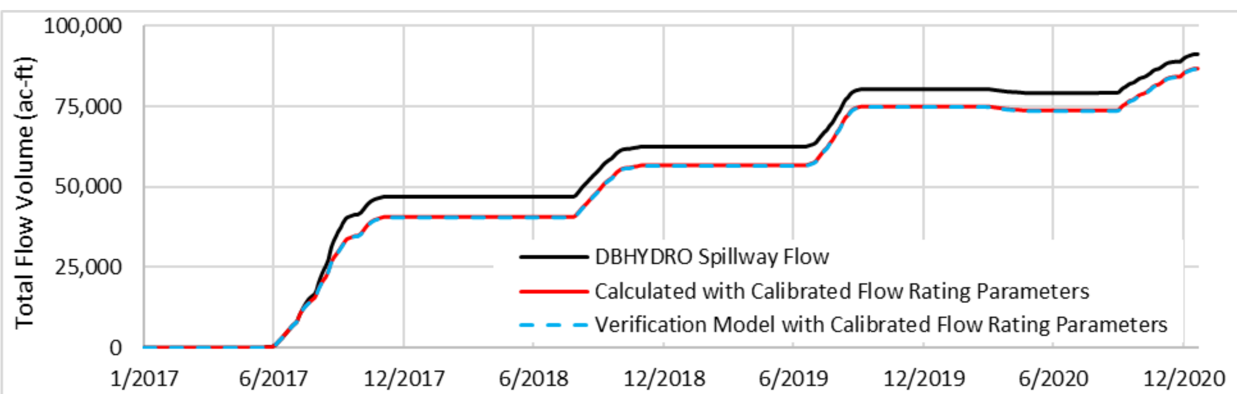

Figure 5-11. COCO3 Cumulative Volume, Calculated Flow and Structure Verification Model Flow versus DBHYDRO Flow

5.5 COCO4

COCO4, also known as Twin Eagles Weir, is a fixed crest weir with two manual steel gates. It controls the flow in the eastern portion of the Cocohatchee Canal. The headwater of the structure is on the west side of the structure, thus, it acts as a basin divide between the east (to the Golden Gate basin) and west (to the Gulf of Mexico) portions of the canal.

High frequency headwater, tailwater and flow are available in DBHYDRO for this structure. Spreadsheet calculations and a structure verification model were developed to compare to the flow from DBHYDRO. The spreadsheet flow calculations with the calibrated flow rating parameters were checked against the reported values in Rakib and Zeng (2020d) to confirm that the calculations were accurate. The comparison resulted in a good match between the calculated flow, DBHYDRO flow and the structure verification model results. The CWI RM was updated with the COCO4 structure set-up and parameters as included in the structure verification model.

The COCO4 structure flow rating development report included a calibrated discharge coefficient for the fixed crest weir and for flow over the top of the gate. While the calibrated discharge coefficient cannot be input directly into MIKE HYDRO model, a head loss factor (a simple multiplier for the discharge from the structure) can be applied to the structure.

For the fixed crest weir, a head loss factor of 1.29 was applied. This was calculated by comparing flow calculated from the SFWMD flow rating equation for the overflow weir with the calibrated discharge coefficient, and flow calculated from the MIKE HYDRO model setup of the revised structure with no head loss factor. Adding the head loss factor of 1.29 resulted in less than 1% error in flow volume from the simulated overflow weir when compared with the weir flow volume calculated from the flow rating equation for the overflow weir with the calibrated discharge coefficient.

For the flow over the top of the gate, flow calculated from the SFWMD flow rating equation for flow over the top of the gate with the calibrated discharge coefficient, and flow simulated in MIKE HYDRO structure verification model were compared. The comparison resulted in less than 1% error in flow volume between the calculated and simulated flow, therefore, no changes were made to the representation of flow over the top of the gate.

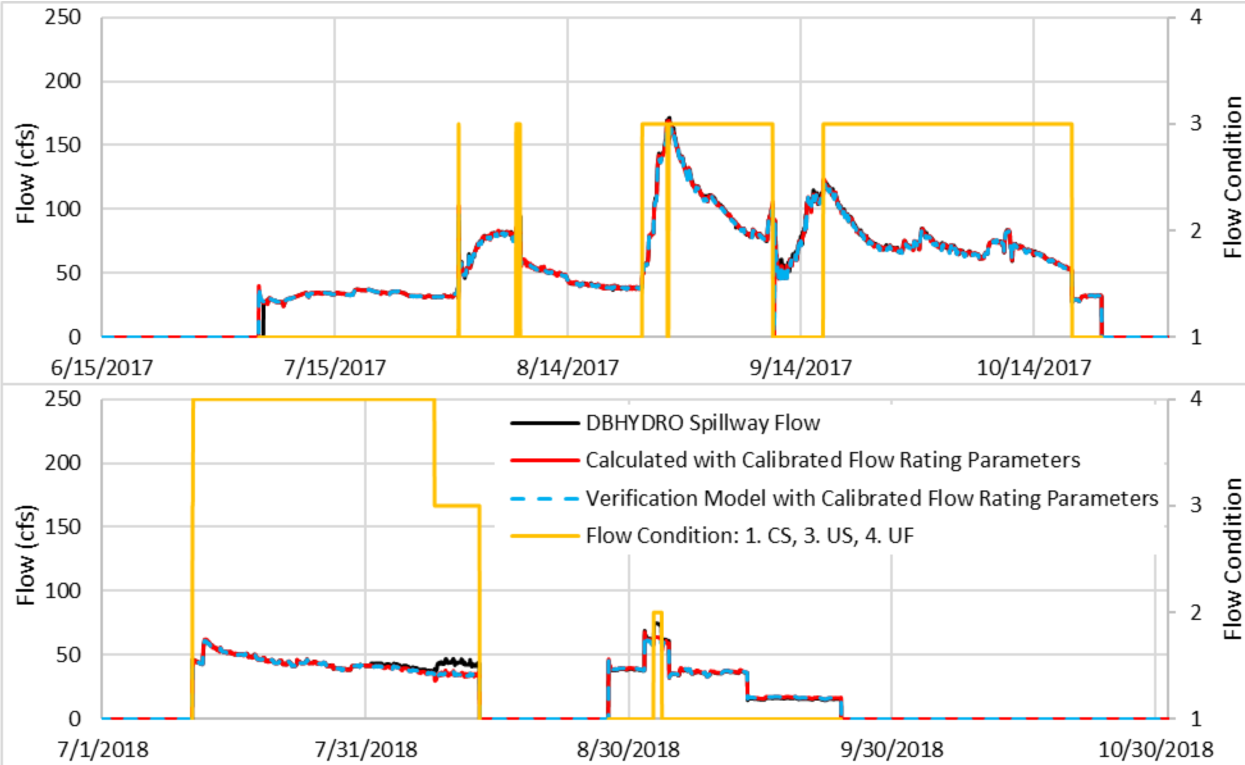

Figure 5-12. COCO4 Flow, Calculated Flow and Structure Verification Model Flow versus DBHYDRO Flow

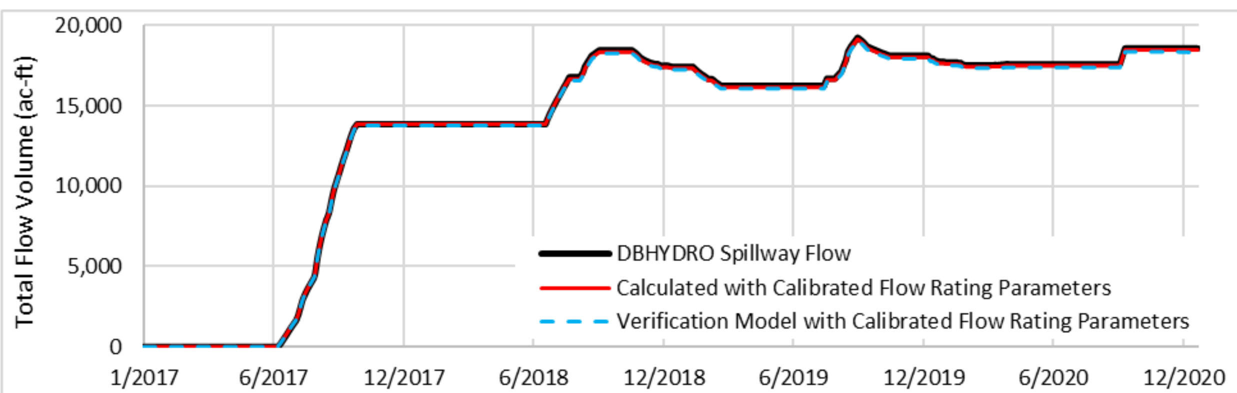

Figure 5-13. COCO4 Cumulative Volume, Calculated Flow and Structure Verification Model Flow versus DBHYDRO Flow

5.6 Kehl Canal Weir

The Kehl Canal structure consist of a 100-foot fixed weir with three side operable gates. Headwater and tailwater stages are available in DBHYDRO since 2003, but no flow or gate operations are available. Lee County provided gate levels, flows and stages starting in November 2019 (Figure 5-14). Based on this information, the structure was adjusted in the CWI RM from the previous setup in the BCB UM. The Kehl

Canal weir crest elevation was corrected and since only one of the gates operates during the calibration period, it was the only one included in the CWI RM for calibration purposes. It was assumed that the gate was closed before this time. Figure 5-14 shows the flow data provided by Lee Count for the last five years. The data shows that even during the times when the gates operate, the flow is around an order of magnitude smaller than the weir flow. Nevertheless, all three gates will be included and operated according to theoretical protocols for the Existing and Future Conditions models.

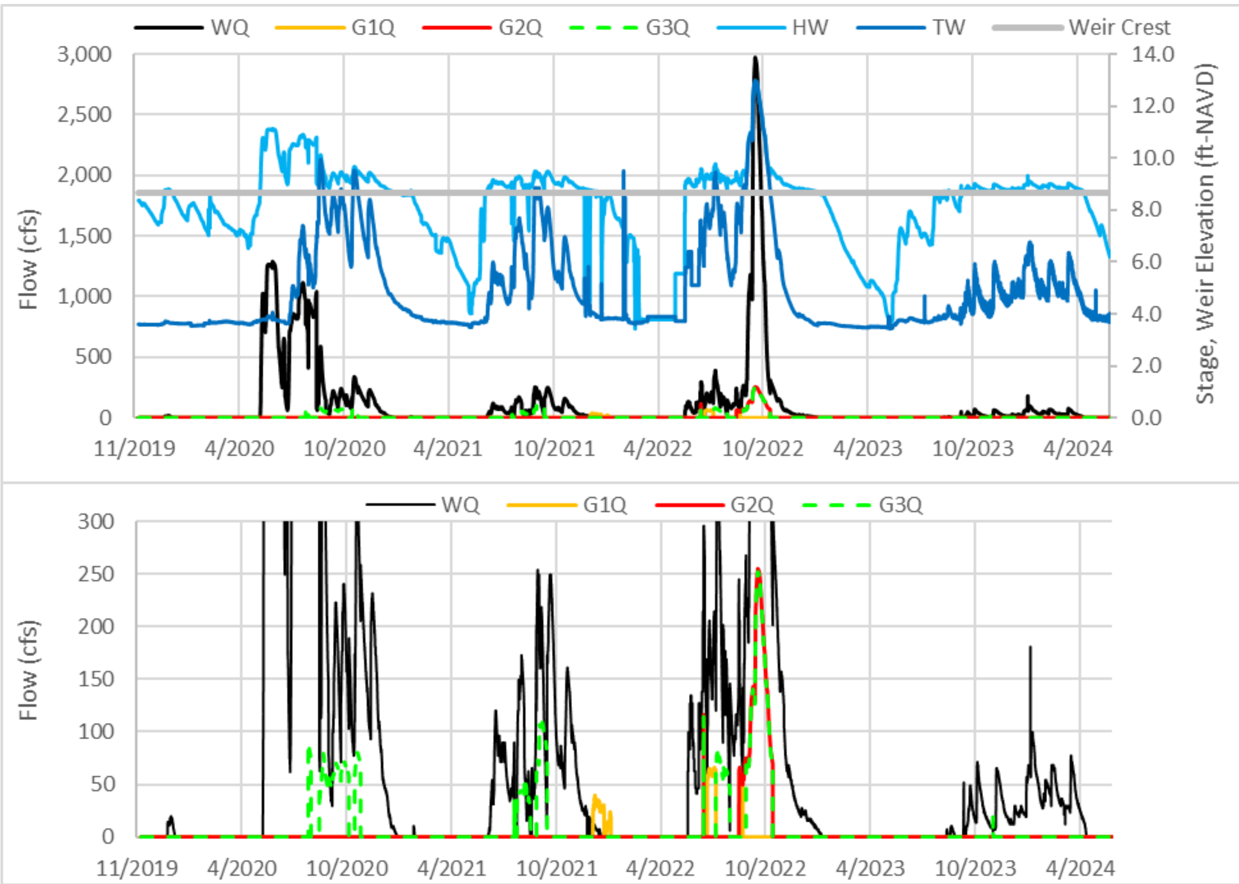

Figure 5-14. Kehl Canal Weir, Flow and Stage Data provided by Lee County

The weir flow was estimated for the full calibration period using the weir discharge coefficient (C = 3.3) in the Lee County flow calculations. However, the County's weir equation was adjusted to account for submerged flow (when the headwater and tailwater stages are above the weir crest) and for negative flow (when the tailwater is higher than the headwater. The Villamonte weir type in MIKE HYDRO is a more direct and comparable weir flow calculation to the common weir equation than the Broad Crested weir type. Thus, the flow time series and structure verification model were developed using this formulation, which accounts for submerged and bi-directional flow. Only the weir flow was verified, since it is where most of the flow through the structure occurs. Figure 5-15 shows a comparison of the Lee County flow calculation versus the calculations conducted for this effort. The plot shows that for unsubmerged conditions, the structure verification model and the calculation with the Villamonte formulation match the Lee County flow calculation, but when the tailwater is above the crest elevation, the structure verification model and the calculation with the Villamonte formulation deviate from the Lee County flow calculation producing lower or negative flow. The CWI RM was adjusted to the Villamonte formulation using the weir coefficient provided by Lee County. Note that the weir coefficient was converted to metric for input into the CWI RM, e.g., C = 3.3 / 3.28084^0.5 = 1.82.

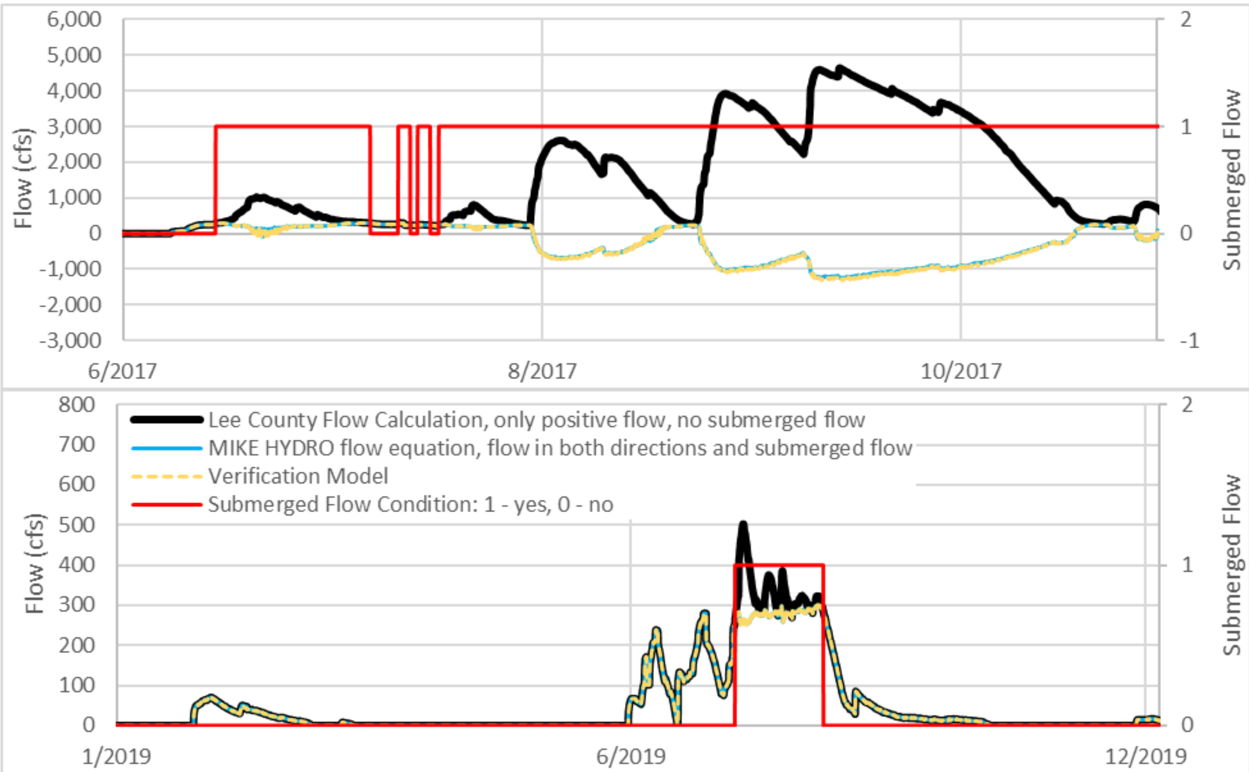

Figure 5-15. Flow Verification for the Kehl Canal Weir

5.7 Curry1

Curry1 is a three-barrel culvert with single stem gates. Each gate is 7-ft wide and 5-ft high and can function as an underflow gate (gate) and an overflow gate (weir). The structure is at the northern end of the Curry Canal, where it connects to the Cocohatchee East Canal. The headwater is on the north side of the structure. The structure was constructed in the summer of 2018 and was manually operated between November 2018 and April 2019 (as per email communication with SFWMD Staff on 3/20/2025) and subsequently operated automatically with remote operation capabilities. A flow rating development report for the Curry1 structure was completed in December 2020 (Rakib and Zeng, 2020e). Gate openings, headwater and tailwater stages, and flows through the structure are available from SFWMD's DBHYDRO database starting in late May 2019.

In the BCB UM, the underflow gates were each represented as a sluice gate (using the calibrated coefficients for the sluice gates available from the Flow Rating Report) and the weirs (flow over the top of the gate) were represented as overflow gates. The sluice gates and overflow gates were operated with gate levels calculated from the DBHYDRO gate openings. In MIKE HYDRO, levels for sluice gates (where water can flow under the gate) should be set to the elevation of the bottom of the gate and levels for overflow gates (where water can flow over the gate) should be set to the elevation of the top of the gate. The overflow gate levels were incorrectly set to the same levels as the sluice gates, allowing too much flow through the structure. This was fixed by setting the overflow gate levels 5 ft higher (the gate height) than the sluice gate levels. Additionally, the overflow gates were incorrectly set to a maximum elevation of 11.7 ft NAVD (13 ft NGVD), which is the elevation of the top of the gates when the underflow gates are closed. This incorrectly allowed flow through the structure whenever the headwater exceeded 11.7 ft NAVD (13 ft NGVD). This was fixed by setting the maximum elevation to 20.2 ft NAVD (21.5 ft NGVD), which is the sluice gate maximum elevation plus the gate height. Additionally, the top of the overflow gates can be brought below 11.7 ft NAVD (13 ft NGVD) to an elevation of 10.2 ft NAVD (11.5 ft NGVD), which is represented in the DBHYDRO gate opening data as a negative gate opening because the bottom of the sluice gate is below the structure sill elevation. These negative gate openings were ignored in the BCB UM. This was fixed by incorporating the negative gate openings into the overflow gate operating levels. Lastly, the Curry1 flow rating development report (Rakib and Zeng, 2020e) included a calibrated discharge coefficient for flow over the top of the gates, which was not included in the BCB UM. While the calibrated discharge coefficient cannot be input directly into MIKE HYDRO model, a head loss factor (a simple multiplier for the discharge from the structure) can be applied to the structure. This was fixed by applying a head loss factor of 1.75, determined as discussed below.

The original BCB UM Curry1 structure and the revisions discussed above (Revised Curry1 structure) were tested in a verification model using the headwater, tailwater, and gate data available from DBHYDRO during the calibration period, June 2019 through December 2020 (May 2019 data was excluded from the verification simulation due to some anomalous very large negative gate opening values). The simulated flow from the BCB UM Curry1 structure and the Revised Curry1 structure was compared with flow calculated using the flow rating equations for the spillway and the overflow weir and with flow values available from DBHYDRO (Figure 5-16). The BCB UM Curry1 structure setup resulted in a 79% error in total flow volume when compared with the flow volume calculated from the DBHYDRO flow time series over the simulation period, due to the additional flow generated from the incorrect overflow weir setup. The revised Curry1 structure provided a significant improvement in the flow at the structure, resulting in only 2% error in total flow volume when compared with the flow volume calculated from the DBHYDRO flow.

The head loss factor of 1.75 was calculated by comparing flow calculated from the SFWMD flow rating equation for the overflow weir with the calibrated discharge coefficient, and flow calculated from the MIKE HYDRO model setup of the revised structure with no head loss factor. The head loss factor of 1.75 resulted in less than 1% error in flow volume from the simulated overflow weir when compared with the weir flow volume calculated from flow rating equation for the overflow weir with the calibrated discharge coefficient.

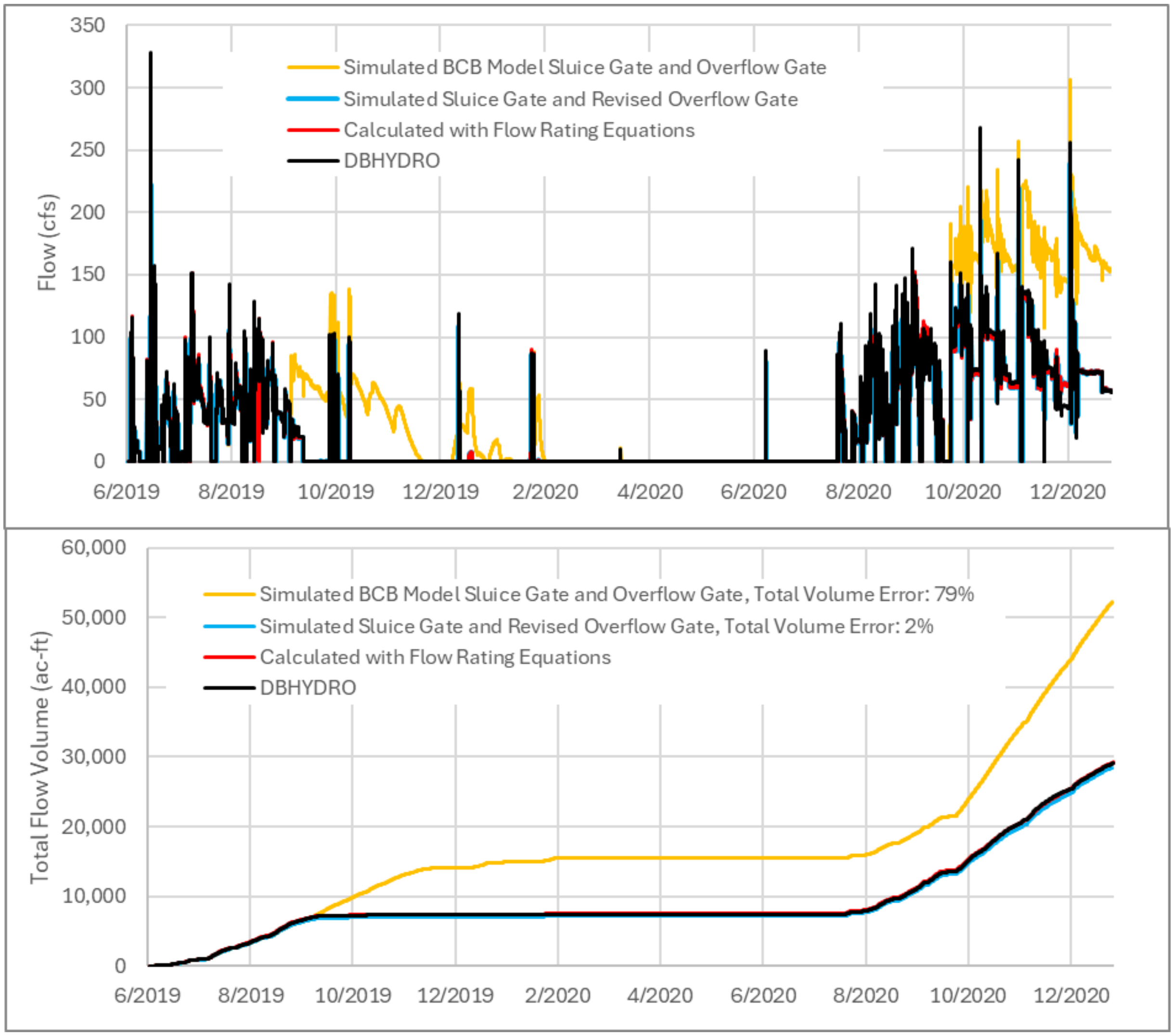

Figure 5-16. Flow Verification for the Curry1 Structure.

6.0 Hydraulic Connections and Constrictions

6.1 Corkscrew Connections to Primary Canals

One of the potential causes of hydroperiod changes in Corkscrew is potential over drainage via connections of the wetland areas to the primary drainage system. Thus, it was considered important for the CWI RM to represent these connections in more detail in order to determine their impact on Corkscrew drainage. To this end, drainage connections that may contribute to the over drainage of Corkscrew wetland were added and revised. The figures below show some of the details added to the refined model.

Figure 6-1 shows the flow ways and structures connecting upstream of the Cork3 structure, including the uncontrolled culverts that can discharge south of the Shady Hollow Boulevard northern ditch and thus, bypass the structure. Figure 6-2 shows the connections added along Immokalee Road to allow flow from the western portions of Corkscrew to connect south via the Immokalee Road swales. Since the swales are shallow and obstructed in some locations, the cross sections were cut 500-ft wide and flood codes added to allow for flooding on either side of the road.

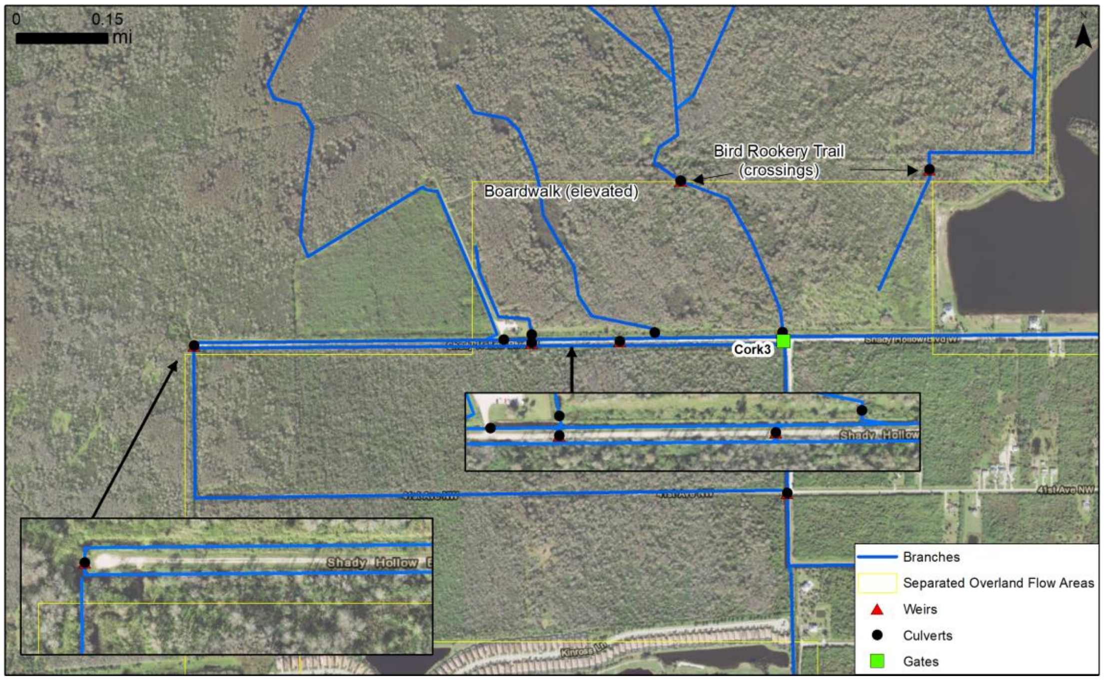

Figure 6-1. Bird Rookery Connections to Cork3 and Uncontrolled Bypasses that can Discharge South of Cork3

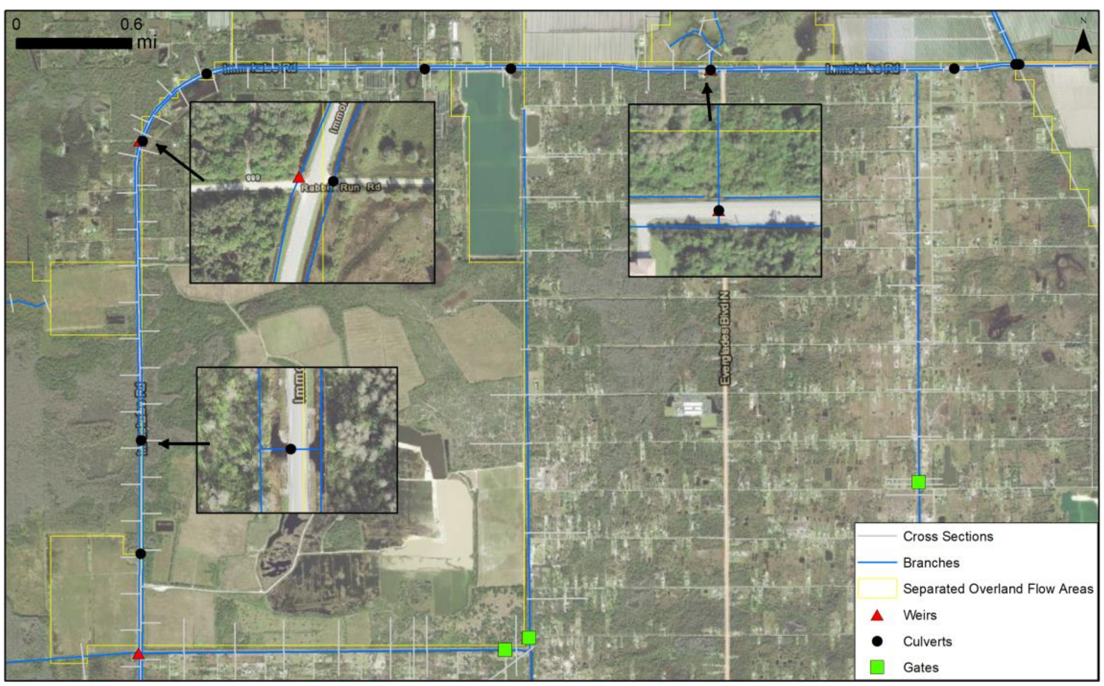

Figure 6-2. Connections to from Corkscrew East-West Immokalee Road

Figure 6-3 shows the southern Corkscrew connections to the Cocohatchee Canal, upstream of COCO3. The Esplanade canal (i.e., Mirasol Pass Through) fixed weirs were checked and adjusted with the development ERP plans and aerial imagery. The canal cross sections were also revised. The elevation of the 955-foot fixed weir that discharges from Corkscrew to the Cocohatchee Canal just east of COCO3 was also adjusted based on the LiDAR elevations. There are several culverts in the Collier County stormwater data under the trail north of Immokalee Road and between the Esplanade development and the COCO3 structure. Google aerial imagery and Street View photos show some of these culverts flowing into the Cocohatchee canal. In conversations with BCB staff, some of the culverts that are shown in the Collier County data may have been removed. Thus, only the ones that were visibly flowing from the aerial imagery were added.

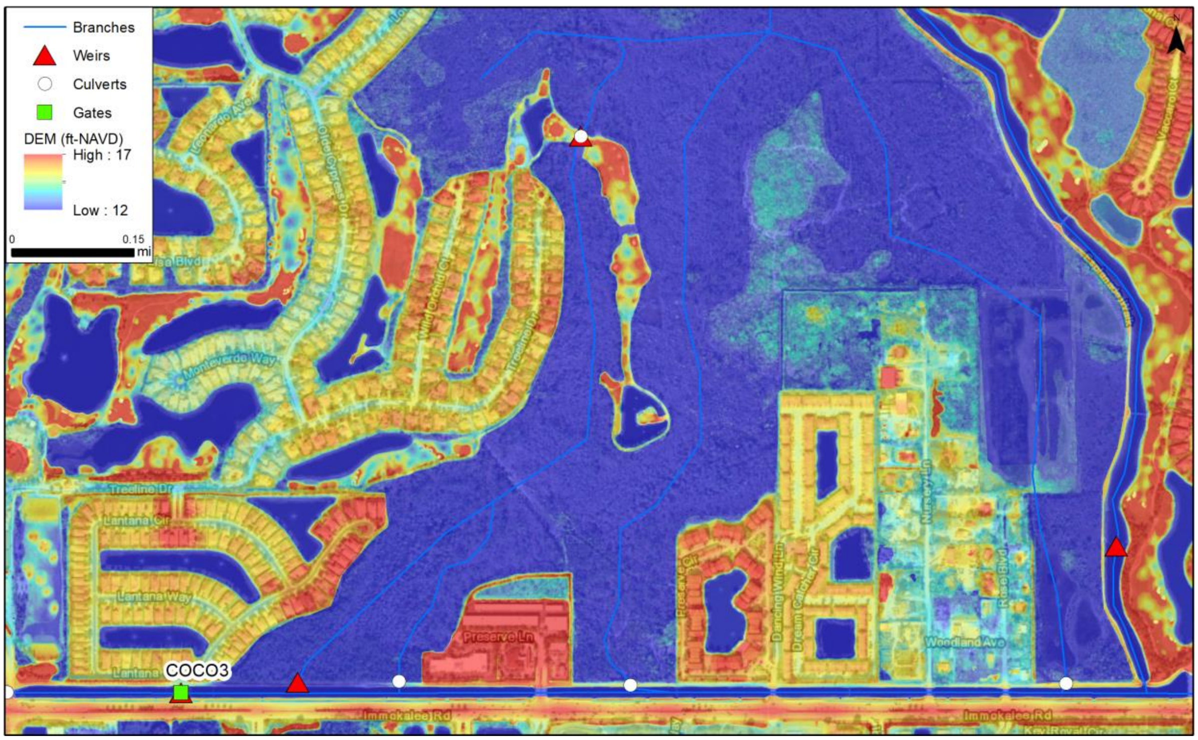

Figure 6-3. Southern Corkscrew Connections to COCO3

Figure 6-4 shows the bridges and culverts along Immokalee Road. Some of these were previously in the BCB UM and some were added or adjusted for locations and sizes.

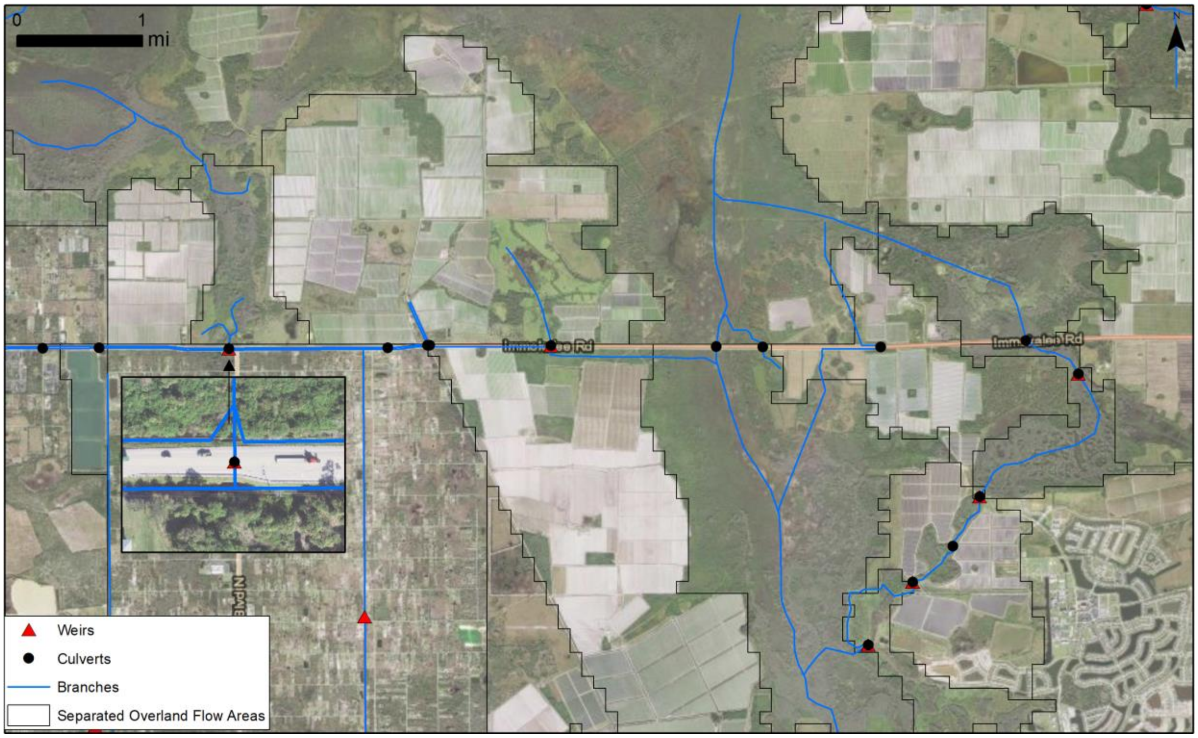

Figure 6-4. Immokalee Road Crossings Eastern Corkscrew and Camp Keis Strand

6.2 Corkscrew Flow Constrictions

Another potential cause of changes in hydroperiod could be due to constrictions to the natural wetland sheet flow, such as roads and berms, that may prevent or limit hydration of areas that were previously better hydrated via upstream flows. Thus, it is important that the modeling tool represents these constrictions in order to assess the potential benefits of their removal. The figures below show areas in the model that were refined by adding blockages to the overland flow component (i.e., Separated Flow Areas (SFA)) and connections through the blockages via culverts and weirs in the 1D surface water component.

Figure 6-5 shows constrictions added to represents the roads along the Immokalee Slough east of Lake Trafford. The data for the crossings was obtained from the Immokalee Regional Water Plan study (Florida Silver Jackets Team, 2023) and the Collier County stormwater database (Collier County Stormwater Management Facilities).

Figure 6-6 shows the constrictions and connections added to represent the Washout Road. Data for the crossings were obtained from Audubon's consultant, Roger Copp (WSA), based on conducted site visits. The flow blockage by the Fish Farm was also represented by a combination of an SFA, canals and structures. The perimeter canals were added to account for potential seepage from the surrounding wetlands to the lower perimeter canal elevations and a storage branch was added to represent the storage of the fish ponds. If the Fish Farm storage is exceed, the berm can be overtopped via weirs that flow into the surrounding wetland areas.

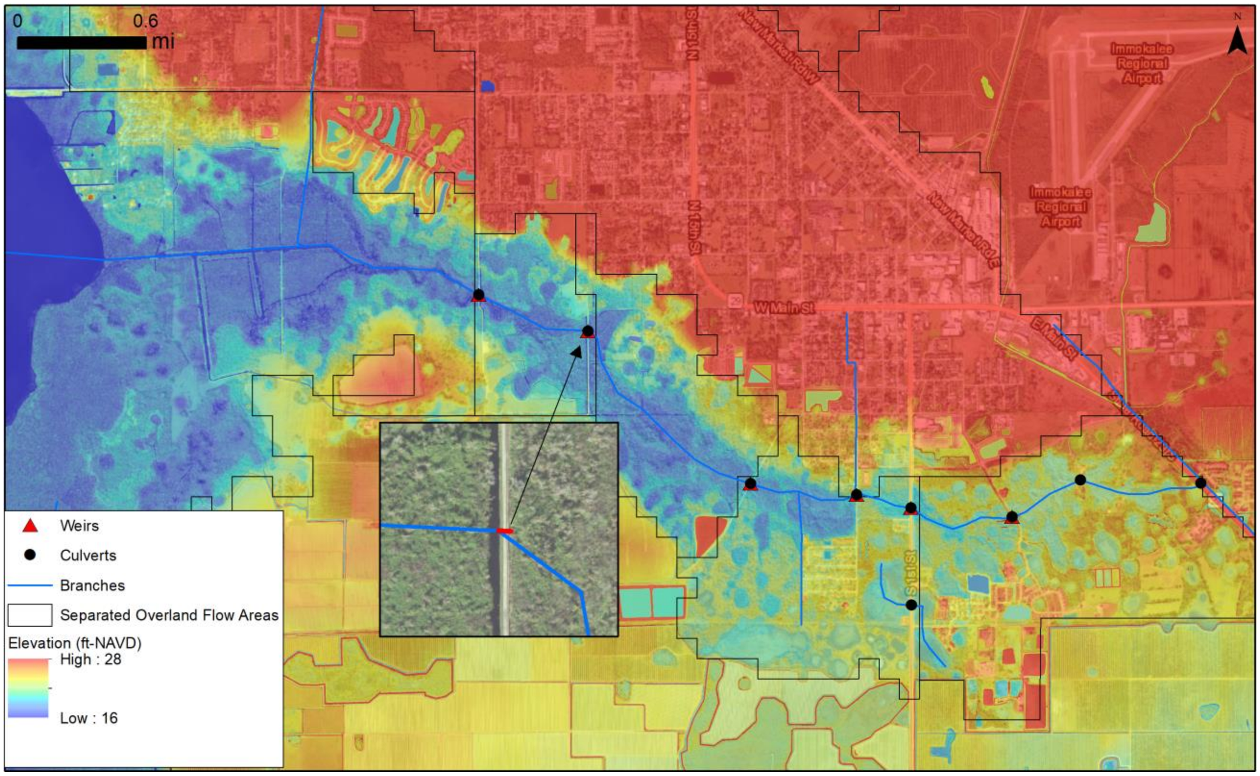

Figure 6-5. Constrictions along Immokalee Slough, East of Lake Trafford

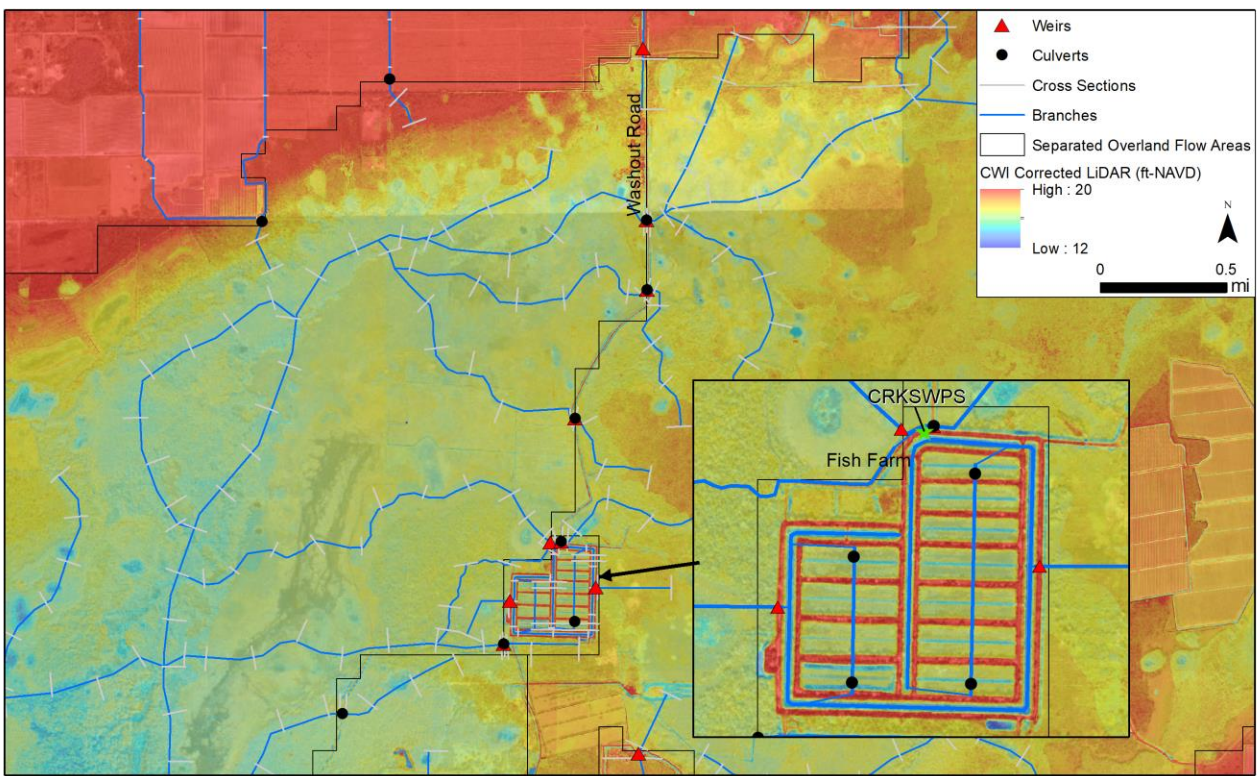

Figure 6-6. Constrictions along Washout Road and Fish Farm

Figure 6-7 shows the constrictions and connections that were refined along the Bird Rookery Trails. Data for these connections was obtained from SFWMD staff and a site visit conducted in August 2024.

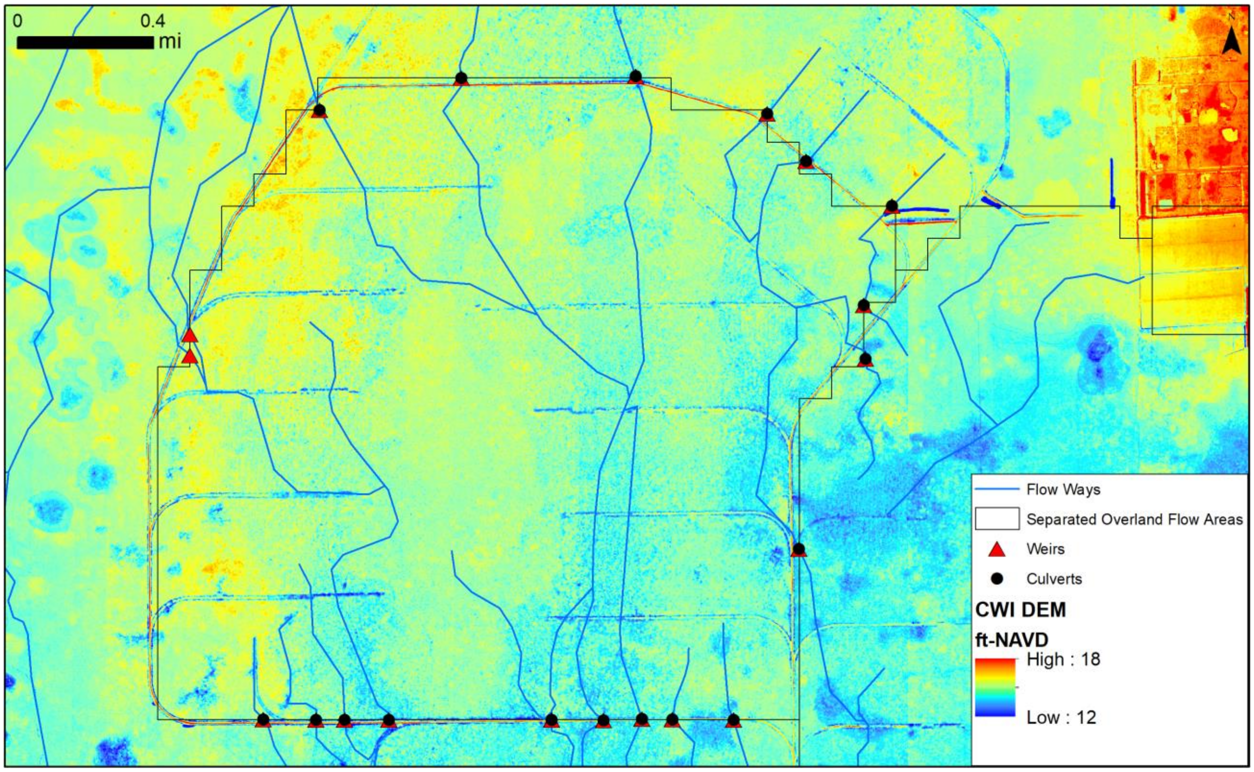

Figure 6-7. Constrictions along the Bird Rookery Trails

6.3 Other Hydraulic Network Revisions

In addition to the hydraulic network revisions described above, general overall checks on the hydraulic network were conducted. These included corrections in channel connections, structure geometries, adjustment of cross sections distances for numerical stability, and redefinition of cross sections based on survey and LiDAR. It was also found that there were several culverts in the model at locations where there are bridges along the Corkscrew and Cocohatchee Canals. The culverts in the BCB UM seem to overestimate the constriction thus producing a higher head loss than expected from a bridge opening (i.e., relatively small openings and higher inverts than the bottom of the cross section) (Figure 6-8). These culverts were modified in the CWI RM to represent the narrowing of the bridge with a larger opening than the previous culverts.

In addition, survey and culvert information provided by the BCB staff along the Shady Hollow Boulevard and Corkscrew Canal were used to adjust cross sections and add the structures to the CWI RM.

Finally, as discussed below in Section 7.0, several outfalls connecting residential and agricultural basins were added to account for discharges to Corkscrew or downstream canals (e.g., Cocohatchee Canal) when control elevations in the basins are exceeded. Cross sections representing the basin storage were also added to selected basins.

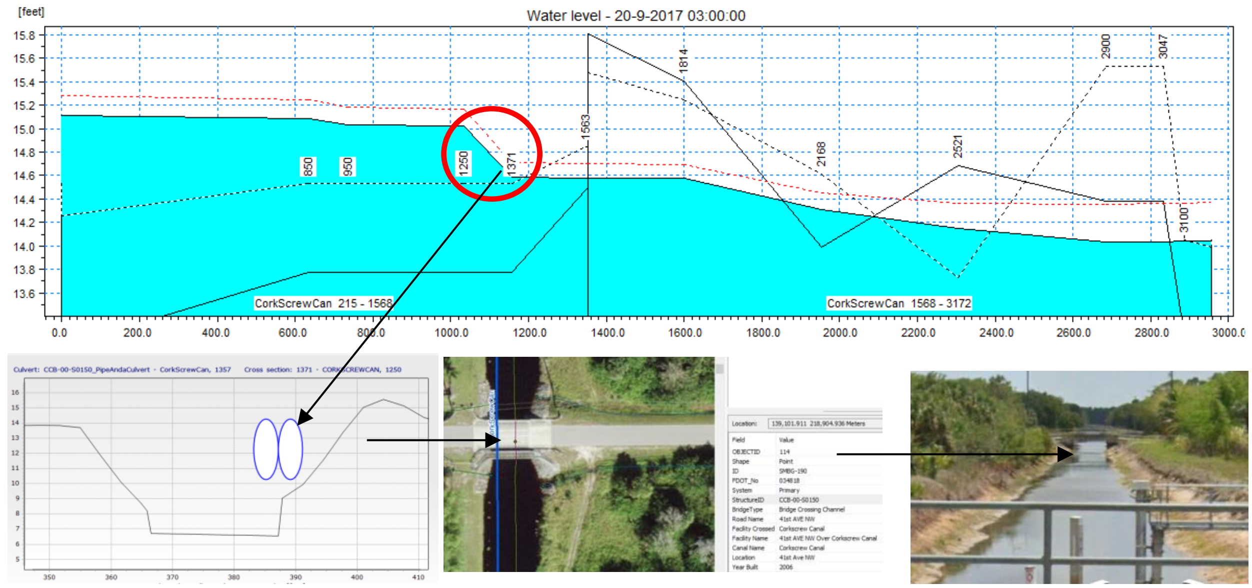

Figure 6-8. Head losses caused by small culverts in the BCB UM that is not evident in the data or images

7.0 Corkscrew-Adjacent Basin Drainage

Numerous ERP documents were reviewed to determine the basin outfalls and connections for urban and agricultural basins adjacent to the Corkscrew wetland areas or to other canals in the drainage system in the project area. Outlet structures and storage and routing features were added to better account for how water is routed from these basins.

Urban drainage includes residential, commercial, and transportation land uses and it is conceptualized in the Ponded Drainage (PD) module. This module is part of the overland flow component and has the purpose of routing impervious stormwater flow to a specified destination. Thus, it is a conceptual method to represent the stormwater pipes that are not included in the surface water model. Agricultural drainage is specified in the groundwater Saturated Zone (SZ) component in MIKE SHE because it is conceptualized as ditches or shallow swales that intercept the water table below the ground surface to drain the soils to optimal crop growth conditions. Thus, while the inner water management systems are excluded from the model, basin water budgets are approximated via physical based process at the cell level (ET, seepage, irrigation, impervious and pervious flow, etc.), storage and discharge control.

For both stormwater (ponded) drainage and agricultural (water table) drainage, the conceptualization in MIKE SHE for a regional model such as the BCB model typically includes the processes, components and model parameters described below. Application of the complete detailed process is time consuming, not only because it requires investigation of many ERP documents to find the information that is applicable to the time period that the model represents, but also because it involves several model components that must be carefully overlayed and synchronized. Thus, it was applied to selected basins in the project area.

1. **Representation of storage and outfalls in MIKE HYDRO**
    a. Basin storage features can be represented either explicitly with wide cross sections along the length of the storage water bodies (e.g., Above Ground Impoundments (AGIs) or wet

detention ponds) or via a conceptual "storage node" that lumps the basin storage in one or more cross sections. For this latter option, the Additional Storage area in the processed data tab of the cross section menu can be used to include the total storage area of the basin.

b. Outfall structures are represented with culverts and/or weirs with inverts and sizes that approximate the control elevations discharge capacities of the actual basin outfall structures.

2. **Representation of basin area, drainage fraction, routing and discharge rate via drain codes, runoff coefficients, drain levels and time constants and separated flow areas in MIKE SHE**

    a. Drain codes are an integer code maps of the basins. The basins can be drawn to include the receiving water body in MIKE HYDRO to which MIKE SHE would directly route the drainage to or can be specified to discharge into a specific location(s) in the MIKE HYDRO network inside or outside the basin. The option depends on the level of detail that is used to represent the basin the routing. For example, if storage features are included, the routing can be specified to those storage features (i.e., lake cross sections or storage nodes) upstream of the discharge structure.

    b. Runoff coefficients are part of the PD module only and define the fraction of ponded water that is routed via the drainage component. Conceptually, it represents the directly connected impervious areas. These fraction were recalculated for the project area basins from those in the BCB UM by establishing a relationship between land use type and impervious fractions conducting detailed analysis in sample cells.

    c. Drain levels and time constants are model parameters that control the threshold depth of drainage flow and rate, respectively. Time constants can be a function or the density or capacities of the stormwater pipes or farm ditches. Drain level in the overland PD module is typically set to the ground elevation and in the target farm water table SZ module. These parameters act in a similar way in the PD and SZ components.

    d. Separated Flow Areas (SFAs) can also be added along the basin boundary to represent the berms that typically surround residential subdivisions and farm basins.

3. **Connection of the outfall with the receiving downstream canal network or via sheet flow**

    If the outfall structure directly connects to a receiving canal in the model a direct link is added. However, in many cases in the CWI project area, the adjacent basins discharge to the Corkscrew wetland via sheet flow. This connection can be made either directly connecting the outfall branch to Corkscrew flow way in MIKE HYDRO or via a flood code specified at the downstream of the outfall structure. This allows the water from an unconnected branch (i.e., the 1D element in MIKE HYDRO) that exceeds the storage of the downstream cross section(s) to flood into the overland flow surface. The outfall branch is also linked to and can be routed via the groundwater component, depending tailwater stage in relation to the water table elevation. MIKE SHE Couplings, which are the sections of the branches that are linked to MIKE SHE, are specified in MIKE HYDRO such that the portions of the outfall branch downstream of the structure are connected to the flood code that communicates with the receiving wetland.

4. **Representation of the storage water bodies interactions with MIKE SHE processes**

Even when the basin storage is lumped in a MIKE HYDRO cross section, flood codes in MIKE SHE can be specified for cells where the storage water bodies are located so that MIKE SHE processes, i.e., drainage, infiltration, seepage, rainfall and ET, are applied and communicated back to MIKE HYDRO. MIKE HYDRO controls how this volume of storage is routed downstream via the outfall structure(s) when the control elevation is exceeded. Note that it is important how these MIKE SHE processes are overlayed or layered in the model on a cell by cell basis, e.g., distinguishing between the drainage cells and the storage cells that receive the drain flow in a basin. Selections of the cells based on land use (e.g., houses versus lakes) are conducted and irrigation, drainage, flood code maps all defined with the same grid definition (origin and cell size) are set up based on these precise cell selections to avoid circulation of drainage and ensure that the conceptualization correctly implemented.

Figure 7-1 and Figure 7-2 show maps of the residential/mining and agricultural basins, respectively, in the project area. Individual permits were reviewed in selected areas to refine the representation of residential/mining and agricultural basins. The selected areas were prioritized by proximity to Corkscrew and available information in the District's ERP website. Drainage for the basins permits were not reviewed due to schedule limitations, are parameterized as the BCB UM.

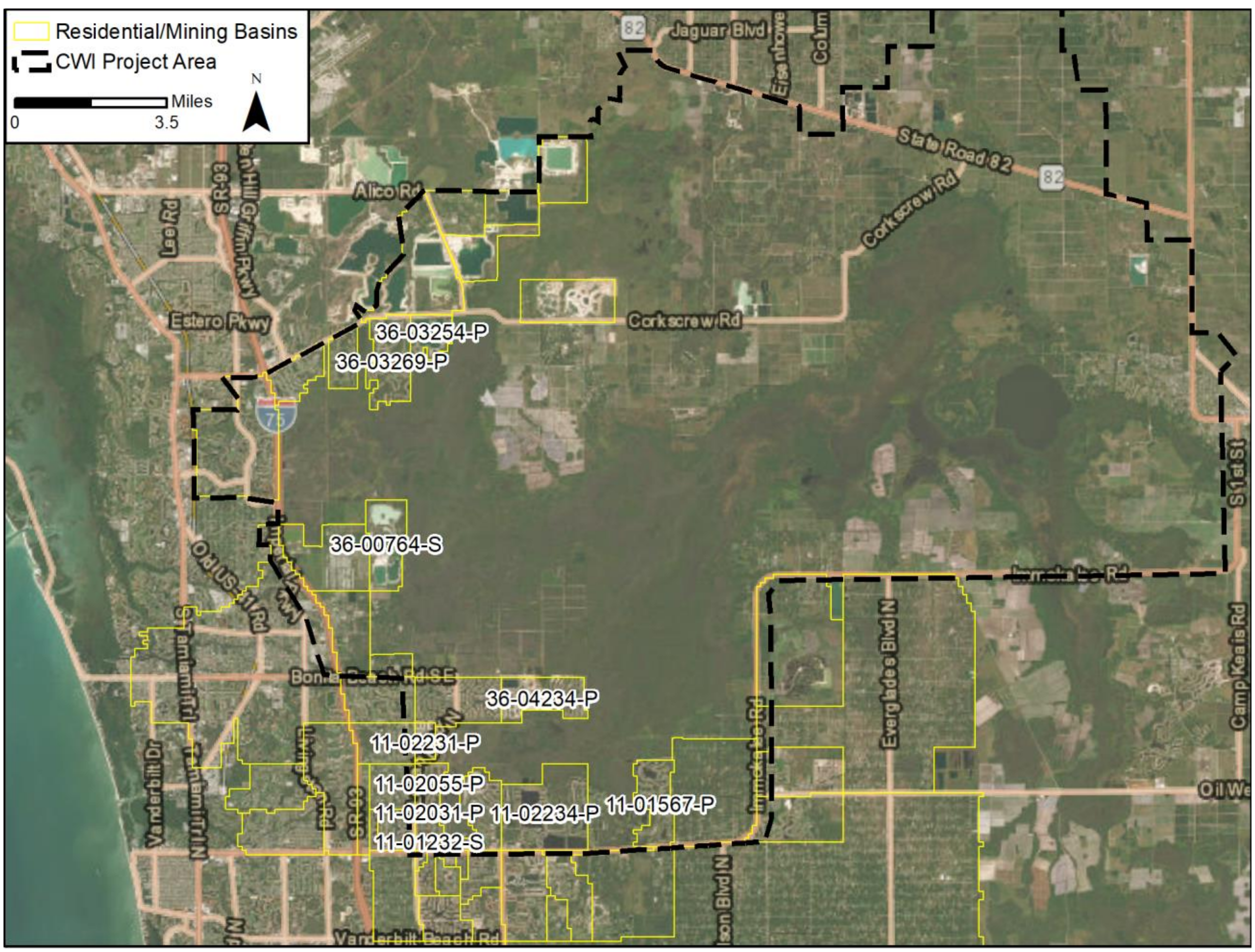

Figure 7-1. Map of Residential/Mining Drainage Basins in the Project Area

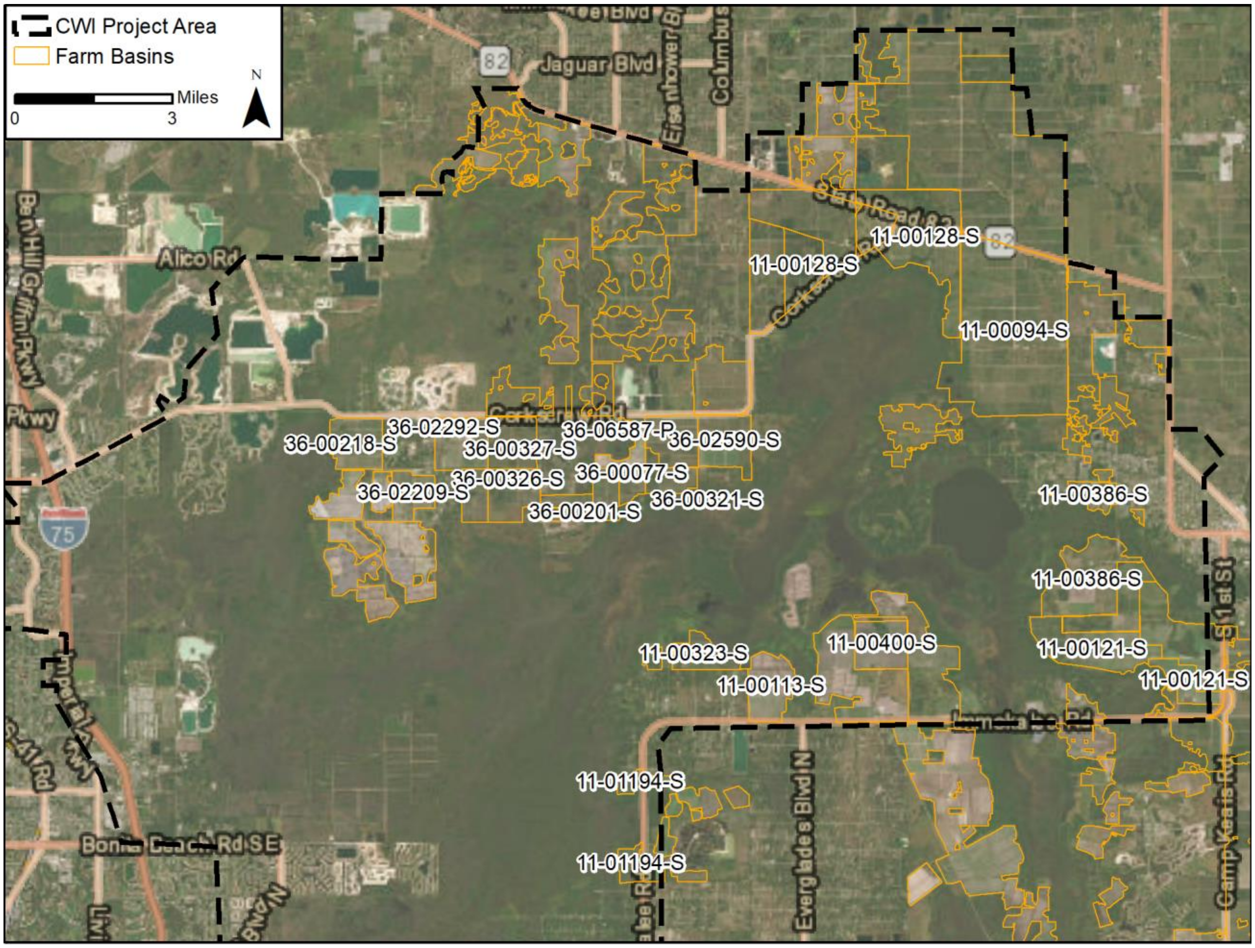

Figure 7-2. Agricultural Drainage Basins in the Project Area

8.0 Revision of Hydrogeological Layers

The BCB UM groundwater model was developed using the Lower West Coast MODFLOW (LWCSIM) model layers and parameters (Bandara et al., 2020), which had been recently updated when the BCB model update effort began. During the BCB UM calibration, the initial hydraulic conductivities that were extracted from the MODFLOW model were adjusted. During the CWI RM optimization, a closer look at layer elevations in areas of interest showed some inconsistencies with borehole data and other Corkscrew models. This in part could be due to the minimum layer thickness used for the LWCSIM model was set to 30 feet and it used the conductivities of the aquifers below a given layer if aquifers are absent. Thus, when the conductivity are adjusted globally it may change the definition of the absent or thin layer. Moreover, recently updated hydrostratigraphic layer SAS and IAS surfaces for the LWC Planning Area were provided by District staff and documented in Zumbro et al. (2023). The hydrostratigraphic surfaces update effort consisted of reviewing the data used for the surfaces developed by Geddes et al. (2015), making adjustments based on the review and incorporating new sources of information. Conductivities were also interpolated from aquifer performance test (APT) sources. These updated layer elevations were input to the CWI RM, as well as the conductivity map for the Lower Tamiami Aquifer and uniform value for the

Tamiami Confining Unit. The impact of this change on the calibration results was analyzed and in most locations, the impact on the calibration was minimal. However, there are some exceptions where either the observed data was better matched than previously or the simulated heads deviate further from the observed data. Given this mixed response, it is recommended that latest surfaces in Zumbro et al. (2023) are used because future calibration efforts can be conducted starting with this updated layering.

9.0 Review of Water Use Abstractions (Groundwater Pumping)

As demonstrated by a sensitivity analysis of a test area (Section 11.3), accurate simulation of groundwater heads in aquifer sources may be sensitive to the input pumping volumes. In both the BCB UM and the CWI RM, the simulated groundwater heads in lower aquifer layers (LTA and SA) are high in some of the monitoring well locations compared to observed data. The performance measures to be used for project evaluations will include potential impacts on water use. If the model underestimates pumping and overestimates groundwater heads, the potential impacts of projects on water use sources may be underestimated.

The pumping volumes in the model are input based on the monthly frequency volumes in the District's water use database. These data are not directly measured by SFWMD, but instead rely on the reported pumping volumes by the permitted users. Moreover, the database excludes smaller users that do not report pumping volumes. Figure 9-1 shows the SFWMD's Water Use Permitting Facilities locations where the aquifer sources are either the water table, Lower Tamiami, or Sandstone aquifers near one of the CWI areas of interest, Lettuce Lake (CorkB well). Those shown with black Xs are not in the withdrawal database.

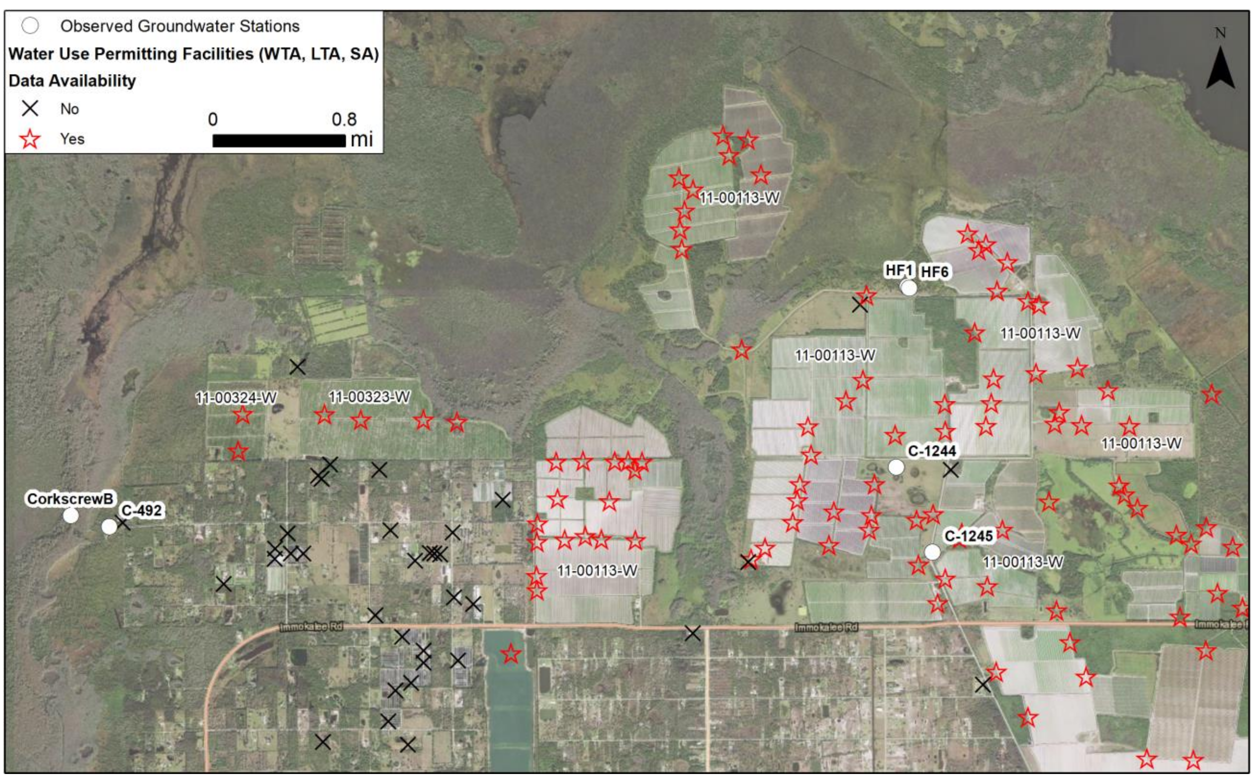

Figure 9-1. Water Use Permitting Facilities Near Central Corkscrew

Select checks on the reported water use for the permits shown in Figure 9-1 were conducted which illustrate differences between volumes of withdrawals in the SFWMD water use database and the amount estimated that a crop needs based on water deficit during the dry season. Table 9-1, Table 9-2, and Table 9-3 shows the total annual reported water use for permits 11-00113-W (i.e., the largest permit reviewed - 2,823 irrigated acres), 11-00323-W (179 irrigated acres), 11-00324-W (103 irrigated acres), respectively, versus estimated requirements based on the simulated net rainfall. The last columns on the tables show the fraction of the reported volume of the estimated requirement, i.e., higher than one if reported is higher than estimated demand and lower than one if reported is lower than estimated demand. The smaller farms show a higher withdrawal than the estimated crop demand, which is the expected outcome due to losses or inefficiencies in the pumping/irrigation system. For example, permit 11-00324-W water use calculations include a 50% efficiency. The larger farm permit, however, reported a much lower volume compared to the estimated crop demand in three out of the four years. Since the larger the area is expected to have relatively higher losses in the system, then there is a disconnect between the anticipated water use and the actual or reported water use. This could be due to changes in crop rotations, unaccounted supply from other sources, or errors in the database.

Table 9-1. Total Annual Reported versus Estimated Requirement for Water Use Permit 11-00113-W

Year	Annual Reported Extraction (MG)	Estimated Requirement (MG)	Reported Fraction of Estimate
2017	1,052	1,026	1.0
2018	769	1,129	0.7
2019	480	1,006	0.5
2020	47	851	0.1

Table 9-2. Total Annual Reported versus Estimated Requirement for Water Use Permit 11-00323-W

Year	Annual Reported Extraction (MG)	Estimated Requirement (MG)	Reported Fraction of Estimate
2017	75	53	1.4
2018	71	49	1.4
2019	47	57	0.8
2020	54	47	1.1

Table 9-3. Total Annual Reported versus Estimated Requirement for Water Use Permit 11-00324-W

Year	Annual Reported Extraction (MG)	Estimated Requirement (MG)	Reported Fraction of Estimate
2017	44	33	1.3
2018	45	40	1.1
2019	28	37	0.7
2020	34	27	1.2

A few sensitivity runs were conducted to test the effect of increasing water use in the farms near Corkscrew in the vicinity of the CorkB/Lettuce Lake area. Pumping increases and effect of increasing and decreasing conductivities with pumping changes were tested. The pumping volumes from the wells associated with the permits above were increased from the reported use by the estimated crop requirements, which is based on the average annual supplemental crop requirements found in the water use permits for those users. In addition, wells that are not in the water use database shown in Figure 9-1 were added with estimated water use requirements. Three simulations were run with the same increased pumping volume but with three conductivity values for the LTA: 1. the baseline or calibrated value (LTA_K_base), 2a. LTA_K_base x 10, and 2b. LTA_K_base x 0.1. Figure 9-2 shows the change in average water table (i.e., layer 1 heads) during a dry period of two weeks in May 2017. The image on the top left shows pumping only effect is contained near the farm fields without much spreading into Corkscrew. The image on the top right shows that increasing conductivity by a factor of 10 removes the effect of pumping in the water table and leads to higher heads. The image on the bottom left shows that decreasing the conductivity by a factor of 10 increases the effect of higher pumping and spreads the drawdown.

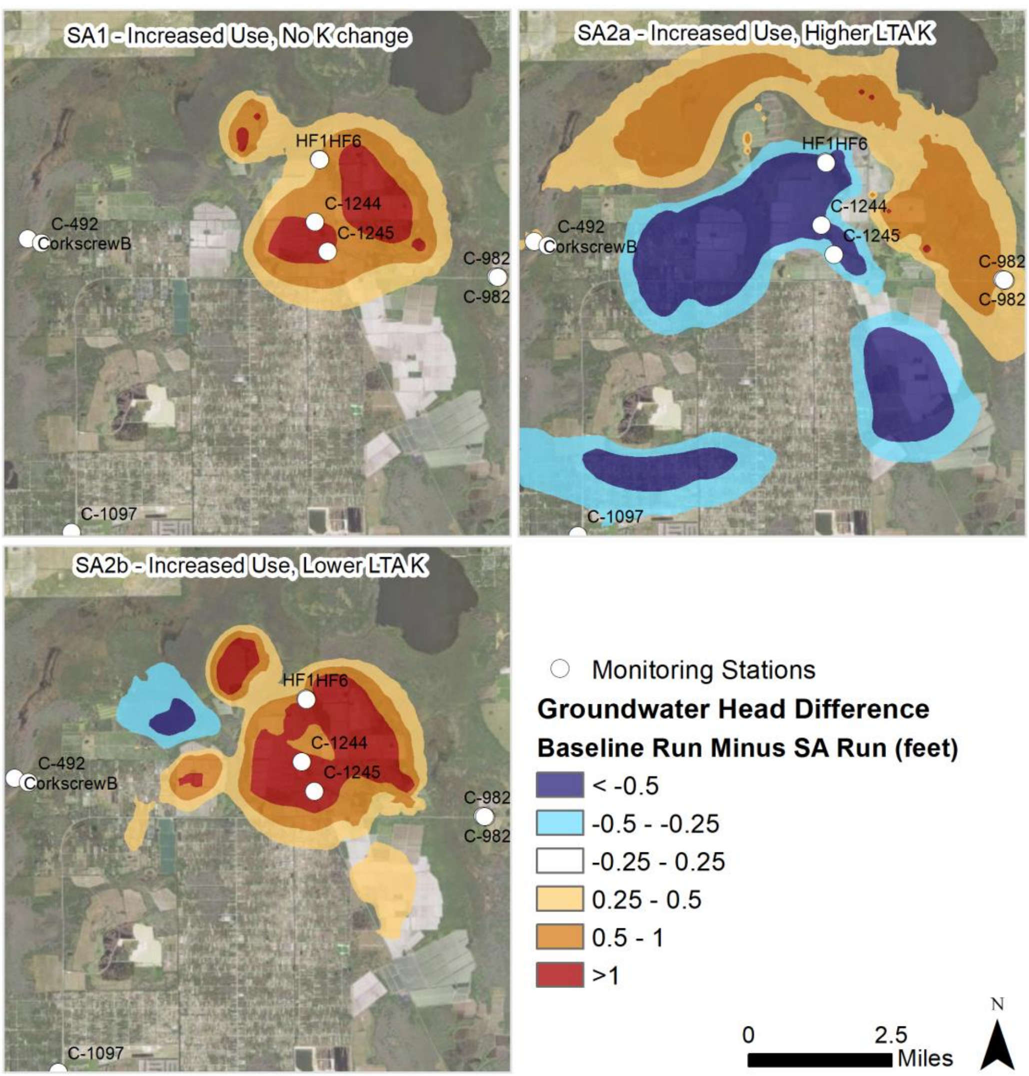

Figure 9-2. Sensitivity Test Runs on the Effect of Groundwater Heads

Further investigation beyond the CWI scope of work is recommended for potential inaccuracies of the pumping volumes, as well as additional calibration of the lower layers to improve the model performance for the lower aquifer layers. However, a way to work around this issue for the current effort and provide a meaningful estimate of project impacts on water use is to evaluate them in the context of this uncertainty, by performing sensitivity analyses on the project results. The effect of the pumping on the groundwater levels is impacted by hydraulic conductivities. Thus, it is important to include both parameters in the sensitivity analysis.

9.1 Domestic Self-Supply (DSS) Wells

Domestic Self-Supply (DSS) wells are typically for residential use in areas that don't have access to a public water supply system (SFWMD, 2025). DSS residential users withdraw less than 0.1 MGD per day and are not required to report their use (SFWMD, 2025). Therefore, pumping volume at each well was estimated using DSS demand and DSS population estimates provided in the Lower West Coast Water Supply Plan (SFWMD, 2022).

Table 9-4. Estimated pumping at each DSS well.

County[1]	DSS 2020 Population[2]	Demand under Average Rainfall Conditions (MGD)[3]	Per capita (gpd)[4]	Per DSS well (gpd)[5]
Collier	72,817	12.09	166	498
Lee	105,379	10.64	101	303

[1]No wells within the model domain were located within Hendry County. [2]DSS Population extracted from Table 2-2: Permanent Resident Population Served By PS and DSS in the LWC Planning Area in 2020 and 2045 Table from SFWMD, 2022. [3]Demand under Average Rainfall Conditions from Table A-8: DSS gross (raw) water demands under average rainfall conditions in the LWC Planning Area from SFWMD, 2022. [4]Per capita demand equals DSS 2020 demand divided by population under average rainfall conditions. [5]Assume 3-person household on average (per DSS well demand equals 3 times per capita demand), based on the LWCSIM's approach for DSS demand estimates (Bandara et al., 2020).

A shapefile of DSS well locations, obtained from the Lower West Coast Model during the BCB UM effort, includes 6,276 DSS wells within the model domain as shown in Figure 9-3.

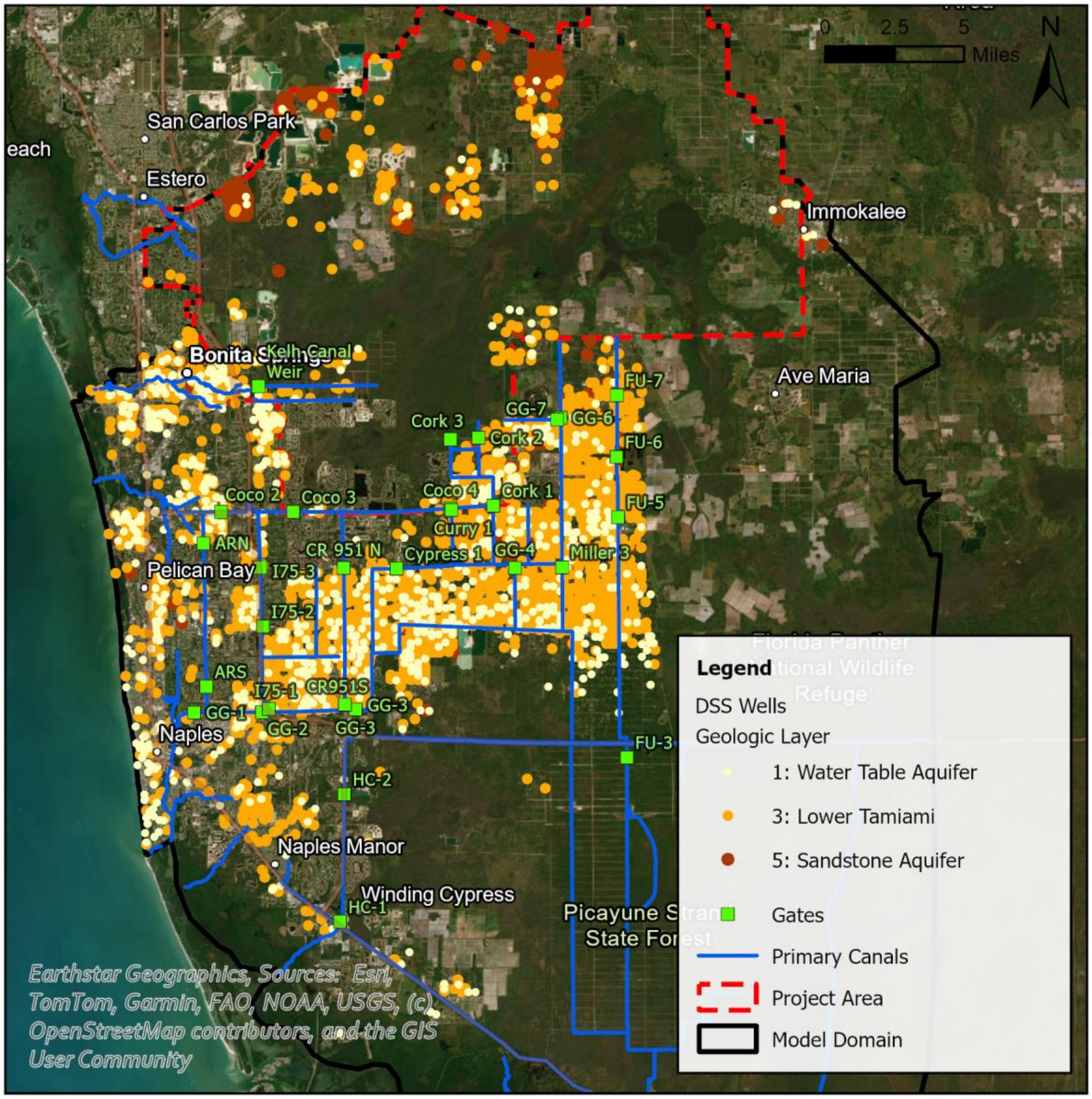

Figure 9-3. Domestic Self-Supply Wells within CWI Model Domain

Due to the high number of wells and the relatively low flow at each well, the wells were aggregated by geologic layer into a 2000 ft grid into 1,804 wells. Figure 9-4 shows a zoomed in area near the Golden Gate Estates. All the DSS wells (yellow, orange, and red circles) within the 2000 ft grid (green grid) were aggregated into 2000 ft point locations (blue squares) by geologic layer and the pumping volume for each DSS well was lumped (volumes for all DSS wells in the 2000 ft grid were added together by layer) into the blue point locations.

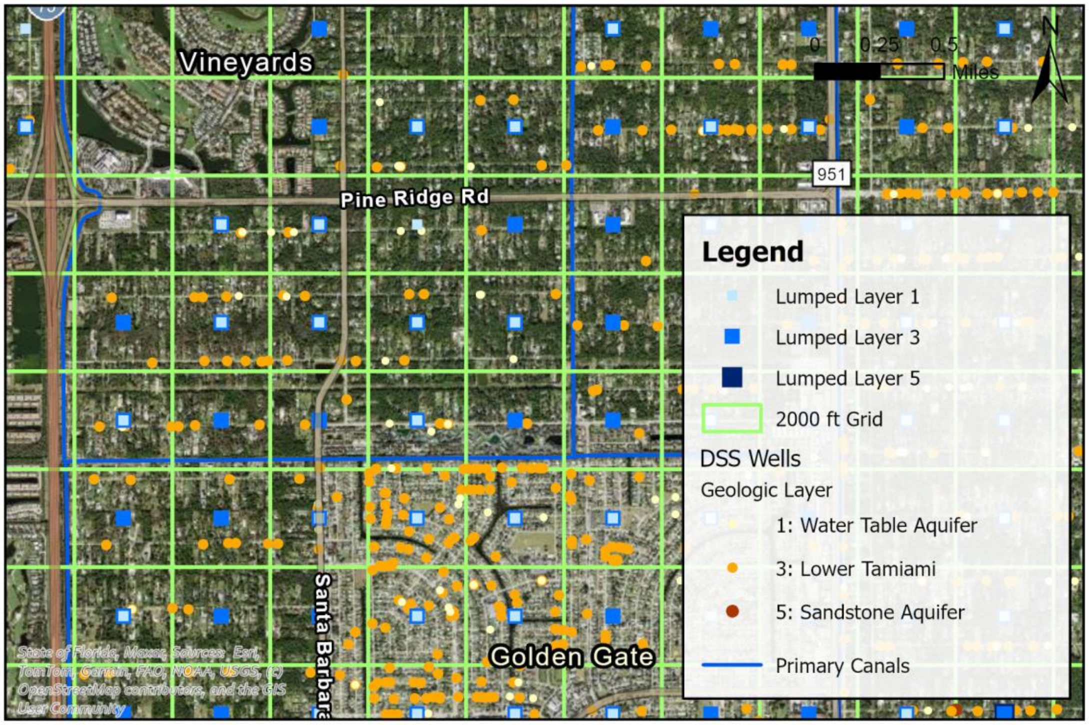

Figure 9-4. Example Area near the Golden Gate Estates to show how Domestic Self-Supply wells were aggregated into a 2000 ft grid

10.0 Revision of Boundary and Initial Conditions

10.1 Groundwater Boundary Conditions

During the calibration checks and optimization process, it was found that the specified boundary conditions in the initial model had a significant impact on some of the calibration results, even at some of the interior well locations. Thus, the BCB UM groundwater boundary conditions for all five layers were modified in the CWI RM. Since there are relatively lower head losses in the top three layers (WTA, TC, and LTA), the same boundary conditions were specified for these three layers based on the nearest observed wells or the tidal stages along the coastal boundary. The stations and the horizontal extent along the boundaries were modified from the ones used for the BCB UM. The Lee County monitoring station data on the northwest boundary was horizontally interpolated at a daily frequency using a distance weighted method. For the rest of the non-coastal boundary, the nearest DBHYDRO station was used.

For the Upper Hawthorn confining unit (layer 4), since permeabilities are very low, a zero-flow boundary was specified. For the Sandstone aquifer (layer 5), since the observed heads are substantially lower than the top layers and the observed data is not as abundant as for the surficial aquifer, a spatial interpolation and time extrapolation of the LWCSIM model results and observed data was used. The simulation period of the LWCSIM model is 1999 - 2014 and the frequency of the output is 30 days. The average monthly differences between each of the LWCSIM model cells and the nearest observation gage location were calculated. These differences were then used to interpolate the daily measurements available for each monitoring well to each of the LWCSIM model cell for the calibration period.

10.2 Groundwater Initial Conditions

The BCB UM initial conditions caused inaccuracies in some of the calibration wells during initial simulation months and were modified for the top two layers based on the observed data interpolation from January 2017. The simulation period was later changed to start in June of 2016 to allow for a six month warm up period. Since the model reaches dynamic equilibrium faster during the summer months and the levels at beginning of June are similar to January in several stations, the static initial condition files were not further revised with the change in the simulation start date.

11.0 Focus Model Areas for CWI, Optimization, and Results

11.1 Project Focus Areas

Three key focus areas for the CWI project evaluation and PM assessment are the Flint Pen/Imperial River Basin in Lee County, Corkscrew West (west of Washout Rd/Lettuce Lake area) and the Corkscrew Canal North/Cocohatchee Basins. Hydrological issues that these areas are facing and that will be evaluated under the CWI project are the following:

- The Flint Pen/Imperial River Basin includes the city of Bonita Springs, which has been experiencing severe flooding issues. Lee County is considering proposed projects to control and retain more water in Corkscrew that may help with both ecosystem restoration and flood control (AIM Engineering, 2020).
- The Corkscrew West basin is experiencing drier conditions during dry months and shorter hydroperiods (Clem and Duever, 2019). Clem and Cornell (2021) investigated potential causes including groundwater withdrawals, increased ET due to introduction of invasive species, and downstream drainage.
- The Corkscrew Canal/Cocohatchee Canals receive discharges from western Corkscrew and may be contributing to its over drainage. Flooding issues have also been significant in these basins. While structure operational changes have been made in recent years to optimize dry season stages in Corkscrew, there are other structural changes that may be considered. For example, uncontrolled flows and other infrastructure improvements.

Efforts to improve the representation in West Corkscrew and Corkscrew/Cocohatchee Basins where mostly spent in adding hydraulic details, structure operations and network representation improvements, as discussed in in the previous sections. While parameter adjustments were conducted for these basins with the purposes of improving the calibration, a larger effort was spent in Flint Pen basin because the flows in the Imperial basin were much lower than observed during the initial simulations. Note that further calibration improvement beyond the scope of work for the effort documented herein is recommended to address remaining issues, as discussed in Section 12.0.

11.2 Surface Water and Groundwater Optimization

While the scope of work for the CWI project did not include a recalibration of the BCB model, it was considered important to spend some effort to try to improve the underprediction of flow in the Imperial River Basin, which was a critical limitation of the BCB UM for CWI purposes. In addition to model parameter adjustments, the hydraulic network representation was also refined. Cross sections in the Kehl Canal, Imperial River, and tributaries were redefined based on survey data and the LiDAR. The weir structure in Kehl Canal was modified, canal connections with other minor structures were adjusted, flow ways were redefined multiple times and connections were adjusted to reduce mass balance instabilities and ensure that routing of flow from the contributing portions of West Corkscrew were incorporated.

An underlying issue in the inability of the model to reproduce the measured flow hydrograph in the Imperial River was that simulated groundwater levels, particularly in the wet season were too low. Since groundwater storage was overestimated, ponded water remaining after ET is extracted in the model will recharge the aquifer during a prolonged portion of the summer and thus, not enough water would reach flow ways of which a large fraction would be lost to the aquifer system. Thus, for the CWI RM, an optimization of the simulated groundwater levels was necessary to improve the prediction of flow in the Imperial River.

11.2.1 Measured Data Analyses

The groundwater monitoring stations in the Flint Pen/Imperial River Basin area with available data for the calibration period are shown in Figure 11-1.

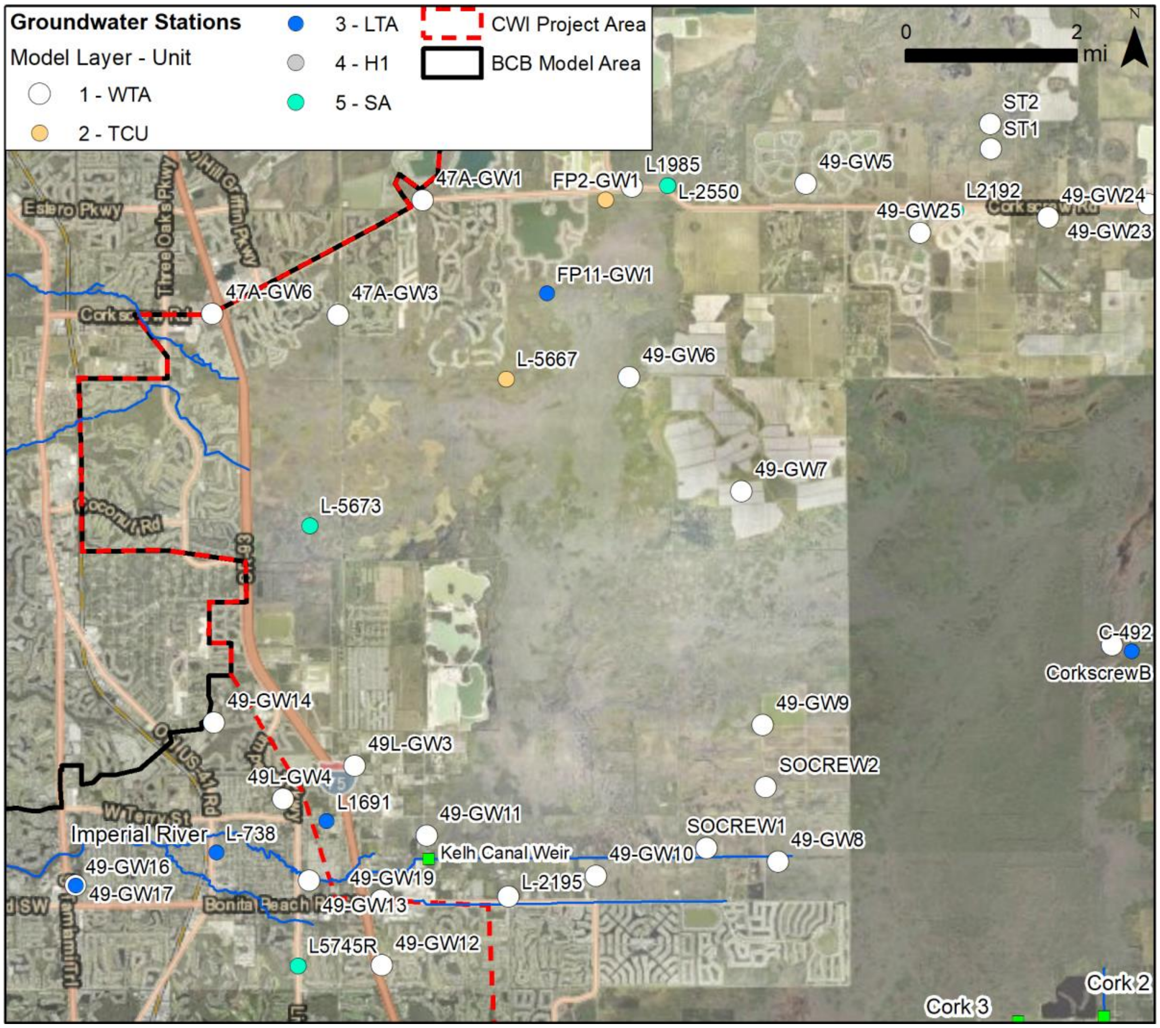

Figure 11-1. Groundwater Monitoring Stations with Available Data for the Calibration Period, Flint Pen Area

Analysis of the measured data in Flint Pen/Imperial River Basin revealed the following:

1) The water table is above the surface during most of the summer months and in some locations up to the end of the year (Figure 11-2).

2) There is an evident vertical layer separation (head losses) between the water table aquifer and the Lower Tamiami Aquifer wells indicating the presence of resistive fine materials that impede vertical flow and thus maintain heads relatively high in the water table aquifer (Figure 11-3).

3) The Imperial River measured flow hydrograph shows delayed peaks, long recessions after rainfall peaks and a continuing source of baseflow that increases over the summer months (Figure 11-4), indicating that the contributing flow is released slowly, which is characteristic of an undeveloped basin, such as Flint Pen.

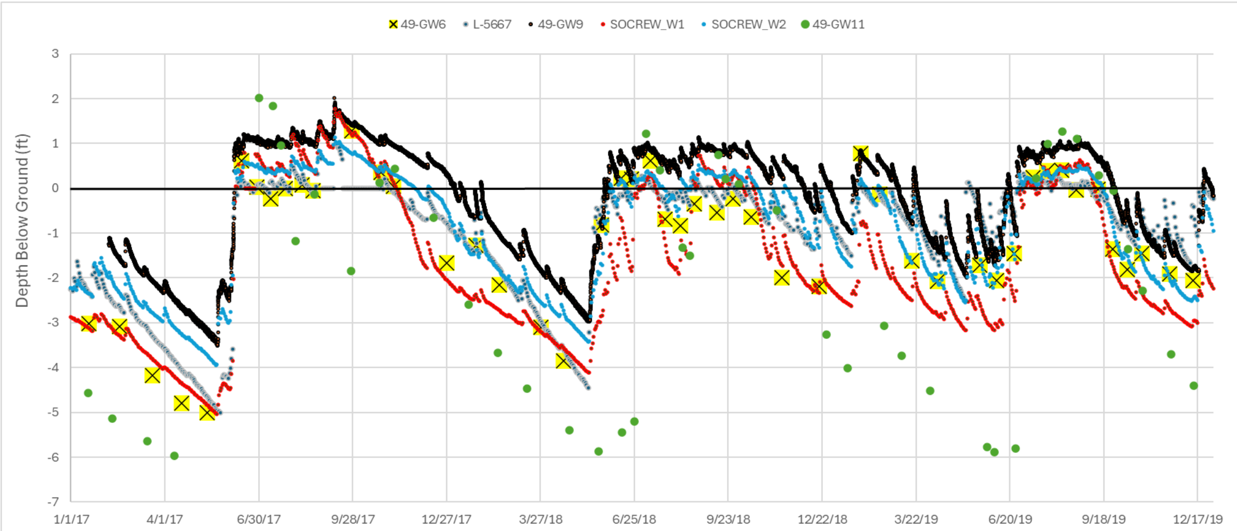

Figure 11-2. Water Table Depths in Flint Pen

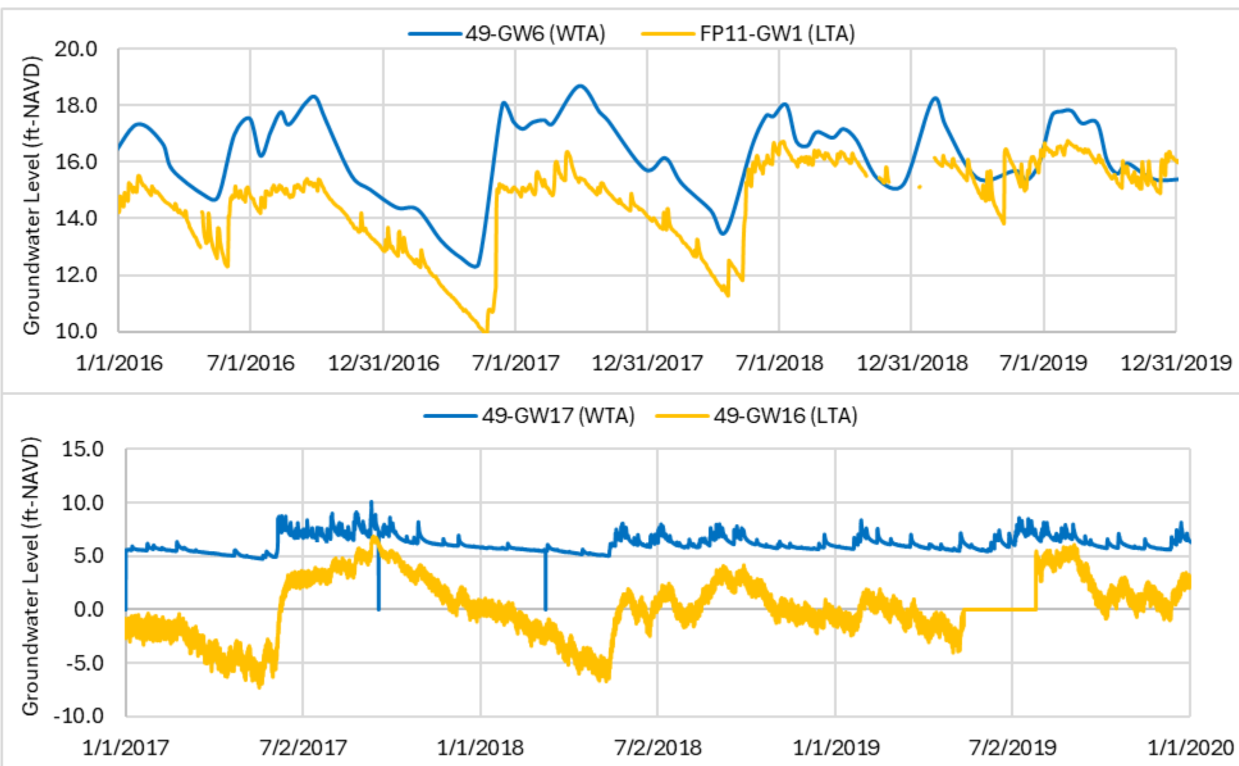

Figure 11-3.Head Differences Between WTA and LTA Monitoring Wells

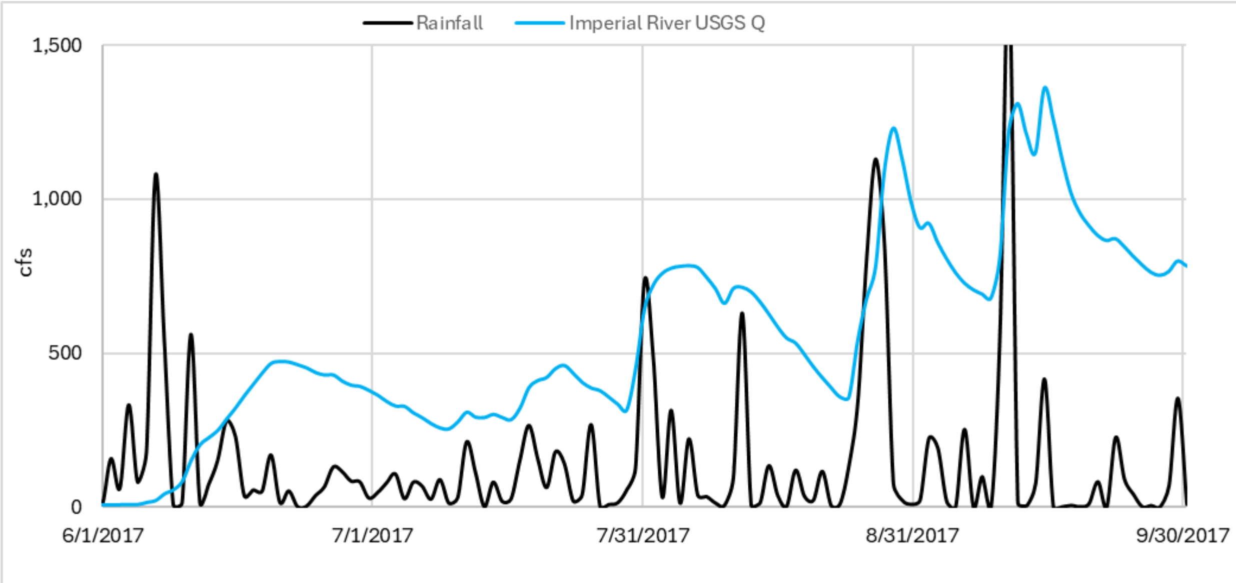

Figure 11-4. Imperial River Flow Hydrograph and Rainfall Volume Rate

11.2.2 Parameter Adjustments

For the groundwater level and flow optimization process, many model parameters were tested and adjusted for most of the model components, including parameters for overland flow, ponded drainage, unsaturated and saturated zone, ET, and MIKE HYDRO. In addition, removal of model components were tested, for example, testing the effect of pumping versus no pumping, removal of flow ways, removal or lower layers, and removal of the entire groundwater component. This latter test served to illustrate the key role of the groundwater component in the Imperial River flow hydrograph; i.e., without groundwater storage, flow is rapidly released after the large rainfall event at the beginning of June 2017, leading to higher than measured flow volumes at the beginning of the summer and rapid "peaky" responses to the subsequent rainfall events. The surface water tributary system, instead of recharging storage in between the larger events, keeps contributing to the flow downstream which remains relatively flat. The simulated flow reaches the flow peak that occurs during Hurricane Irma in September 2017 but very quickly recedes to a much lower flow volume than measured. Thus, the goal of the CWI RM optimization process was to improve this surface water – groundwater dynamics, i.e., the rainfall – storage – runoff response behaving closer to observed.

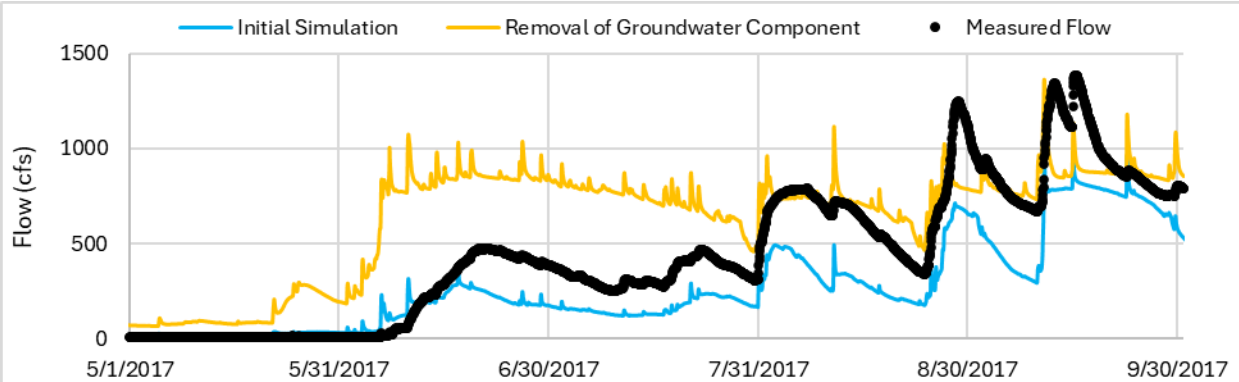

Figure 11-5. Effect of removing the groundwater component on the Imperial River simulated flow

Hydraulic conductivity is a key parameter in optimizing the groundwater level response, but it is not sufficient to implement global changes for a given layer due to several factors aside from differences in the layer materials (such as proximity of canals and other landscape features, influences of water use, etc.). Global changes to hydraulic conductivity results in better matching of simulated levels to historical data in some areas and worse in others. Thus, hydraulic conductivity adjustments had to be conducted by breaking down areas into zones. Lee County water table contours maps served to guide in distributing the zones of various degrees of flow resistance. Automatic runs were attempted to optimize the conductivities in each zone, but manual adjustments proved to be more effective. Automatic calibration tries to minimize a defined objective function based on many model simulations and since the model takes a long time to run, it is difficult to achieve the desired calibration results in a practical amount of time even with simpler versions of the model.

In addition to hydraulic conductivities, decreasing crop coefficients (Kc) for some of the wetland vegetation types during the summer months lowered ET volumes, leading to increases in simulated groundwater levels. Lower wet season Kc values can be justified based on ET data from the FPWX station (located north in Flint Pen), which are lower in the summer than the satellite-based reference ET. Other parameters that were adjusted and had some impact on the simulated groundwater levels and flow performance were overland flow Manning's M (which is the flow resistance parameter input in the MIKE SHE overland flow component, M=1/n), detention storage, and flow way Manning's n values and conductances. Flow way or channel Manning's n values did not have a substantial impact on the performance. Table 11-1 shows the list of parameters adjusted in the CWI refinement process.

Table 11-1. List of Parameters Adjusted in the CWI Refined Model

Model Component	Parameter	Location	Initial	Final
Overland Flow	Manning's M (1/n)	Corkscrew	1.8	5
Overland Flow	Detention Storage (inches)	Corkscrew	1.1 to 2.5	0 [1]
Overland Flow	Separated Flow Areas (integer codes, # added)	Corkscrew and adjacent basins	146	165 [2]
Overland Flow Ponded Drainage	Runoff Coefficients (fraction)	Urban areas model domain	[3] LDR: 0.05 MDR: 0.15 HDR: 0.45	LDR: 0.28 MDR: 0.40 HDR: 0.58
	Drain Codes (integer codes)	Corkscrew adjacent basins	-	New codes added, Specified Drainage routing to reaches[4].
	Inflow Time Constant (1/s)	Model domain	-	Zeroed flood cells
	Outflow Time Constant (1/s)	Flint Pen/Imperial River Basin	Same as Inflow TC	Lowered Inflow TC by a factor of 100
ET	Crop Coefficients	Model domain	See Table 11-2	See Table 11-2
	Root Depths	Model domain	See Table 11-2	See Table 11-2
SHE-HYDRO Coupling	Flood Codes (integer codes)	Corkscrew and adjacent canals	-	Added new codes, adjusted locations and branch connections for previous codes that were not linked in MIKE HYDRO.
	Conductance	Corkscrew and adjacent canals	-	Conductance type, leakage coefficients, spatially variable.
Saturated Zone	K, Elev. [5] L1	Model domain	(283-77,185), 13,097 [6]	(181-553,587), 60,946 [6]
	K, Elev. [5] L2	Model domain	(12-46,806), 3,140 [6]	(0.02-0.6), 0.3 [6]
	K, Elev. [5] L3	Model domain	(457-71,952), 17,961 [6]	(522-426,681), 91,503 [6]
	K, Elev. [5] L4	Model domain	(2.8-847), 187 [6]	(0.2-687), 79 [6]
	Elev. [5] L5	Model domain	(1.7-6,050), 1,015 [6]	(0.5-15,750), 2,979 [6]
SZ Drainage	Drain Codes	Corkscrew and adjacent basins	-	Added new codes and Specified Drainage routing added.
	Time Constant	Model domain	-	Zeroed flood cells

[1] Overland storage removed because wetland storage is represented in the saturated zone component,
[2] Total number of areas (19 added in CWI RM), [3] LDR, MDR, HDR – low, medium, high density residential,
[4] Reaches are locations in the MIKE HYDRO network where drainage flow is routed to, [5] K, Elev. = Conductivities and layer bottom elevations, [6] Transmissivity range (min-max), average (ft^2/d).

Table 11-2. Adjustments to Vegetation Parameters from the BCB UM

Month			Jan[3]	Feb	Mar	Apr	May	Jun	Jul	Aug	Sep	Oct	Nov	Dec	EOY[4]
Urban Low Density	BCB	RD[1]	7.9	7.9	7.9	7.9	7.9	7.9	7.9	7.9	7.9	7.9	7.9	7.9	7.9
		KC[2]	0.6	0.5	0.5	0.6	0.6	0.6	0.6	0.7	0.7	0.7	0.7	0.6	0.6
	CWI	RD	7.9	7.9	7.9	7.9	7.9	7.9	7.9	7.9	7.9	7.9	7.9	7.9	7.9
		KC	1.0	1.0	1.0	1.0	1.0	0.6	0.6	0.7	0.7	0.7	0.7	1.0	1.0
Urban Med. Density	BCB	RD	7.9	7.9	7.9	7.9	7.9	7.9	7.9	7.9	7.9	7.9	7.9	7.9	7.9
		KC	0.7	0.7	0.7	0.7	0.7	0.7	0.5	0.6	0.6	0.6	0.6	0.5	0.7
	CWI	RD	7.9	7.9	7.9	7.9	7.9	7.9	7.9	7.9	7.9	7.9	7.9	7.9	7.9
		KC	1.0	1.0	1.0	1.0	1.0	0.6	0.6	0.7	0.7	0.7	0.7	1.0	1.0
Urban High Density	BCB	RD	7.9	7.9	7.9	7.9	7.9	7.9	7.9	7.9	7.9	7.9	7.9	7.9	7.9
		KC	0.7	0.7	0.7	0.7	0.7	0.7	0.4	0.4	0.5	0.5	0.5	0.4	0.7
	CWI	RD	7.9	7.9	7.9	7.9	7.9	7.9	7.9	7.9	7.9	7.9	7.9	7.9	7.9
		KC	1.0	1.0	1.0	1.0	1.0	0.6	0.6	0.7	0.7	0.7	0.7	1.0	1.0
Bare Ground	BCB	RD	29.5	29.5	29.5	29.5	29.5	29.5	29.5	29.5	29.5	29.5	29.5	29.5	29.5
		KC	0.6	0.7	0.7	0.9	1.0	1.0	1.0	1.0	1.0	0.9	0.9	0.8	0.6
	CWI	RD	2.0	2.0	2.0	2.0	2.0	2.0	2.0	2.0	2.0	2.0	2.0	2.0	2.0
		KC	0.6	0.7	0.5	0.5	0.5	0.7	0.7	0.7	0.7	0.7	0.7	0.7	0.7
Hydric Flatwood	BCB	RD	48.0	48.0	48.0	48.0	48.0	48.0	48.0	48.0	48.0	48.0	48.0	48.0	48.0
		KC	0.8	0.8	0.8	0.9	0.9	0.9	0.9	1.0	1.0	0.9	0.9	0.8	0.8
	CWI	RD	48.0	48.0	48.0	48.0	48.0	48.0	48.0	48.0	48.0	48.0	48.0	48.0	48.0
		KC	1	1	1	1	1	0.6	0.6	0.6	0.6	0.7	1	1	1
Hydric Hammock	BCB	RD	24.0	24.0	24.0	24.0	24.0	24.0	24.0	24.0	24.0	24.0	24.0	24.0	24.0
		KC	0.8	0.8	0.8	0.9	0.9	0.9	0.9	1.0	1.0	0.9	0.9	0.8	0.8
	CWI	RD	24.0	24.0	24.0	24.0	24.0	24.0	24.0	24.0	24.0	24.0	24.0	24.0	24.0
		KC	1.0	1.0	1.0	1.0	1.0	0.6	0.6	0.6	0.6	1.0	1.0	1.0	1.0
Wet Prairie	BCB	RD	6.0	6.0	6.0	6.0	6.0	6.0	6.0	6.0	6.0	6.0	6.0	6.0	6.0
		KC	0.8	0.8	0.8	0.8	0.9	0.9	0.9	0.9	0.9	0.9	0.8	0.8	0.8
	CWI	RD	6.0	6.0	6.0	6.0	6.0	6.0	6.0	6.0	6.0	6.0	6.0	6.0	6.0
		KC	1	1	1	1	1	0.6	0.6	0.6	0.6	0.7	1	1	1
Dwarf Cypress	BCB	RD	60.0	60.0	60.0	60.0	60.0	60.0	60.0	60.0	60.0	60.0	60.0	60.0	60.0
		KC	0.8	0.8	0.8	0.8	0.9	1.0	1.0	1.0	1.0	0.9	0.8	0.8	0.8
	CWI	RD	12.0	12.0	12.0	12.0	12.0	12.0	12.0	12.0	12.0	12.0	12.0	12.0	12.0
		KC	1	1	1	1	1	0.6	0.6	0.6	0.6	0.6	1	1	1
Marsh	BCB	RD	6.0	6.0	6.0	6.0	6.0	6.0	6.0	6.0	6.0	6.0	6.0	6.0	6.0
		KC	0.8	0.8	0.8	0.8	0.8	0.8	0.8	0.8	0.8	0.8	0.8	0.8	0.8
	CWI	RD	36.0	36.0	36.0	36.0	36.0	36.0	36.0	36.0	36.0	36.0	36.0	36.0	36.0
		KC	0.7	0.7	0.7	1.3	1.1	1.0	0.7	0.7	0.7	0.7	0.7	0.7	0.7
Cypress	BCB	RD	60.0	60.0	60.0	60.0	60.0	60.0	60.0	60.0	60.0	60.0	60.0	60.0	60.0
		KC	0.8	0.8	0.8	0.9	0.9	0.9	0.9	1.0	1.0	0.9	0.9	0.8	0.8

Month			Jan[3]	Feb	Mar	Apr	May	Jun	Jul	Aug	Sep	Oct	Nov	Dec	EOY[4]
	CWI	RD	12.0	12.0	12.0	12.0	12.0	12.0	12.0	12.0	12.0	12.0	12.0	12.0	12.0
		KC	1.0	1.0	1.0	1.0	1.0	0.6	0.6	0.6	0.6	0.6	0.7	0.7	0.7
Swamp Forest	BCB	RD	60.0	60.0	60.0	60.0	60.0	60.0	60.0	60.0	60.0	60.0	60.0	60.0	60.0
		KC	0.7	0.7	0.7	0.7	0.8	0.8	0.9	0.9	1.0	0.9	0.9	0.8	0.7
	CWI	RD	36.0	36.0	36.0	36.0	36.0	36.0	36.0	36.0	36.0	36.0	36.0	36.0	36.0
		KC	0.7	0.7	0.7	1.3	1.1	1.0	0.7	0.7	0.7	0.7	0.7	0.7	0.7
Mangrove	BCB	RD	60.0	60.0	60.0	60.0	60.0	60.0	60.0	60.0	60.0	60.0	60.0	60.0	60.0
		KC	0.8	0.8	0.8	0.8	0.9	1.0	1.0	1.0	1.0	0.9	0.8	0.8	0.8
	CWI	RD	12.0	12.0	12.0	12.0	12.0	12.0	12.0	12.0	12.0	12.0	12.0	12.0	12.0
		KC	1.0	1.0	1.0	1.0	1.0	1.0	1.0	1.0	1.0	0.9	1.0	1.0	1.0

[1] Root depth (inches)
[2]Kc = crop coefficient (unitless)
[3] Beginning of the year (January 1st)
[4] End of the year (December 31st), values are linearly interpolated between the beginning and end of the months.

11.2.3 Effects of Model Topography in Groundwater Levels and Introduction of a Vegetation Partial Layer in the Groundwater Model

While adjusting parameters mentioned above led to a closer match between the simulated heads and the observed values, the model was not able to simulate water levels above ground surface for prolonged periods of time as the observed data indicates for a number of well locations. In some of the observed well locations (e.g., 49-GW6, -GW9, -GW11, L-5667, SOCREW1, SOCREW2, etc.), levels would plateau at or near the model topography of those cells. This happens because ponded water above the MIKE SHE topography is no longer part of the SZ component and it is moved via overland flow. Movement of overland flow is relatively fast compared to ground flow velocities. Yet, multiple attempts to lower the overland component Manning's M values in the Corkscrew wetlands (i.e., increasing resistance, equivalent to increasing n) did not produce the observed water level response and instead led to a reduction in peak flows downstream. One outcome of using the corrected LiDAR in the model is that it overrepresents available storage above ground in reality is occupied tall and dense vegetation, which is more representative of a shallow, open lake flow effect than the slower highly resistive wetland effect. This reduction in open above ground storage caused by wetland vegetation could be one of the physical mechanisms that contributes to water levels well above ground for prolonged periods of time. While increasing the overland component detention storage can lead to higher water levels, it does not lead to accurate timing of the flow hydrograph because the storage has to be exceeded before overland flow occurs. Thus, adjustments in the overland flow parameters alone do not produce the accurate wetland water levels and flows that are critical for the CWI performance measure evaluation.

Studies in Florida stormwater treatment wetlands (STAs) such as, Lal et al. (2015), have shown that wetland flow does not behave as described by the Manning's equation, instead in the shallow zones of dense vegetation, it behaves more similar to porous groundwater flow. Specifically the Lal paper states: "the Manning's equation is not applicable for wetlands with thick emergent vegetation, as well as the difficulty of applying a single power law-type expression for vegetation resistance over a wide range of depths and energy slopes without errors. This is partly due to the existence of multiple flow regimes and different power exponents over depth and energy slopes in these regimes. Results show that the flow regime at low depths is similar to porous media flow, and the flow regime at higher depths is more turbulent”. Moreover, calibration of an STA with a surface water model has shown that the Manning’s n power functions can vary substantially between cells and flow regimes and in some cases may have such high head losses that the depth-dependent function that fits simulated stages to observed stages leads to Manning’s n values much higher than the typical values at shallow depths (MHW and ADA, 2015).

Other studies, such as Lightbody et al. (2008), have shown that wetland flow velocities are heterogenous due to preferential (short circuiting) pathways, where a significant portion of the flow occurs. Thus, in the context of an integrated model like MIKE SHE, wetland flow can be conceptualized as consisting of three model components representing different zones of vegetation and flow regime:

1. a lower, preferential pathway zone simulated by the 1D surface water flow ways,

2. a zone of turbulent flow above the dense vegetation simulated by the 2D overland flow, and

3. a shallow, laminar flow zone that represents the dense wetland vegetation, soil and variable microtopography simulated by the 3D groundwater flow component (Figure 11-6).

This shallow zone was added to the groundwater component by raising the model topography in the Corkscrew wetlands to a height representative of the vegetation zone, which was assumed to be 1.5 feet. Thus, movement in the overland flow component will occur above the dense vegetation height. Flow ways in MIKE HYDRO acting as the short circuit pathways can move water below the height of the vegetation zone. This 3-component conceptualization helps overcome the model coarse resolution limitations and the inability of the overland flow component to simulate a power function.

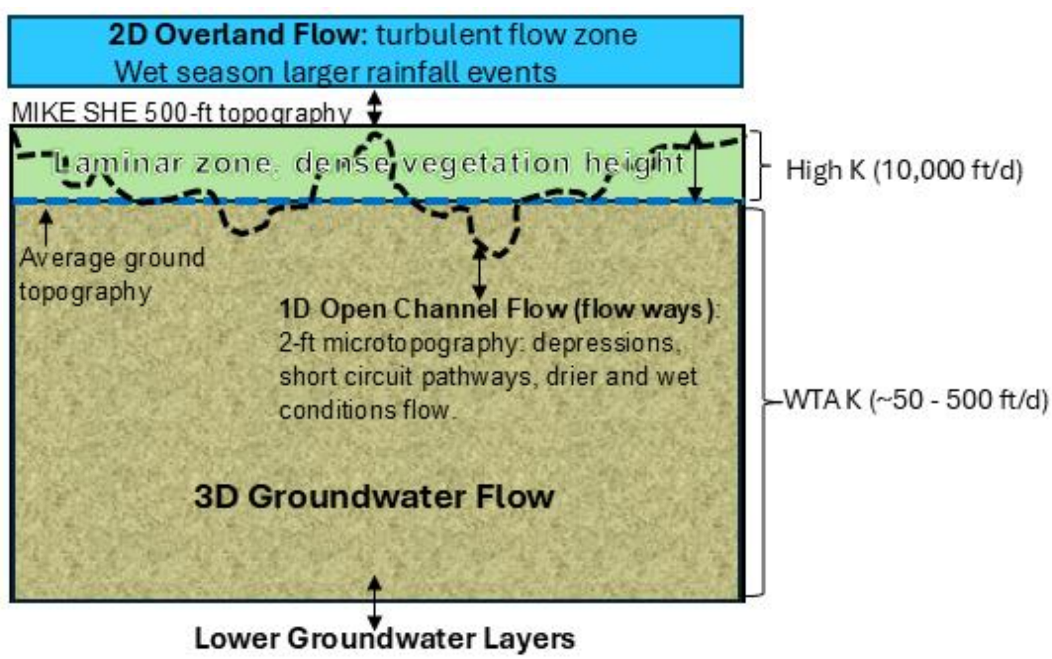

Figure 11-6. Conceptual Diagram of a Wetland Cell Top Groundwater Layer

To conceptually separate this vegetation zone from the lower aquifer material in the groundwater model, a partial layer (called a Lense in the MIKE SHE interface) was introduced that extends in the upper 2 feet (1.5-ft vegetation zone, plus a 0.5-ft buffer). In this upper zone hydraulic conductivities are higher and in the lower zone conductivities are lower to represent the resistance vertical flow that is suggested by the measured data. The aquifer properties of lenses are numerically interpolated as part of the computational layer that they are in. Thus, in this case the actual conductivity of the first layer is an interpolation of the specified conductivity for the lens and the specified conductivity for layer 1 based on the horizontal extent and thickness of the lens in relation to the thickness of layer 1. The resulting conductivity can be seen in the Processed tab in the MIKE SHE interface. While ideally this shallow vegetation layer would be numerically separated as an individual layer instead of a partial layer, this would have a negative impact on the calibration, particularly in the dry season. This is because the minimum heads in a numerical layer is the bottom elevation of the layer, so as the cells below the shallow layer would dry below the bottom of the top layer, it an artificially high level would remain in the shallow layer.

It should be noted that while this raised DEM partial groundwater layer concept proved to be effective in raising the water levels and increasing flow in the Imperial River, it should be further refined and calibrated beyond the scope of this project as more data becomes available in Corkscrew. Figure 11-7 shows example plots of the model performance at three stations with (red lines) and without the raised DEM (black lines). Figure 11-8 show example plots of the model performance at the same stations comparing the raised DEM/lens with higher M, i.e., lower overland flow resistance (red lines) and without the raised DEM/lens with lower M, i.e., higher overland flow resistance (black line). In both cases the plots show a better performance with the raised DEM/lens setup. Note that these plots are prior versions of the final refined model calibration shown in Section 11.4. These are included here to demonstrate the proof of concept The final revised model calibration showed similar results.

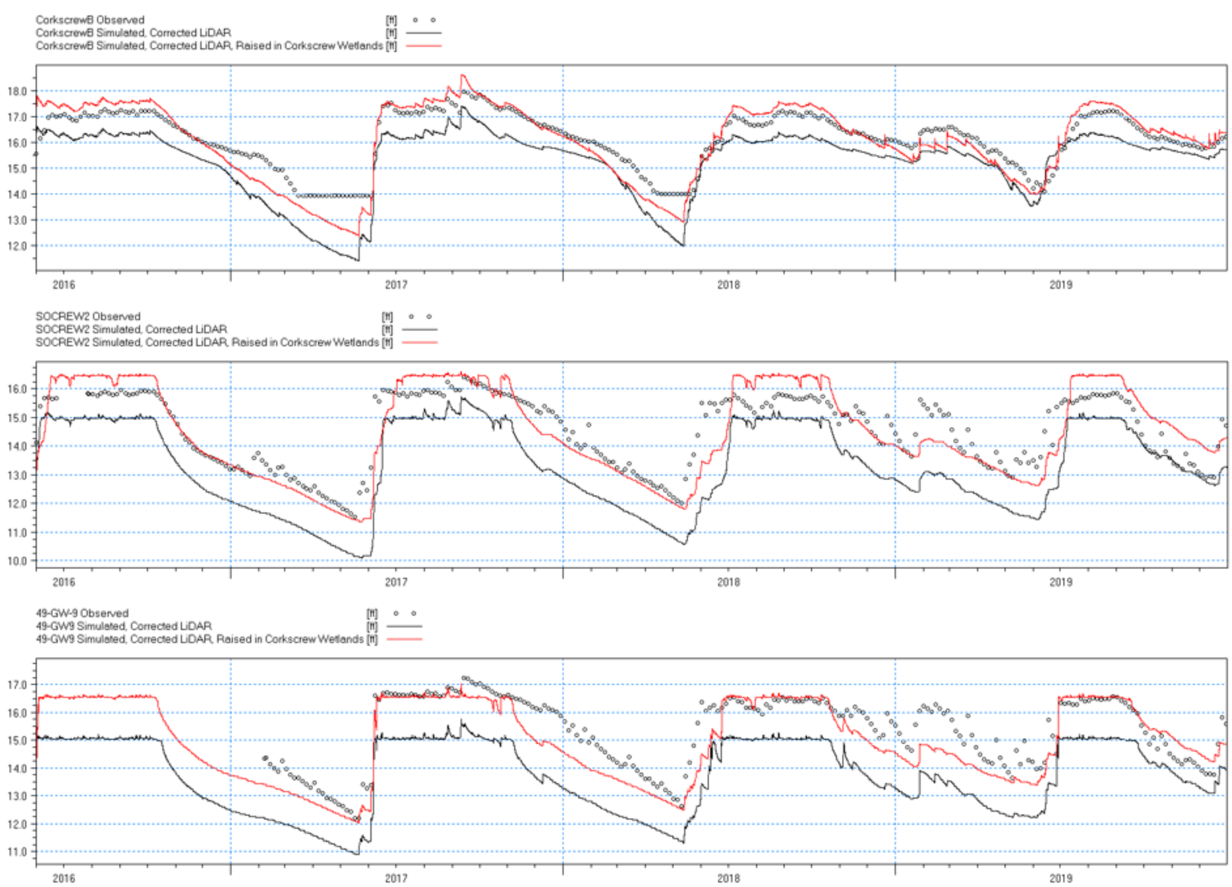

Figure 11-7. Example Plots Comparing Groundwater Levels With and Without the Raised DEM

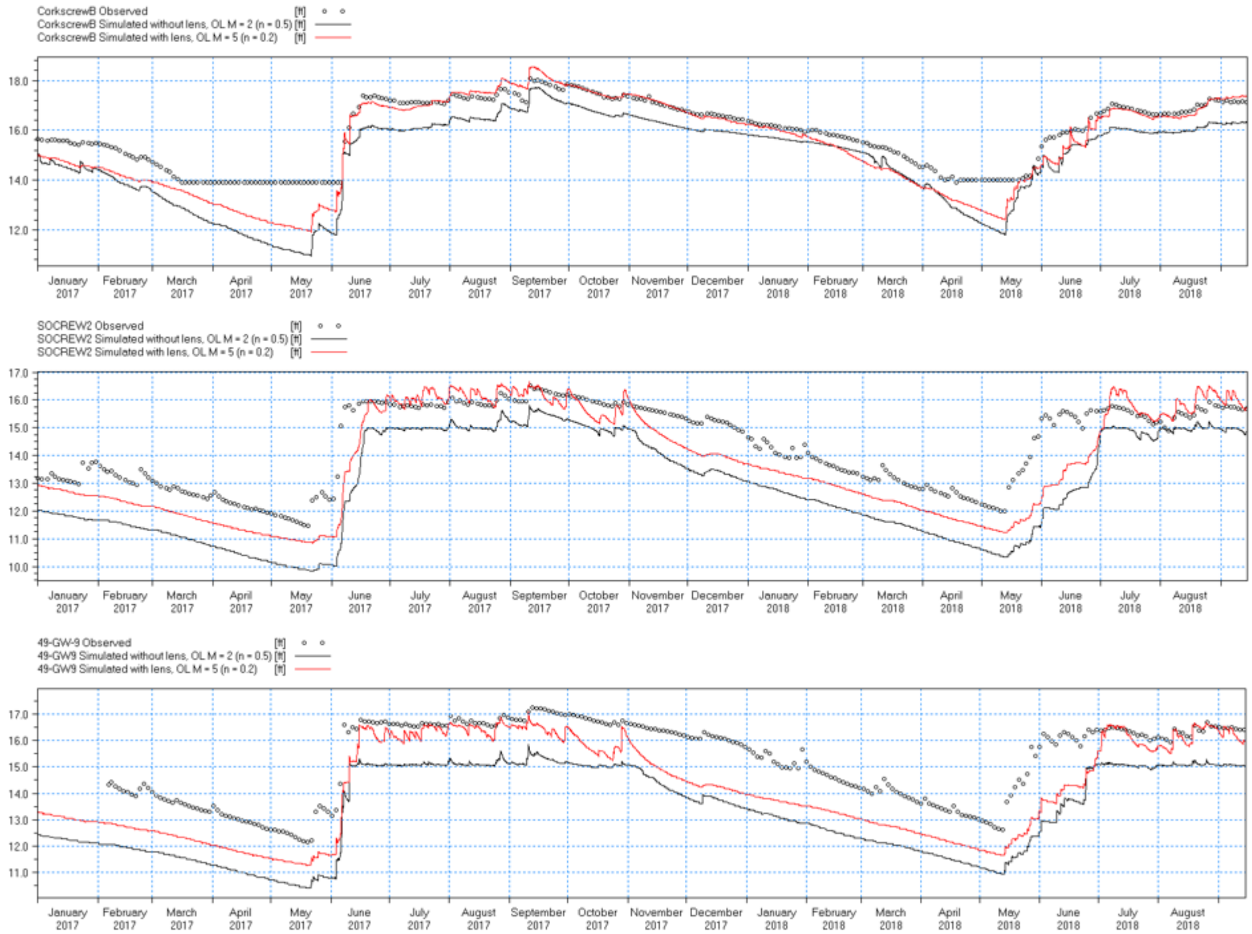

Figure 11-8. Example Plots Comparing Groundwater Levels With and Without the Raised DEM, Lens and Overland flow M values

11.3 Sensitivity Analysis of a Corkscrew Sub-Model

A sensitivity analysis using a sub-model of an area of interest in Corkscrew was conducted to test the effect of some of the applied concepts and adjusted model parameters in output results related to the CWI performance measures. Although the small model is a simplification of the real system and the impacts on the real system may differ, it provides the ability to conduct many simulations in a reasonably short amount of time and it is useful in terms of assessing the relative impacts of the setup concepts and parameters. Figure 11-9 shows the sub-model area and inputs.

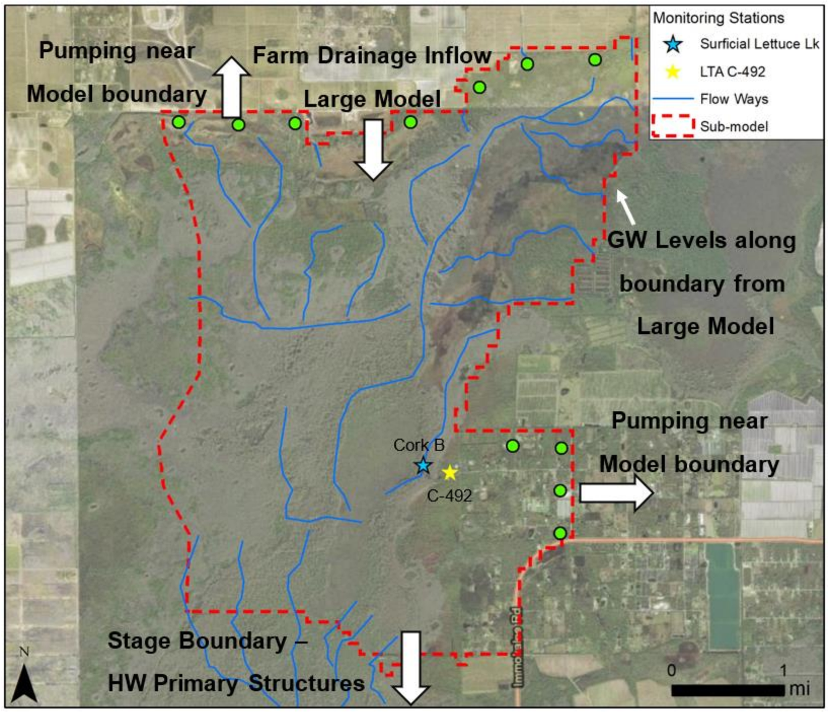

Figure 11-9. Sub-Model for Sensitivity Analysis

The model components evaluated in the sub-model included the items below. Table 11-3 lists the parameters adjusted in each of the simulations.

- The flow way definitions – direction and connections
- SZ hydraulic conductivities for the top layers of the model (WTA, TCU, LTA)
- The wetland lens concept and related inputs (DEM height and K vs overland detention storage), as described above, in Section 11.2.
- ET parameters – crop coefficients
- Pumping volumes and aquifer source
- Flow way and overland flow Manning's n

The sensitivity runs were conducted for a two-year period (January 1, 2017 to December 31, 2018). The first month of the simulation was not used in the analysis to exclude effects of initial conditions.

Figure 11-10 shows the change in the average number of days during the dry season above ground in four of the wetland indicator locations that were provided by members of the Technical Working Group. The baseline model resulted in an average of 219 days above ground out of a total of 392 dry season days in the two year evaluation period (i.e., 56%). To convert the model output to days above ground, the water table elevation was converted to a depth using the same reference DEM for all of the simulations. Most parameters tests had some impact in this measure of hydroperiod, but the largest changes have to do with the wetland lense setup and the flow way definition and connections.

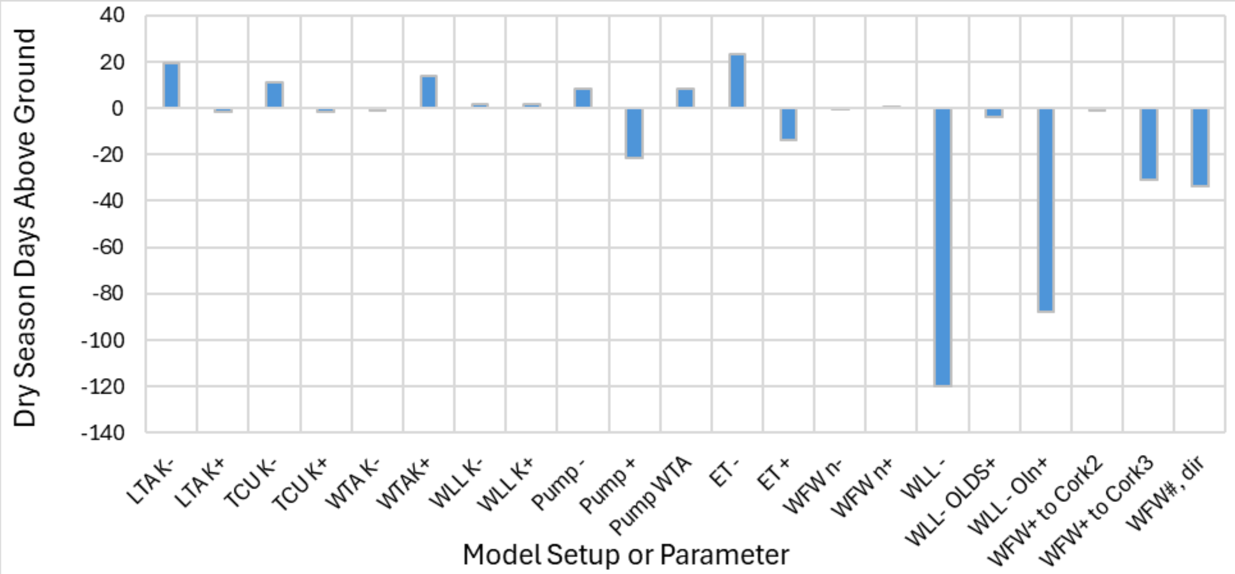

Figure 11-10. Change in the Average Number of Days Above Ground in Four Wetland Indicator Locations (descriptions are provided in Table 11-3)

Table 11-3. Parameters Changed in Sensitivity Analysis

Parameter Acronym	Description
LTA K-	Decrease conductivity of the Lower Tamiami aquifer (layer 3) x0.1
LTA K+	Increase conductivity of the Lower Tamiami aquifer (layer 3) x10
TCU K-	Decrease conductivity of the Tamiami confining unit (layer 2) x0.1
TCU K+	Increase conductivity of the Tamiami confining unit (layer 2) x10
WTA K-	Decrease conductivity of the Water Table aquifer (layer 1) x0.1
WTAK+	Increase conductivity of the Water Table aquifer (layer 1) x10
WLL K-	Decrease conductivity of the wetland lense
WLL K+	Increase conductivity of the wetland lense
Pump -	Decrease pumping in the LTA x0.25
Pump +	Increase pumping in the LTA x4
Pump WTA	Change the source of northern wells to the WTA.
ET -	Decrease crop coefficients
ET +	Increase crop coefficients
WFW n-	Decrease Manning’s n in wetland flow ways
WFW n+	Increase Manning’s n in wetland flow ways
WLL -	Remove wetland lens and set top elevation to original DEM
WLL- OLDS+	Same as WLL- and add overland detention storage
WLL - Oln+	Same as WLL- and decrease overland flow Manning’s M (1/n)

Parameter Acronym	Description
WFW+ to Cork2	Add a flow way connecting to Cork 2
WFW+ to Cork3	Same as WFW+ to Cork2, add flow way connection to Cork 3
WFW#, dir	Reduce the number of flow ways and change direction (previous model flow ways)

11.4 Calibration Plots and Statistics

Surface water and groundwater plots and statistics for locations of interest to the CWI project are provided in this section. Calibration statistics tables for the all the monitoring stations in the BCB model domain are provided below and all of the calibration plots are available within the model files and results as part of this deliverable. Recommendations for future calibration improvements are provided in Section 12.2.

Figure 11-11 shows the groundwater monitoring stations with available data for the calibration period and corresponding the groundwater model layer. Plots comparing simulated to observed groundwater head elevations for selected locations are shown below (Figure 11-12 to Figure 11-44). The groundwater calibration plots also include a line representing the elevation of the model topography. For stations that fall in a cell in which the model topography has been raised as part of the conceptual lens layer, a line representing the corrected LiDAR elevation averaged over the model cells at a 500 ft resolution, is also shown on the plot. See Section 11.2, for more details on the conceptual vegetation lens layer.

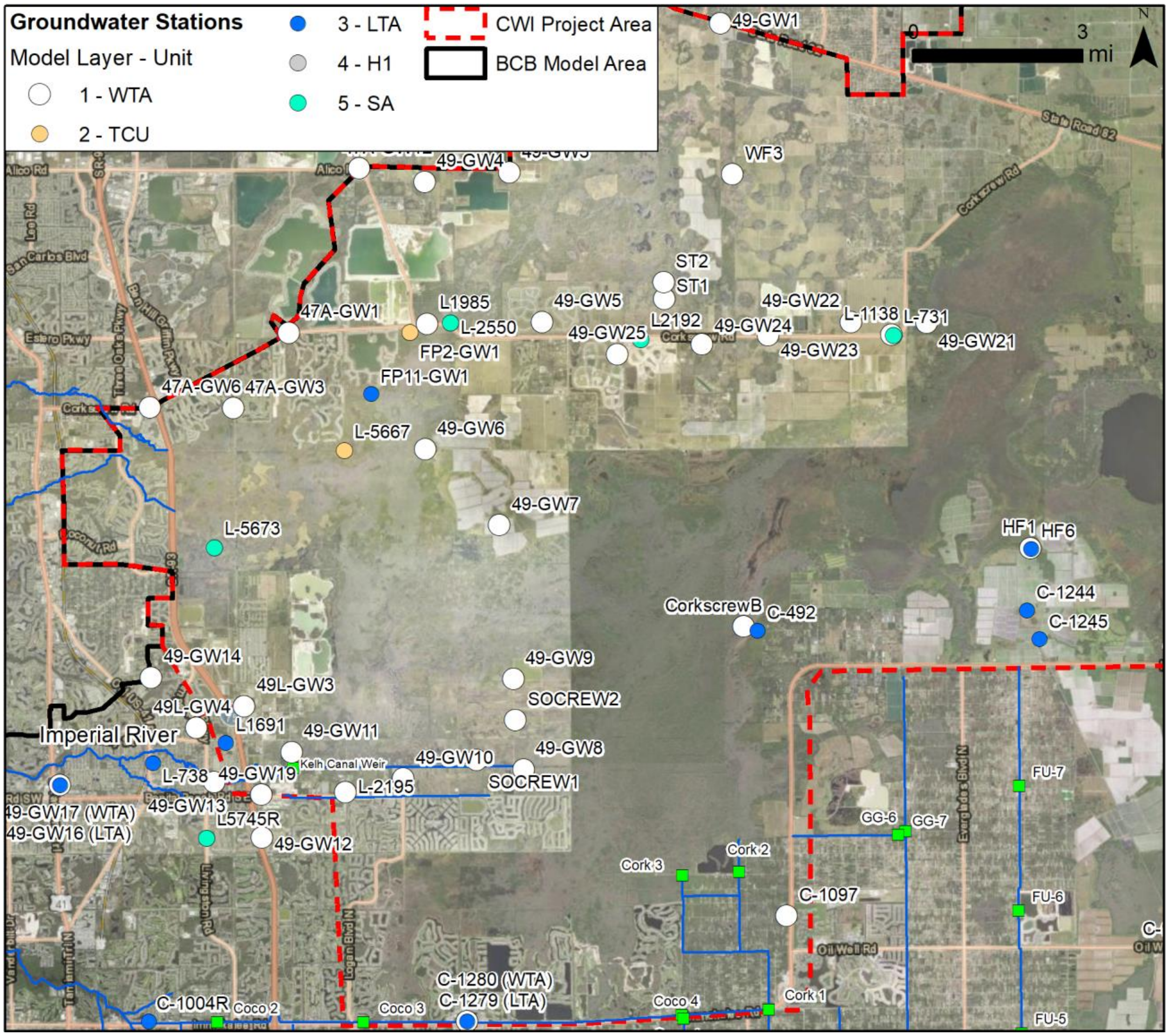

Figure 11-11. Groundwater Monitoring Stations with Available Data for the Calibration Period, Project Area

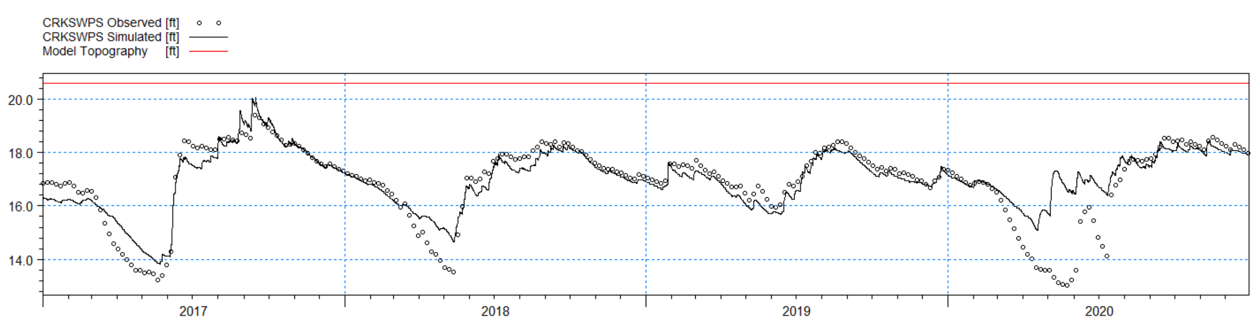

Figure 11-12. Simulated Versus Observed Groundwater Head Elevation (ft-NAVD) at the CRKSWPS Station

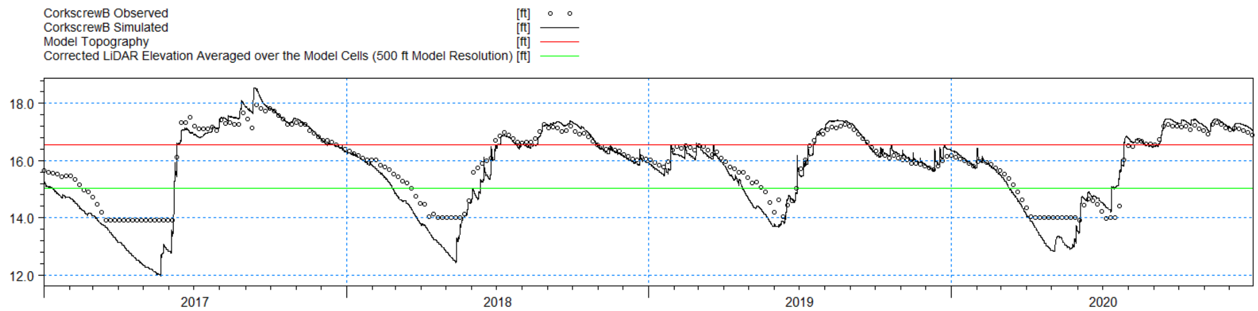

Figure 11-13. Simulated Versus Observed Groundwater Head Elevation (ft-NAVD) at the CorkscrewB Station

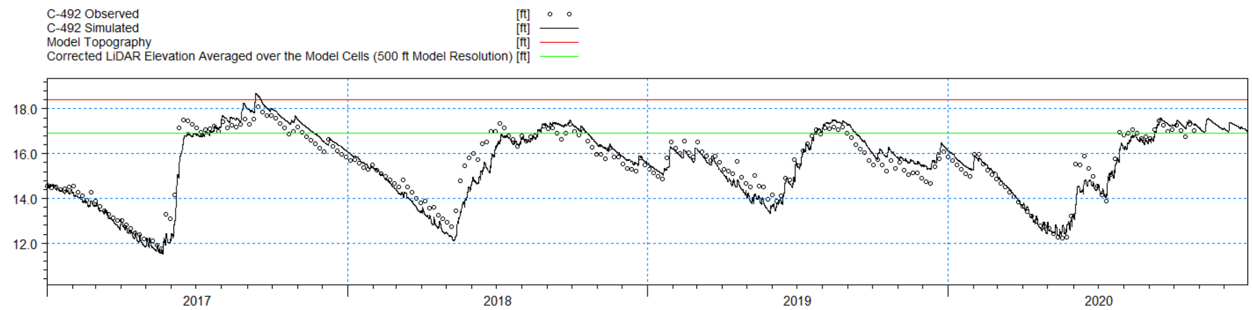

Figure 11-14. Simulated Versus Observed Groundwater Head Elevation (ft-NAVD) at the C-492 Station (LTA)

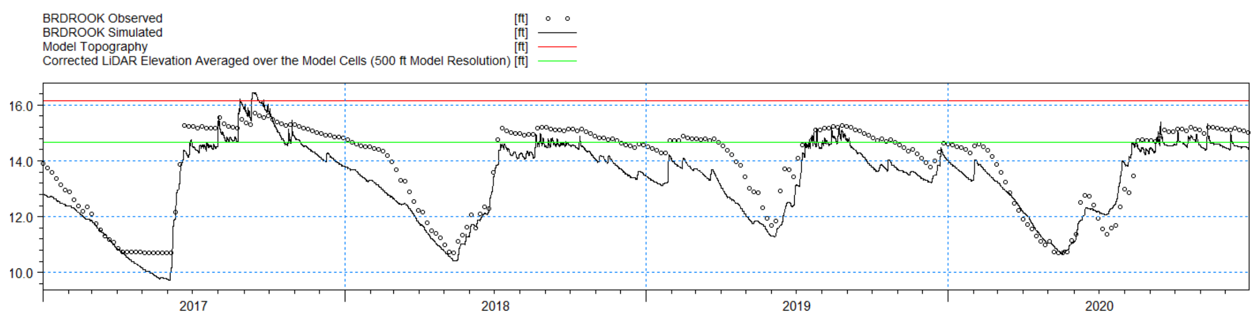

Figure 11-15. Simulated Versus Observed Groundwater Head Elevation (ft-NAVD) at the BRDROOK Station

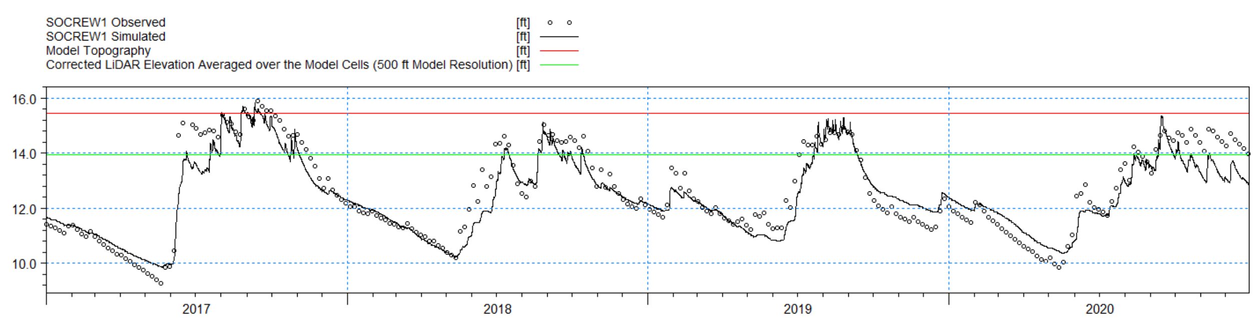

Figure 11-16. Simulated Versus Observed Groundwater Head Elevation (ft-NAVD) at the SOCREW1 Station

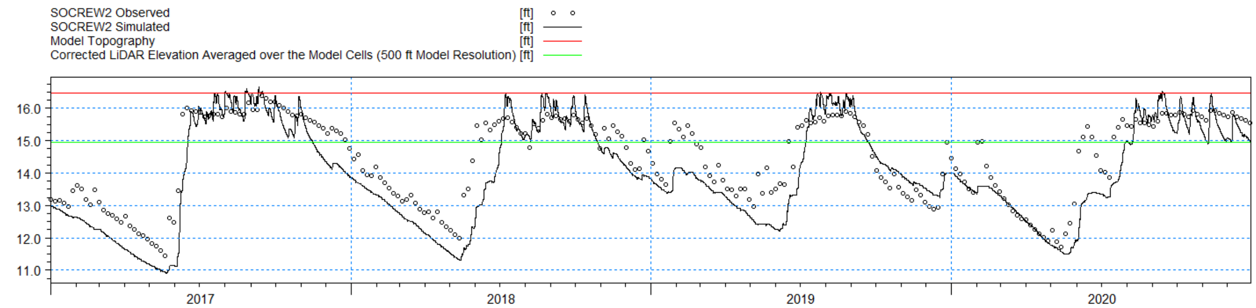

Figure 11-17. Simulated Versus Observed Groundwater Head Elevation (ft-NAVD) at SOCREW2 Station

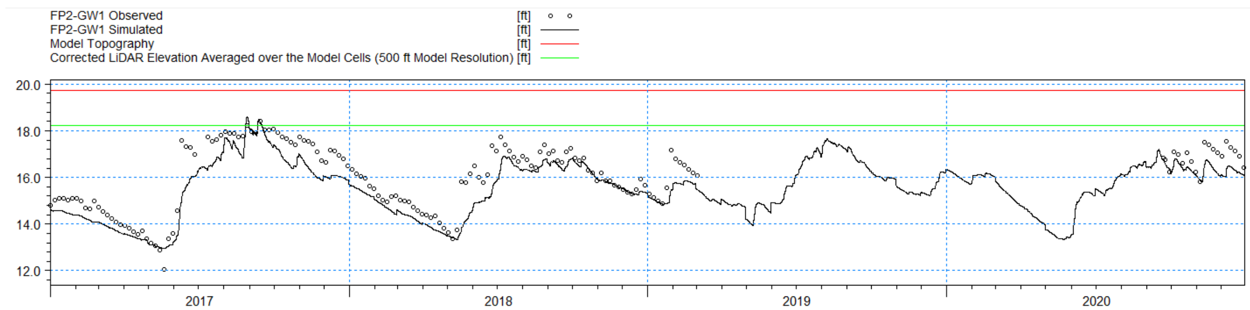

Figure 11-18. Simulated Versus Observed Groundwater Head Elevation (ft-NAVD) at the FP2-GW1 Station

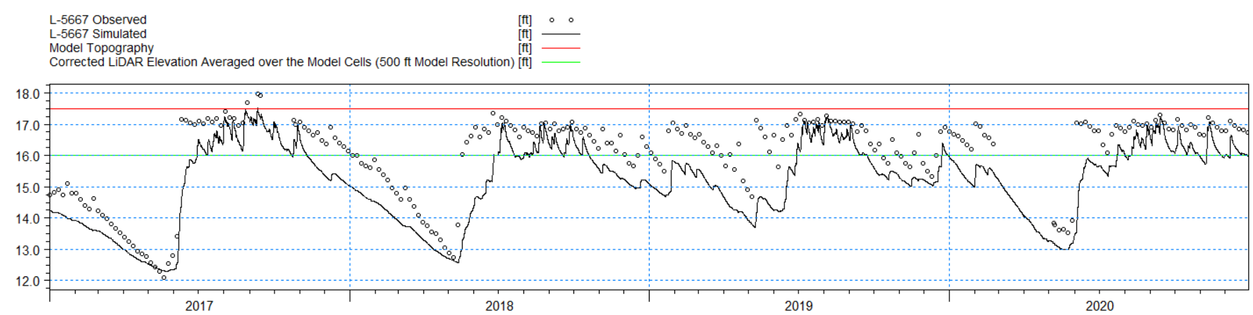

Figure 11-19. Simulated Versus Observed Groundwater Head Elevation (ft-NAVD) at the L-5667 Station

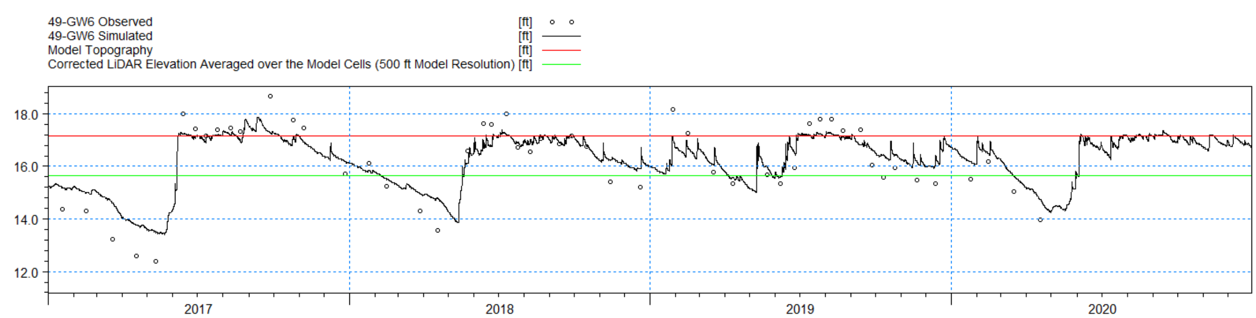

Figure 11-20. Simulated Versus Observed Groundwater Head Elevation (ft-NAVD) at the 49-GW6 Station

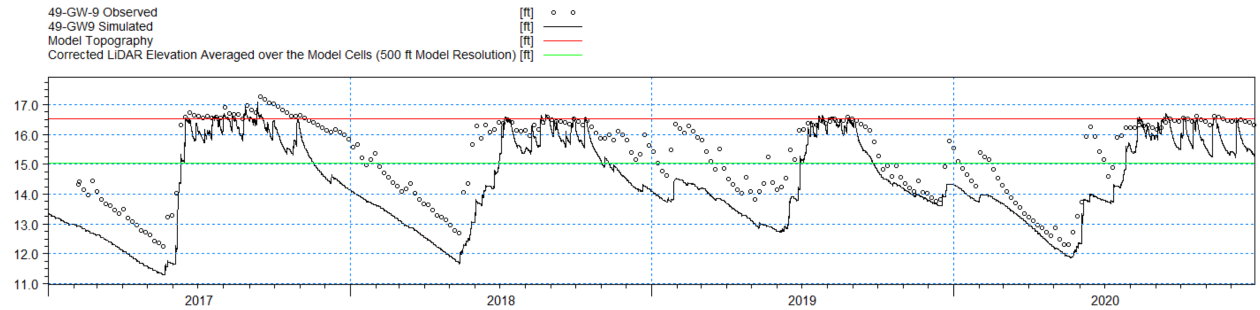

Figure 11-21. Simulated Versus Observed Groundwater Head Elevation (ft-NAVD) at the 49-GW9 Station

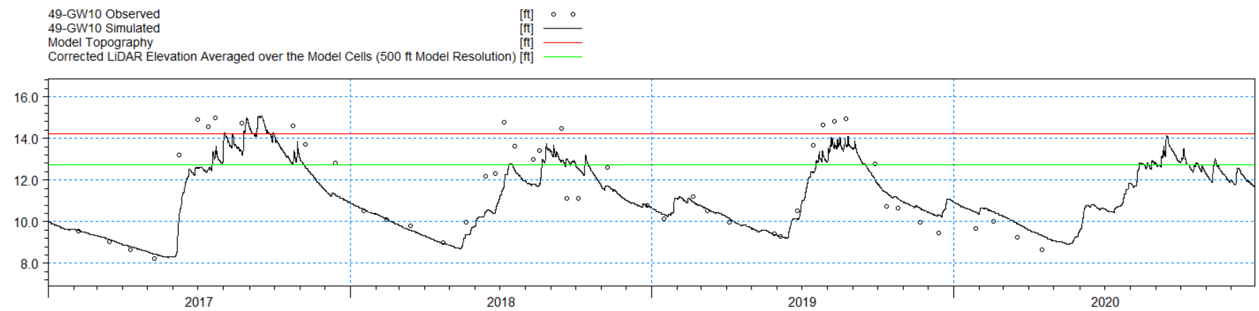

Figure 11-22. Simulated Versus Observed Groundwater Head Elevation (ft-NAVD) at the 49-GW10 Station

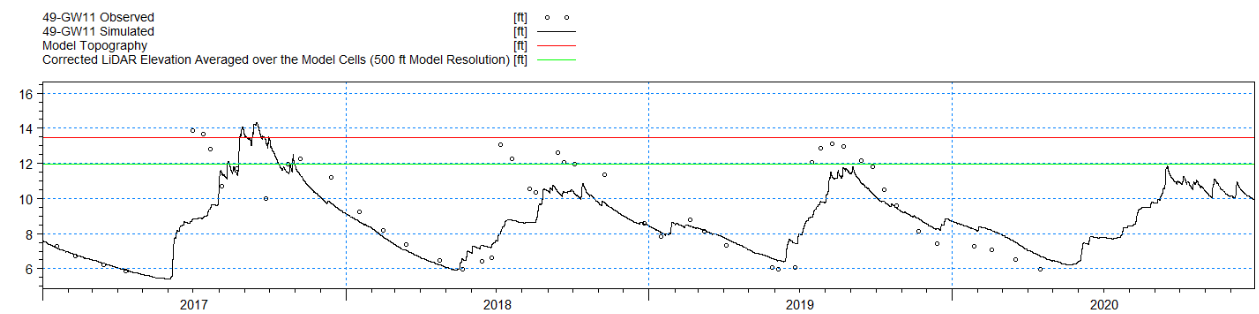

Figure 11-23. Simulated Versus Observed Groundwater Head Elevation (ft-NAVD) at the 49-GW11 Station

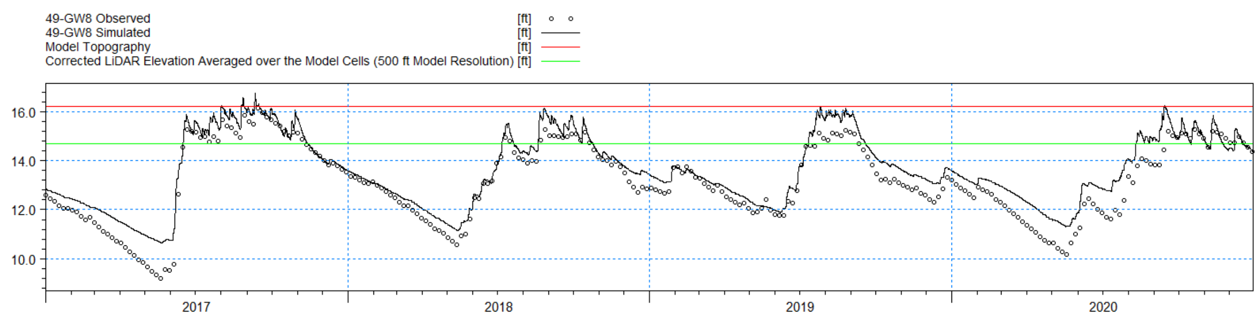

Figure 11-24. Simulated Versus Observed Groundwater Head Elevation (ft-NAVD) at the 49-GW8 Station

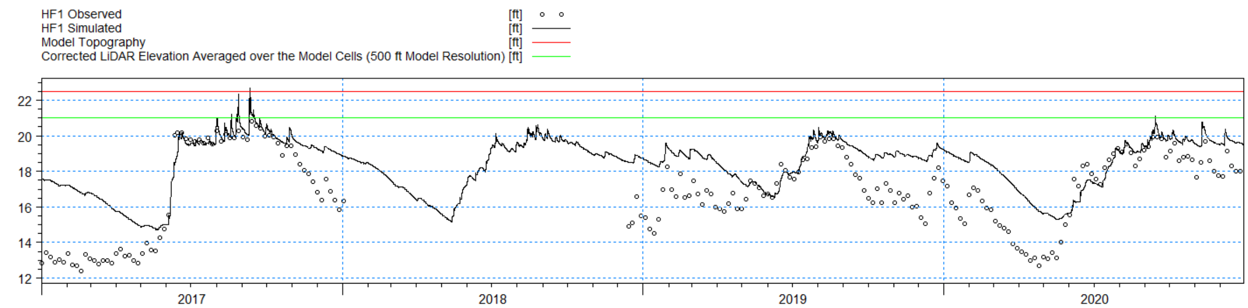

Figure 11-25. Simulated Versus Observed Groundwater Head Elevation (ft-NAVD) at the HF1 Station

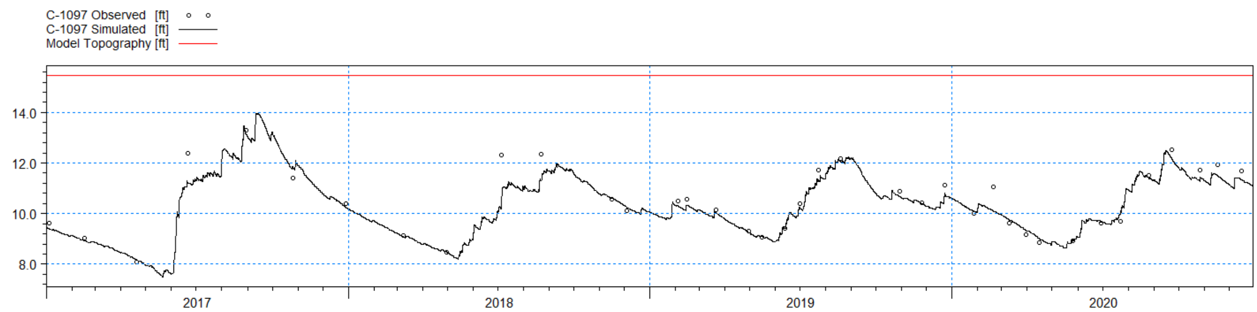

Figure 11-26. Simulated Versus Observed Groundwater Head Elevation (ft-NAVD) at the C-1097 Station

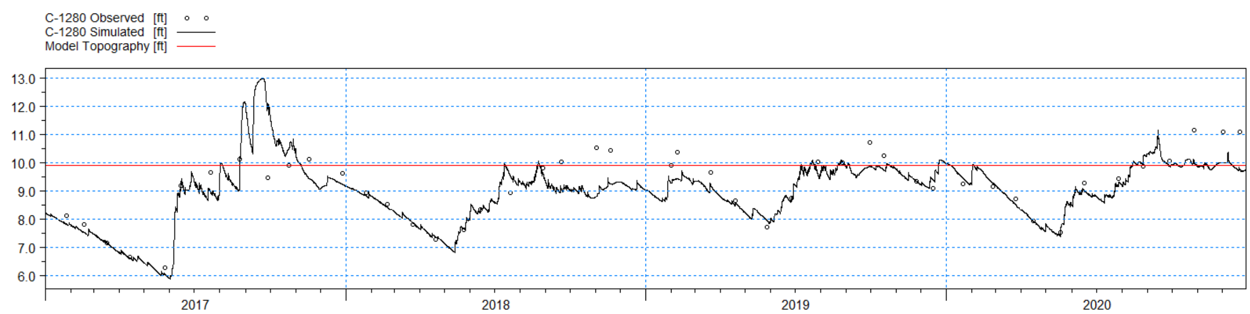

Figure 11-27. Simulated Versus Observed Groundwater Head Elevation (ft-NAVD) at the C-1280 Station

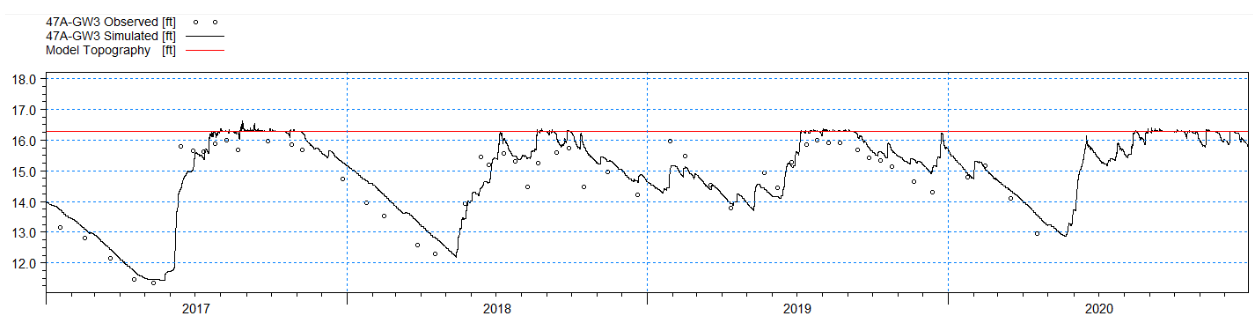

Figure 11-28. Simulated Versus Observed Groundwater Head Elevation (ft-NAVD) at the 47A-GW3 Station

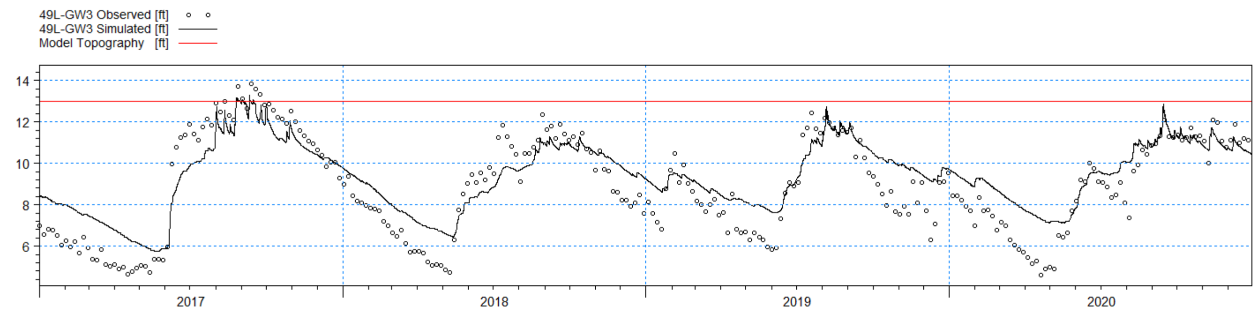

Figure 11-29. Simulated Versus Observed Groundwater Head Elevation (ft-NAVD) at the 49L-GW3 Station

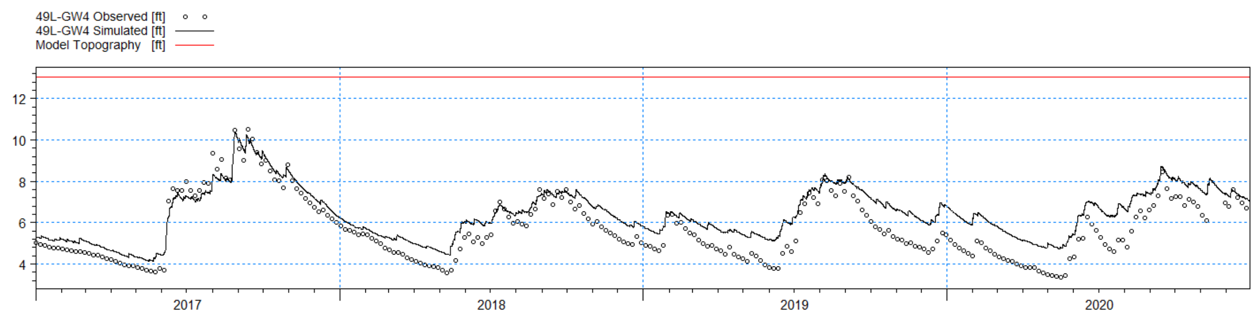

Figure 11-30. Simulated Versus Observed Groundwater Head Elevation (ft-NAVD) at the 49L-GW4 Station

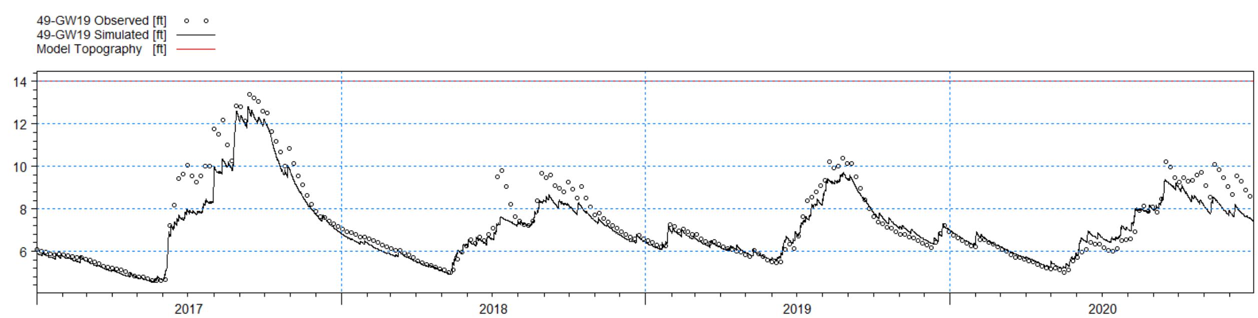

Figure 11-31. Simulated Versus Observed Groundwater Head Elevation (ft-NAVD) at the 49-GW19 Station

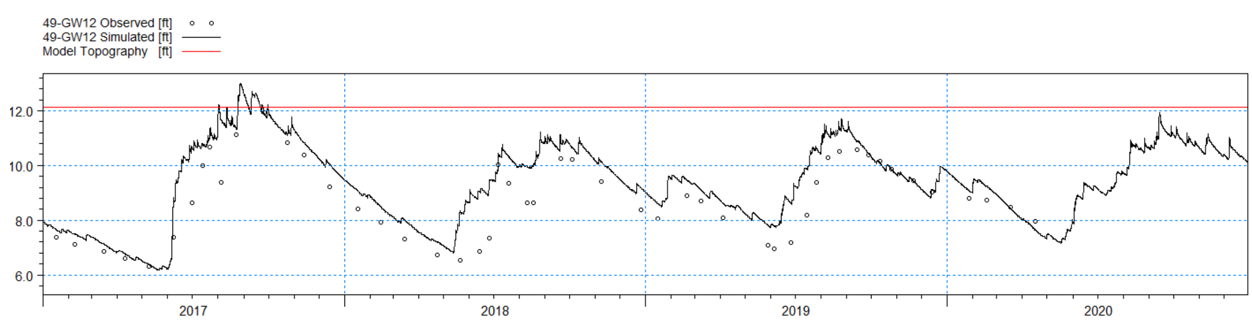

Figure 11-32. Simulated Versus Observed Groundwater Head Elevation (ft-NAVD) at the 49-GW12 Station

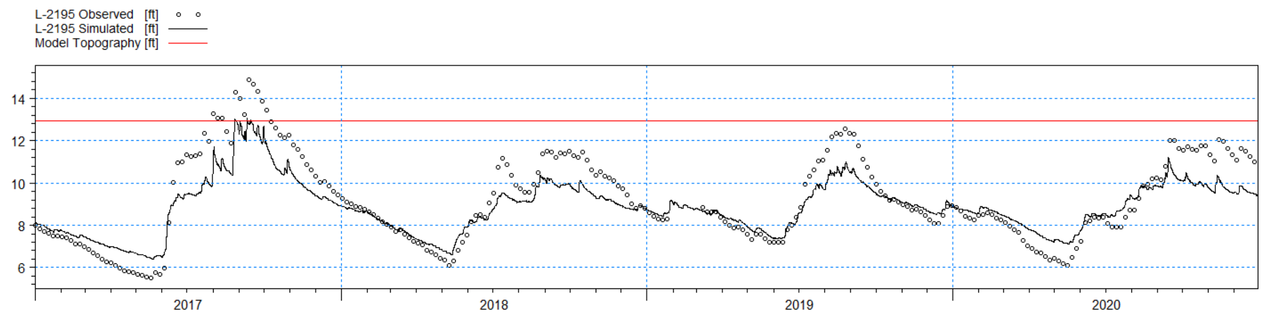

Figure 11-33. Simulated Versus Observed Groundwater Head Elevation (ft-NAVD) at the L-2195 Station

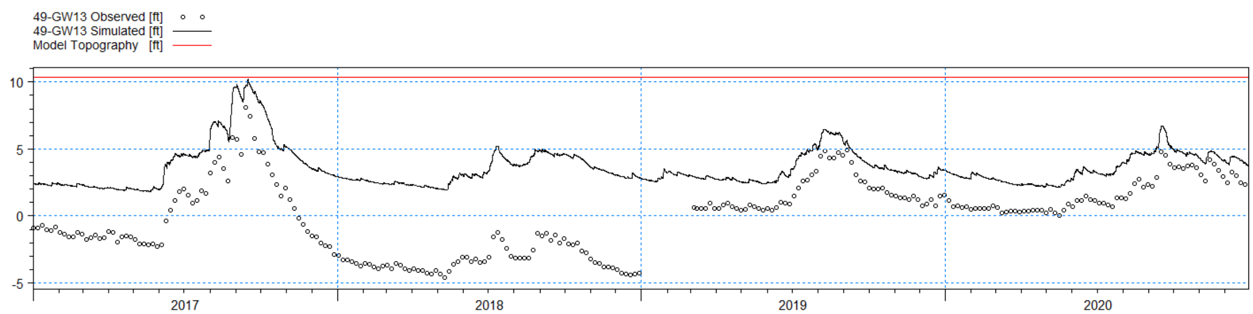

Figure 11-34. Simulated Versus Observed Groundwater Head Elevation (ft-NAVD) at the 49-GW13 Station

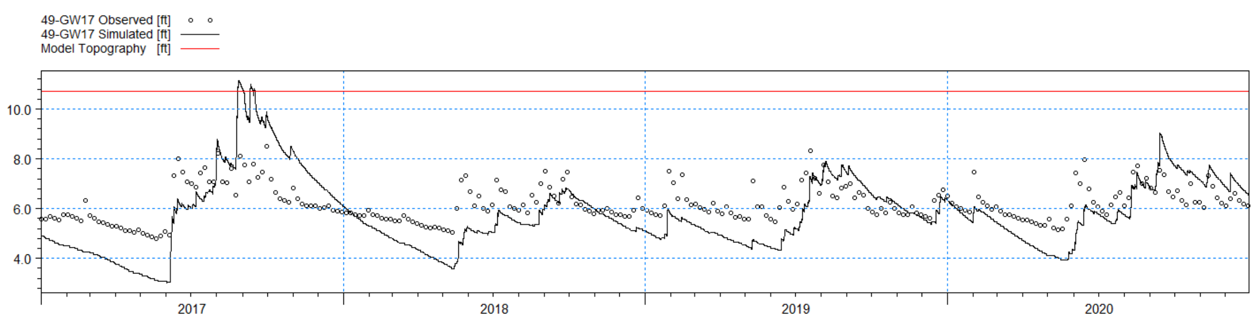

Figure 11-35. Simulated Versus Observed Groundwater Head Elevation (ft-NAVD) at the 49-GW17 Station

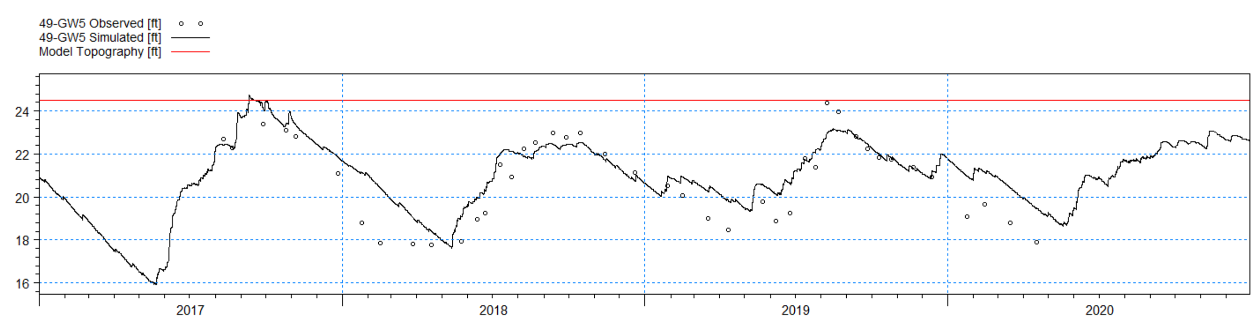

Figure 11-36. Simulated Versus Observed Groundwater Head Elevation (ft-NAVD) at the 49-GW5 Station

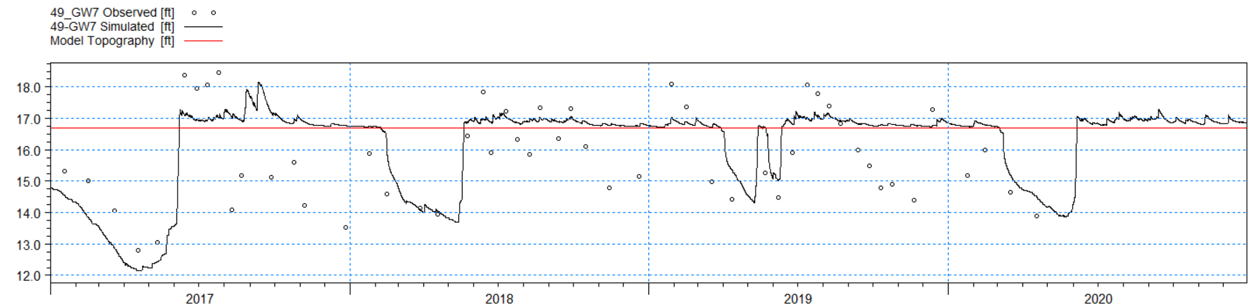

Figure 11-37. Simulated Versus Observed Groundwater Head Elevation (ft-NAVD) at the 49-GW7 Station

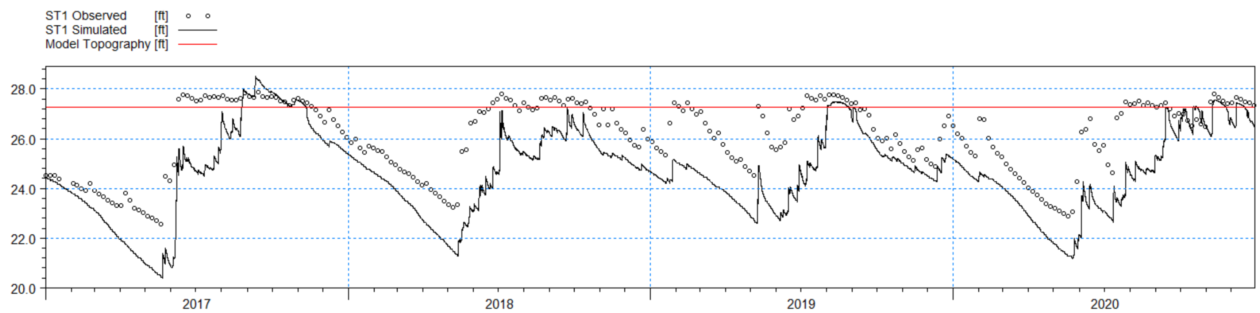

Figure 11-38. Simulated Versus Observed Groundwater Head Elevation (ft-NAVD) at the ST1 Station

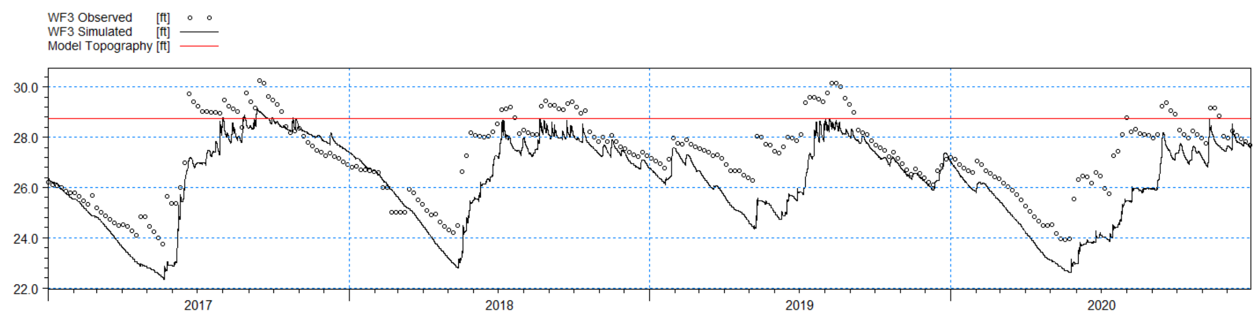

Figure 11-39. Simulated Versus Observed Groundwater Head Elevation (ft-NAVD) at the WF3 Station

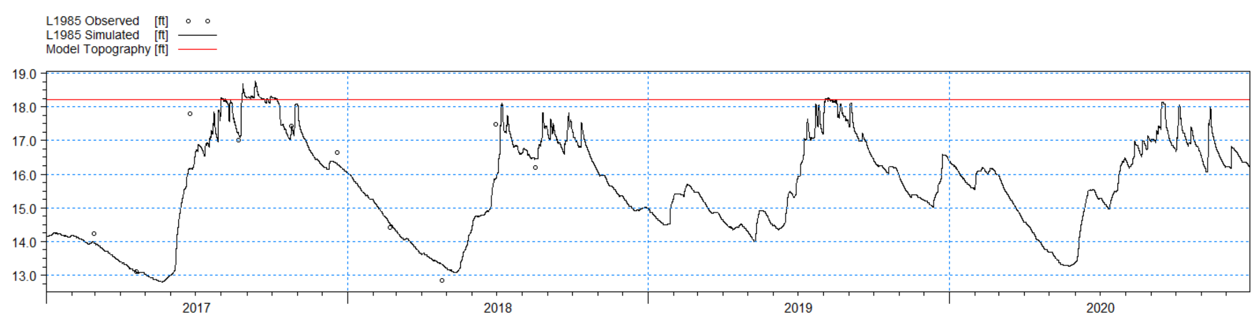

Figure 11-40. Simulated Versus Observed Groundwater Head Elevation (ft-NAVD) at the L1985 Station

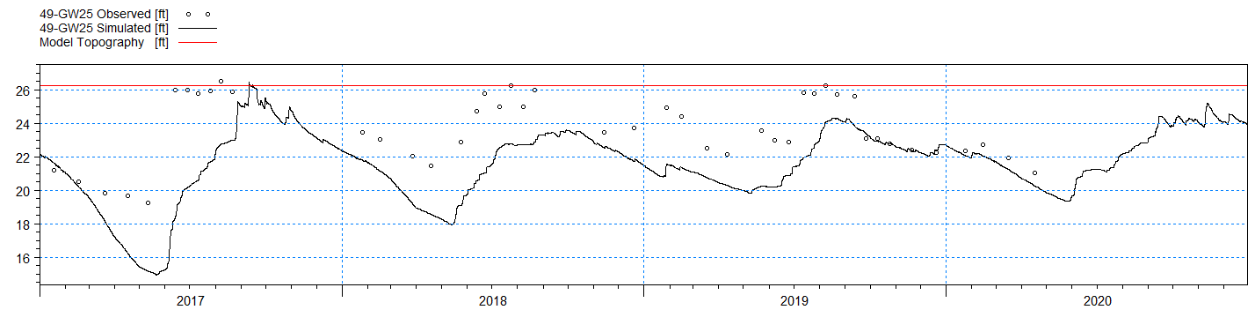

Figure 11-41. Simulated Versus Observed Groundwater Head Elevation (ft-NAVD) at the 49-GW25 Station

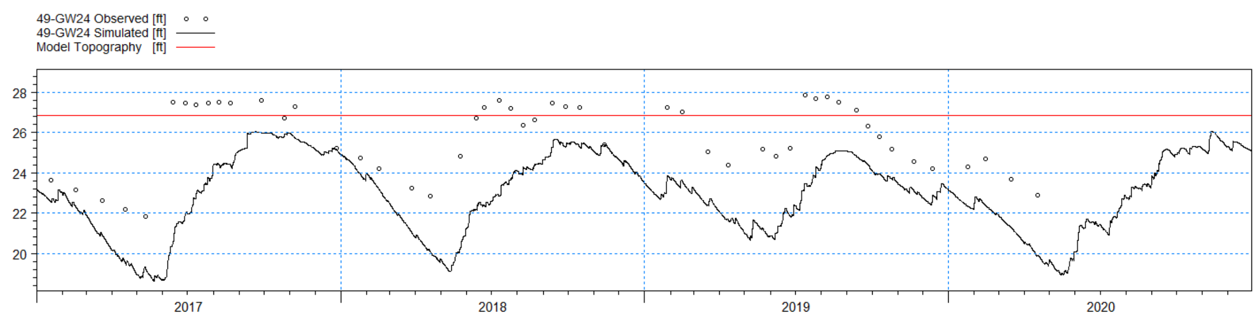

Figure 11-42. Simulated Versus Observed Groundwater Head Elevation (ft-NAVD) at the 49-GW24 Station

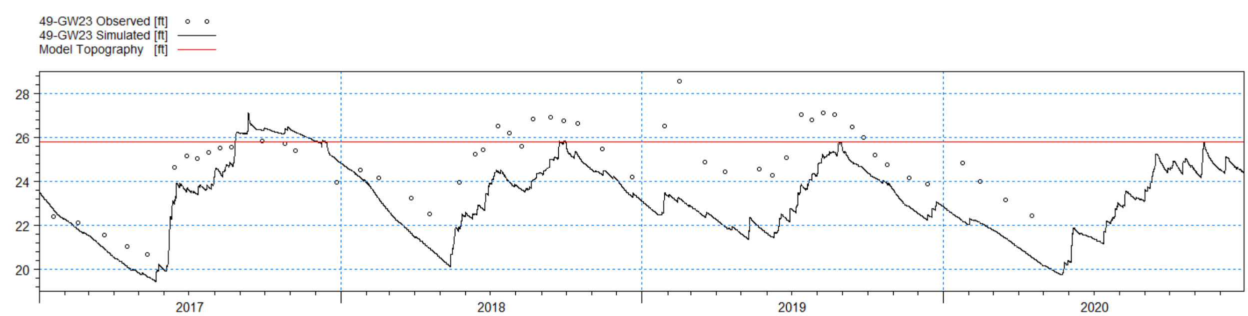

Figure 11-43. Simulated Versus Observed Groundwater Head Elevation (ft-NAVD) at the 49-GW23 Station

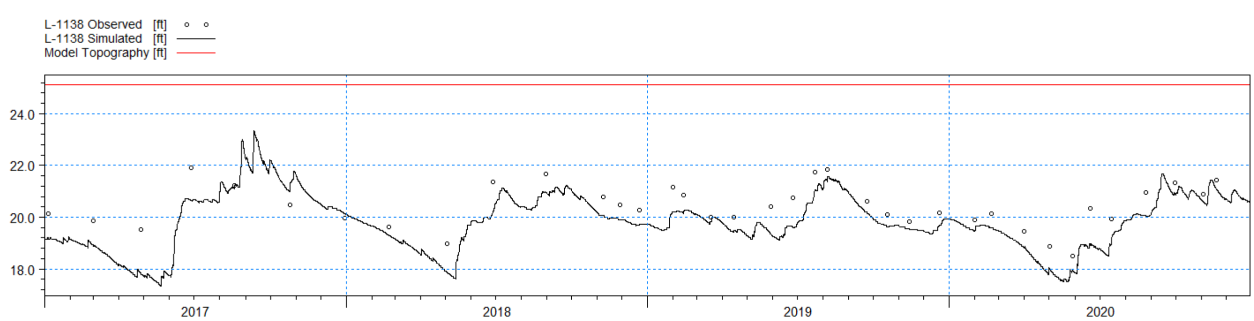

Figure 11-44. Simulated Versus Observed Groundwater Head Elevation (ft-NAVD) at the L-1138 Station

Figure 11-45 shows the surface water monitoring stations with available data for the calibration period. Figure 11-46 through Figure 11-61 show plots comparing simulated to observed surface water stages and flows for selected locations.

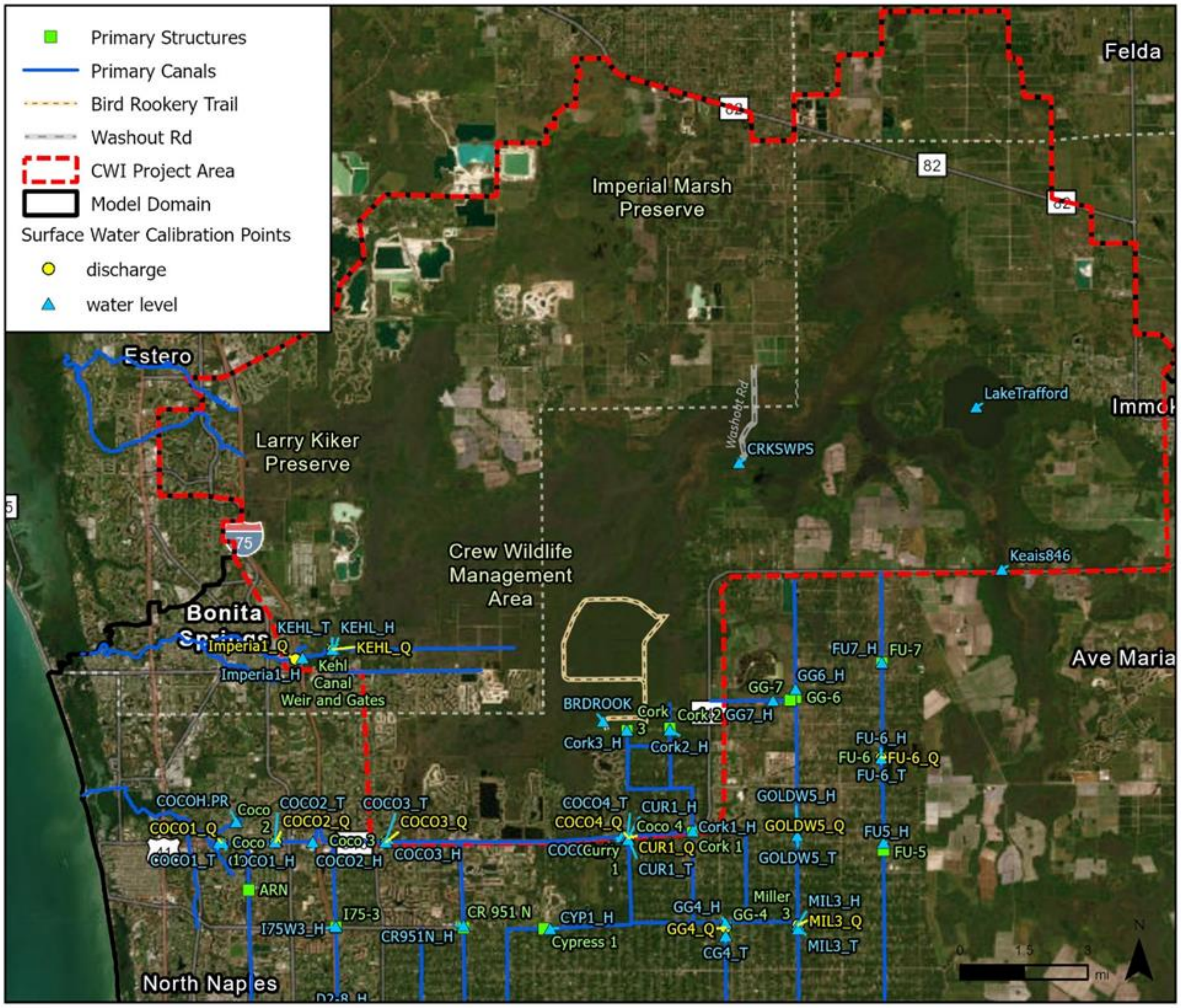

Figure 11-45. Surface Water Monitoring Stations with Available Data for the Calibration Period, Project Area

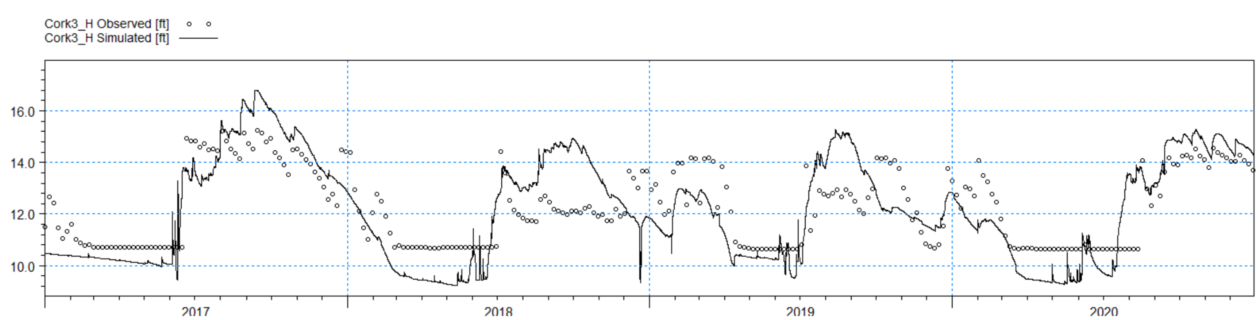

Figure 11-46. Simulated Versus Observed Stages (ft-NAVD) at the Cork3 Headwater Station

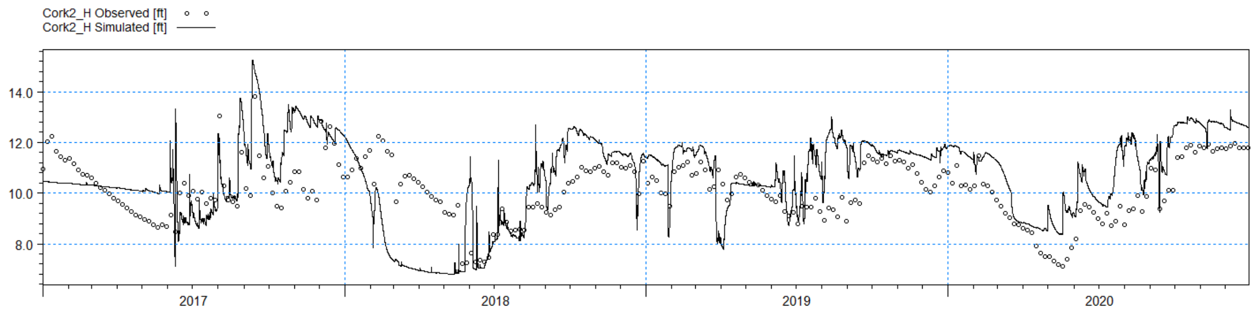

Figure 11-47. Simulated Versus Observed Stages (ft-NAVD) at the Cork2 Headwater Station

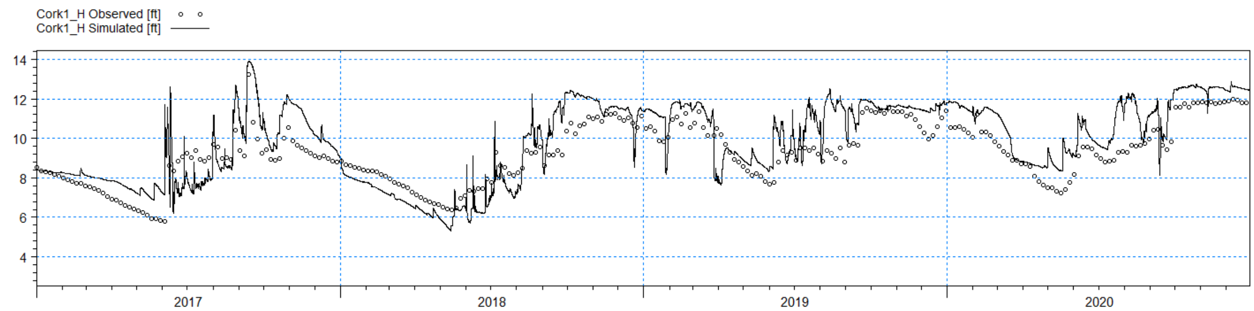

Figure 11-48. Simulated Versus Observed Stages (ft-NAVD) at the Cork1 Headwater Station

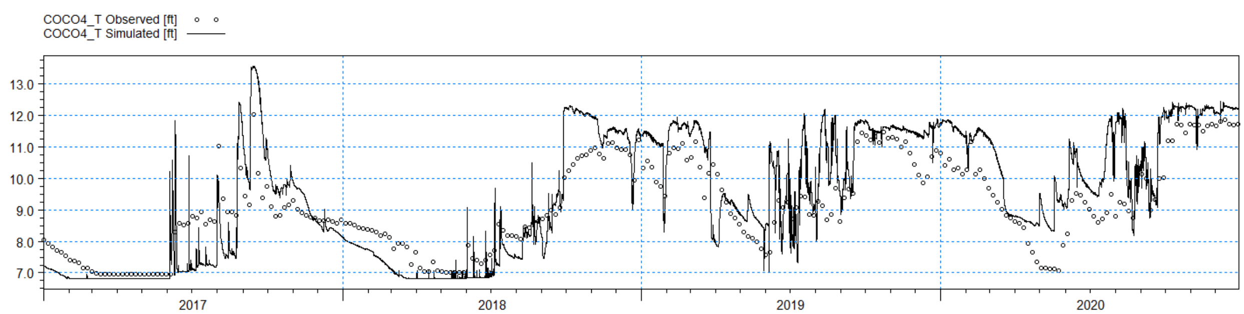

Figure 11-49. Simulated Versus Observed Stages (ft-NAVD) at the COCO4 Tailwater Station (East)

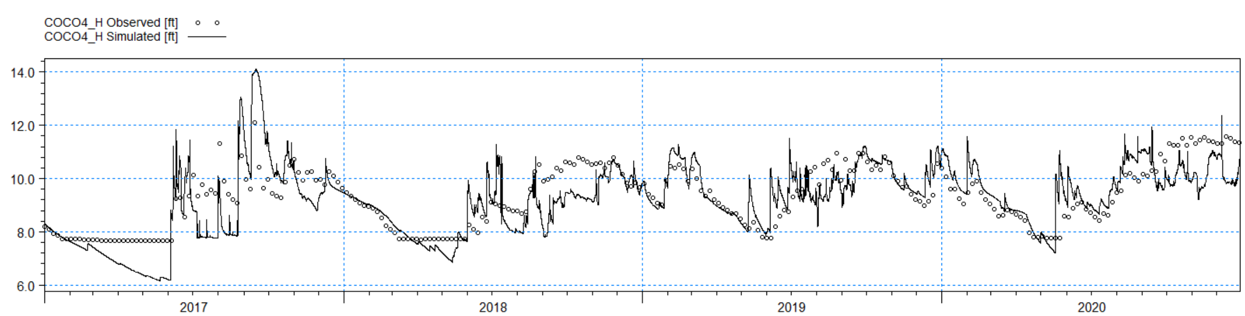

Figure 11-50. Simulated Versus Observed Stages (ft-NAVD) at the COCO4 Headwater Station (West)

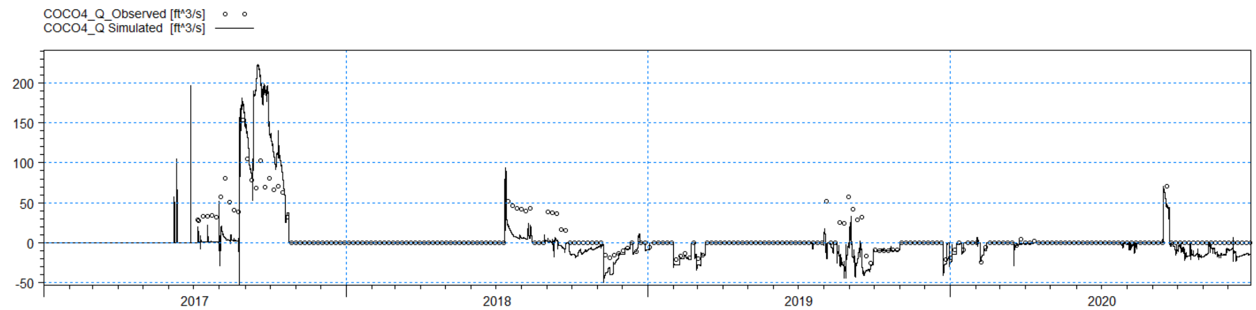

Figure 11-51. Simulated Versus Observed Flow (cfs) at the COCO4 Station

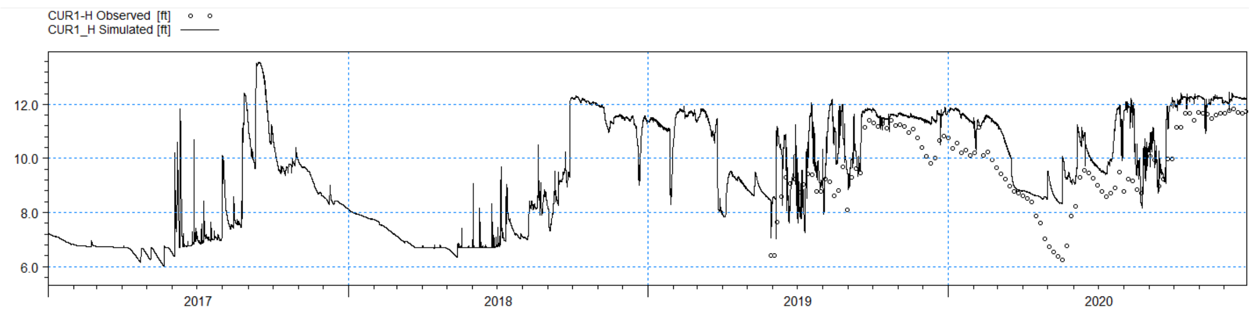

Figure 11-52. Simulated Versus Observed Stages (ft-NAVD) at the CUR1 Headwater Station

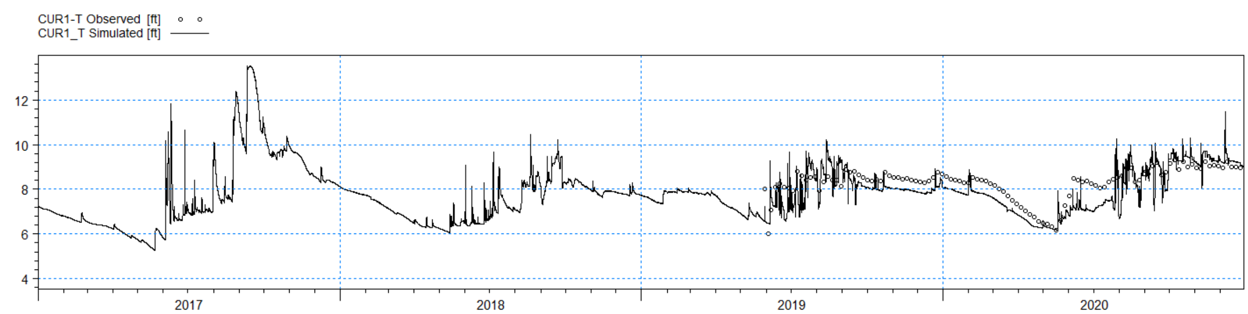

Figure 11-53. Simulated Versus Observed Stages (ft-NAVD) at the CUR1 Tailwater Station

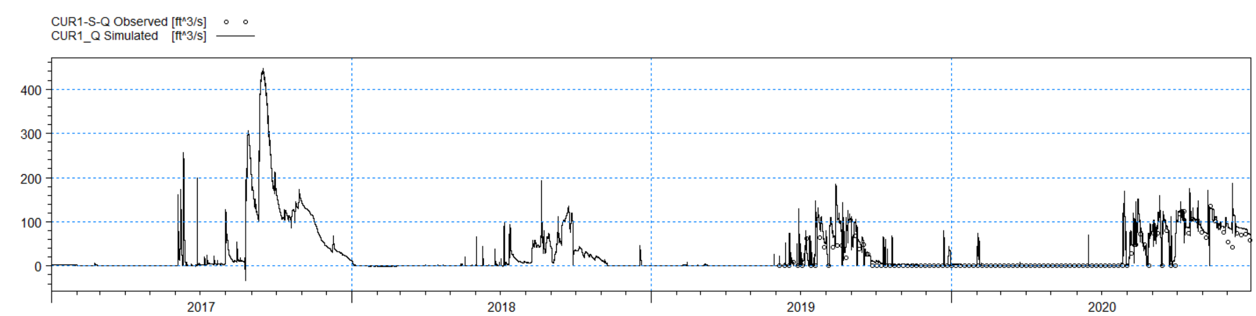

Figure 11-54. Simulated Versus Observed Flow (cfs) at the CUR1 Station

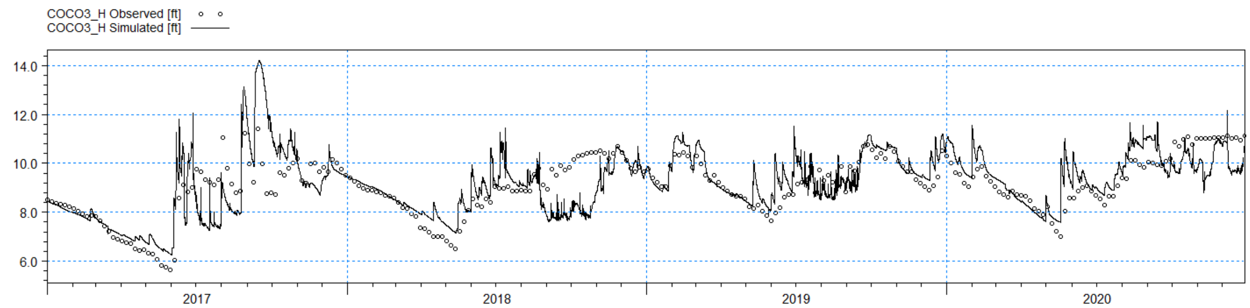

Figure 11-55. Simulated Versus Observed Stages (ft-NAVD) at COCO3 Headwater Station

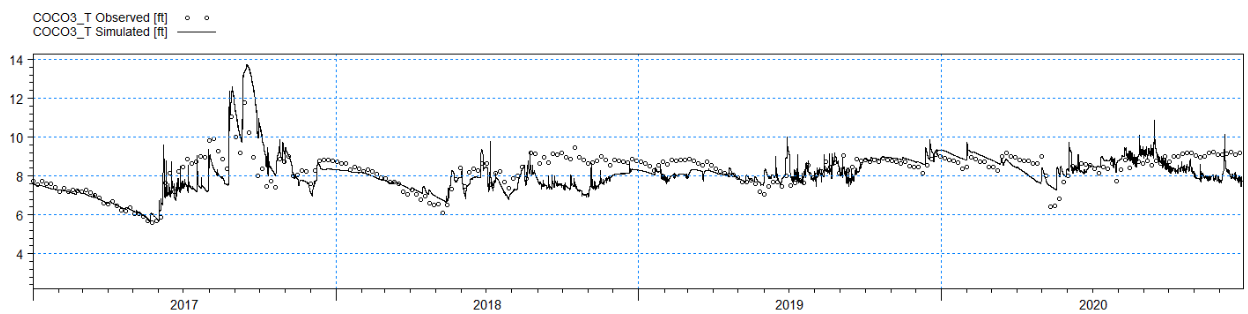

Figure 11-56. Simulated Versus Observed Stages (ft-NAVD) at the COCO3 Tailwater Station

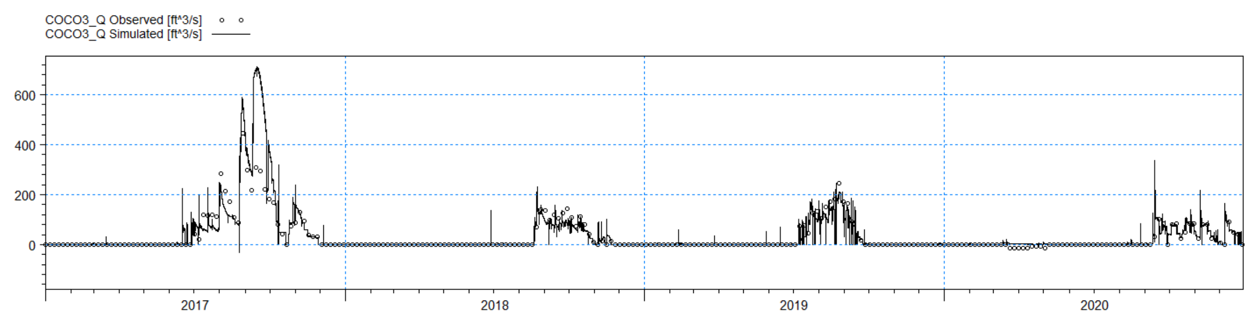

Figure 11-57. Simulated Versus Observed Flow (cfs) at the COCO3 Station (Spillway +Weir)

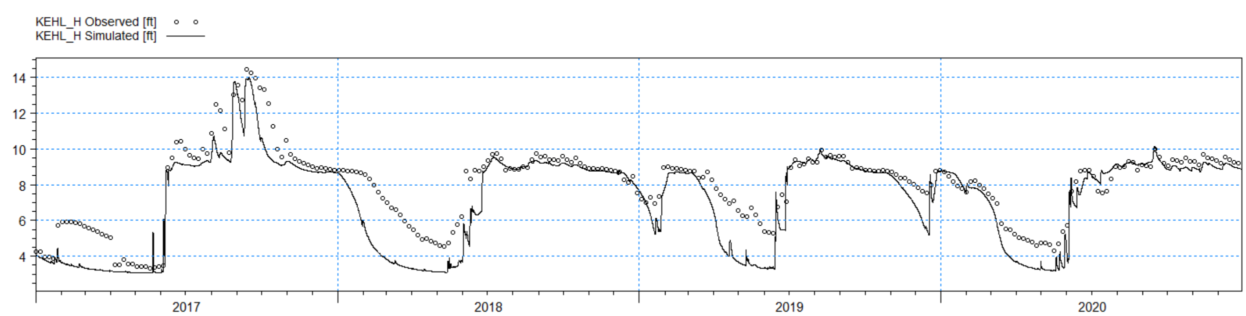

Figure 11-58. Simulated Versus Observed Stages (ft-NAVD) at Kehl Canal Headwater Station

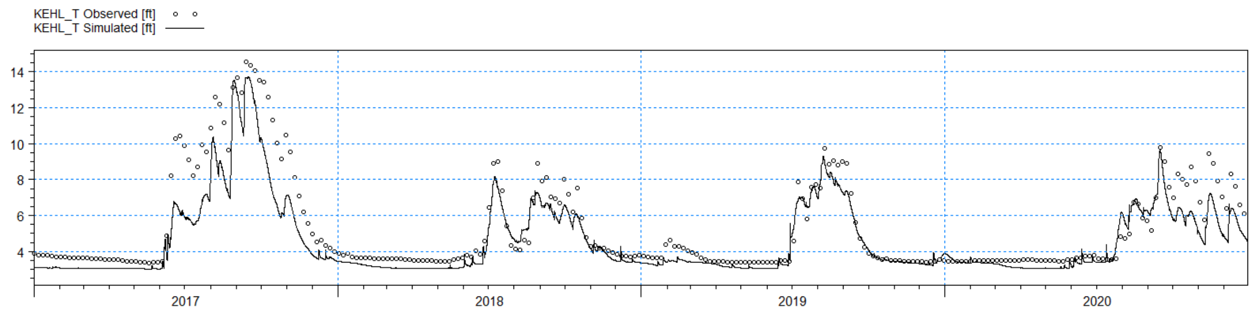

Figure 11-59. Simulated Versus Observed Stages (ft-NAVD) at Kehl Canal Tailwater Station

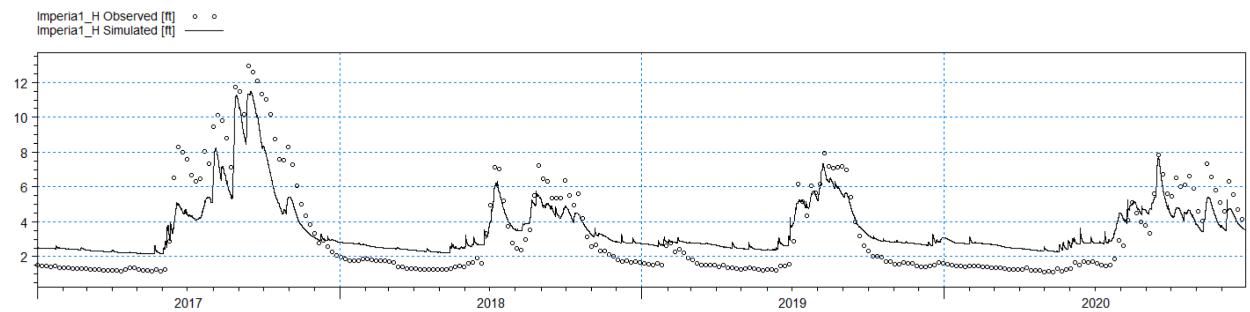

Figure 11-60. Simulated Versus Observed Stages (ft-NAVD) at Imperial River Station

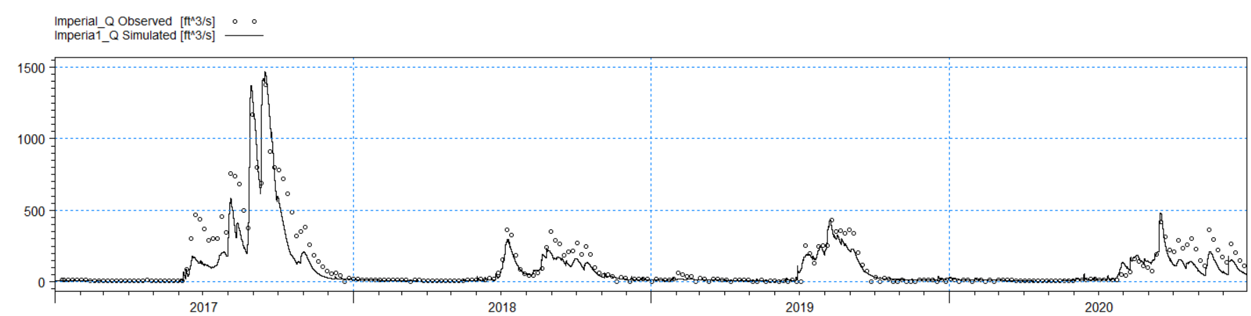

Figure 11-61. Simulated Versus Observed Flow (cfs) at the IMPERIAL Station

Figure 11-62 through Figure 11-64 show plots comparing simulated and observed cumulative flow for three flow locations: the COCO4 structure, the COCO3 structure, and the Imperial River flow monitoring station for the calibration period. Note that the cumulative flow calculation for COCO4 starts on 7/6/2017 because there is no COCO4 observed data available within the simulation period before this date.

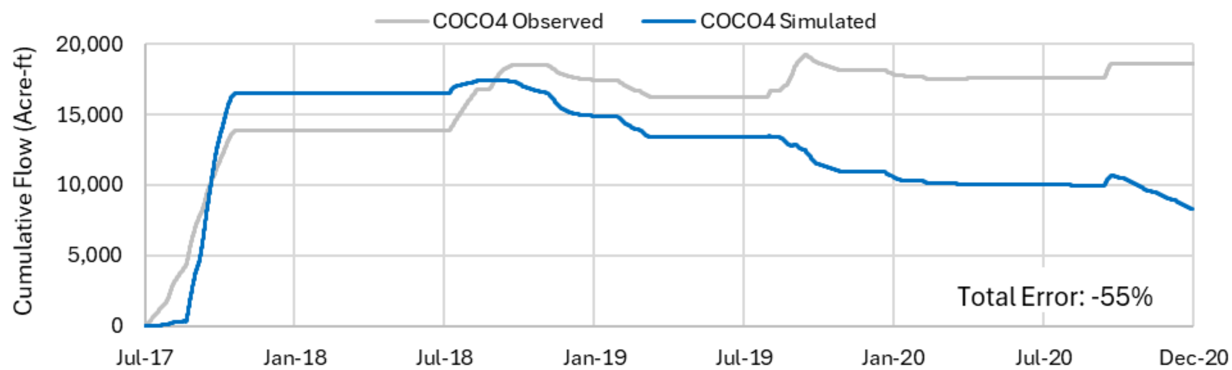

Figure 11-62. Simulated Versus Observed Cumulative Flow at the COCO4 structure.

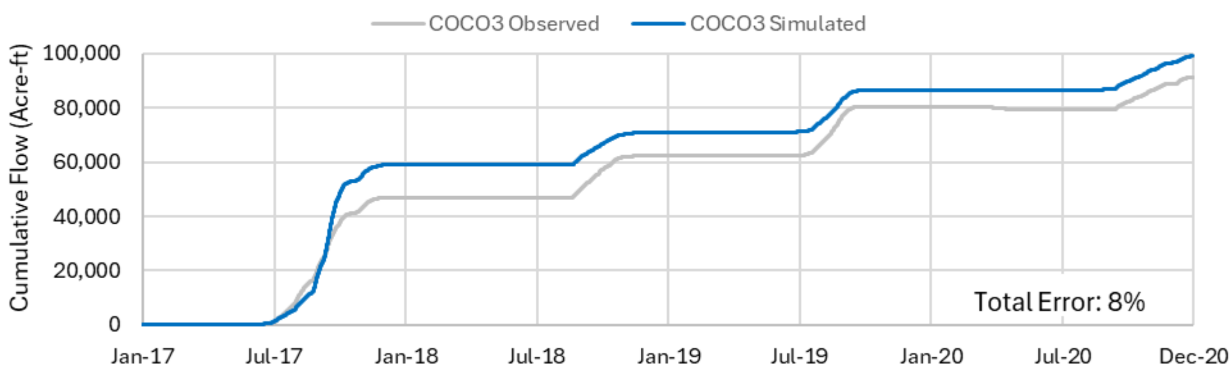

Figure 11-63. Simulated Versus Observed Cumulative Flow at the COCO3 structure.

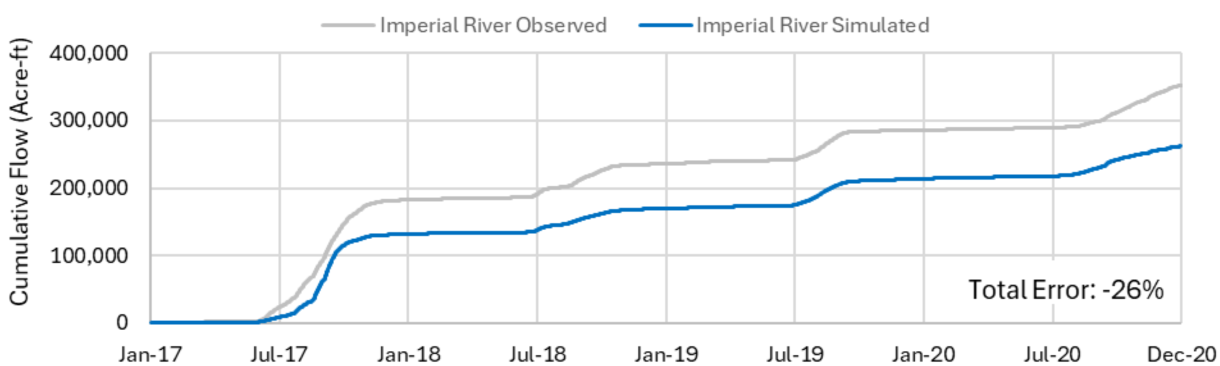

Figure 11-64. Simulated Versus Observed Cumulative Flow at the Imperial River Flow Monitoring Station.

Table 11-4 shows simulation statistics for all groundwater calibration points and Table 11-5 and Table 11-6 for show simulation statistics for all surface water calibration points for stage and flow, respectively. Simulation statistics were generated in MIKE SHE for the January 1, 2017 to December 31, 2020 time period at an hour frequency. Figure 11-65 shows stations that are in the southern portion of the model domain that are not shown in Figure 11-11 and Figure 11-45. Simulation statistics in Table 11-4 through Table 11-6 may vary from those shown in the calibration plots in Figure 11-12 through Figure 11-44 and Figure 11-46 through Figure 11-61 because the calibration plots show statistics for the entire simulation period June 1, 2016 through December 31, 2020, which includes the model warm up period (June 1, 2016 – January 1, 2017).

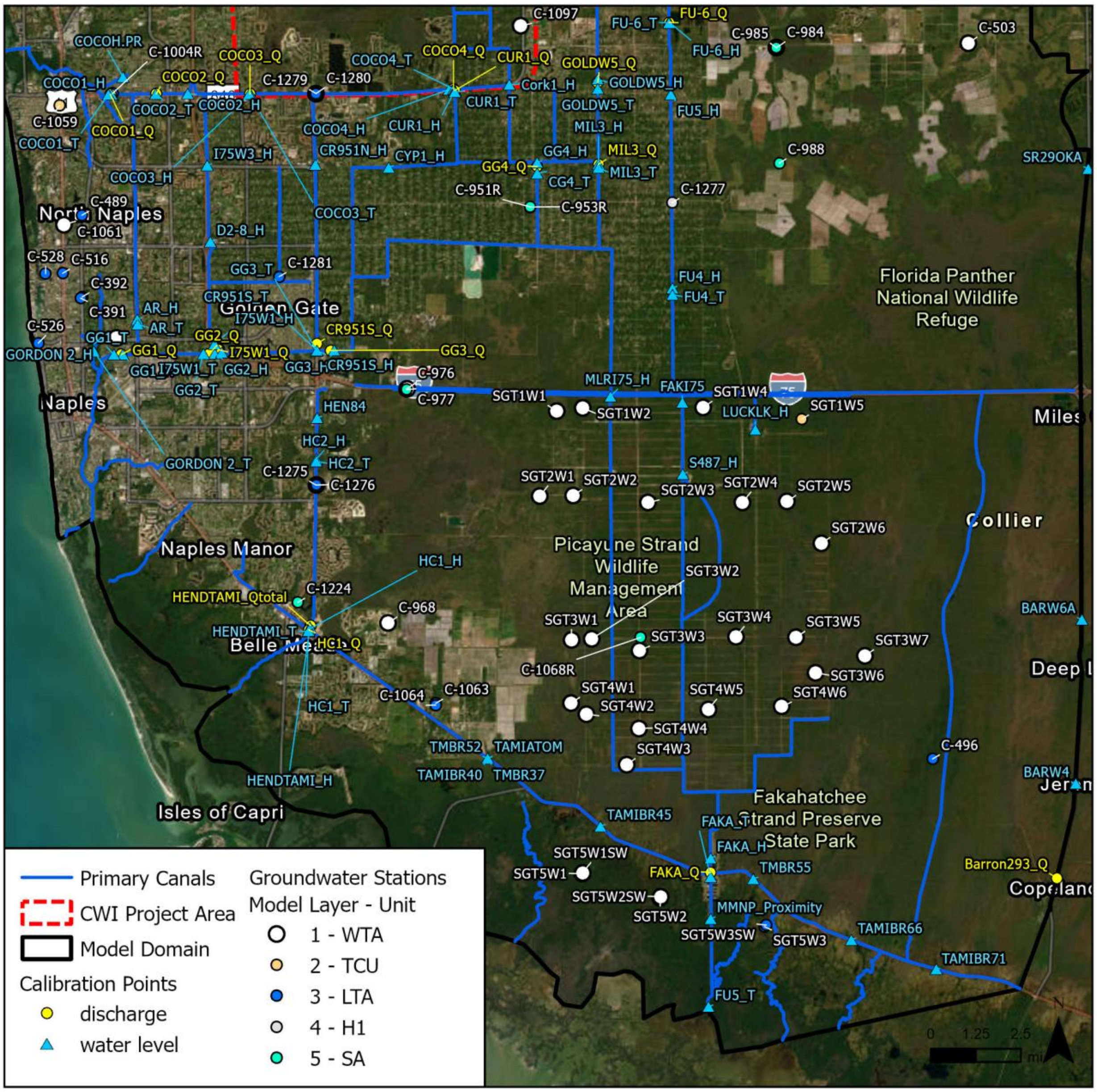

Figure 11-65. Groundwater and Surface Water Monitoring Stations with Available Data for the Calibration Period in the Southern Portion of the Model Domain, South of the CWI Project Area.

Table 11-4. Simulation Statistics for Groundwater Calibration Points within the Model Domain for the simulation period of January 1, 2017 through December 31, 2020.

Name	Layer	ME[1] (ft)	MAE[2] (ft)	RMSE[3] (ft)	STD[4]	R[5]	R2[6]
BRDROOK	1	0.6	0.6	0.7	0.5	0.95	0.76
CRKSWPS	1	-0.1	0.5	0.8	0.8	0.87	0.72
CorkscrewB	1	0.2	0.3	0.5	0.5	0.97	0.81
C-1097	1	0.2	0.3	0.5	0.4	0.95	0.88
C-1280	1	0.2	0.5	0.7	0.6	0.84	0.66
49-GW1	1	-0.3	0.6	0.7	0.6	0.86	0.40
49-GW2	1	-0.2	0.3	0.3	0.2	0.99	0.95
49-GW3	1	-0.6	0.8	1.0	0.8	0.90	0.66
49-GW4	1	0.1	0.4	0.6	0.6	0.91	0.82
WF3	1	1.0	1.1	1.3	0.9	0.86	0.27
ST1	1	1.4	1.5	1.7	0.9	0.84	-0.40
ST2	1	1.6	1.6	1.9	1.0	0.84	-0.77
L1985	1	0.3	0.5	0.8	0.7	0.93	0.82
FP2-GW1	2	0.6	0.6	0.7	0.5	0.94	0.71
49-GW5	1	-0.6	0.8	1.0	0.9	0.93	0.71
49-GW25	1	2.4	2.4	3.0	1.7	0.60	-1.22
49-GW24	1	2.7	2.7	3.0	1.4	0.69	-1.99
49-GW23	1	1.6	1.7	2.0	1.1	0.76	-0.40
49-GW6	1	-0.1	0.6	0.7	0.6	0.96	0.80
49-GW7	1	-0.5	1.1	1.3	1.2	0.63	0.21
49-GW9	1	0.9	0.9	1.1	0.6	0.92	0.29
SOCREW1	1	0.2	0.4	0.6	0.6	0.94	0.86
SOCREW2	1	0.5	0.6	0.8	0.7	0.90	0.62
49-GW10	1	0.5	0.9	1.2	1.1	0.89	0.68
49-GW8	1	-0.5	0.5	0.6	0.4	0.97	0.86
L-2195	1	0.4	0.8	1.0	0.9	0.97	0.77
47A-GW1	1	0.0	0.3	0.4	0.4	0.94	0.88
47A-GW12	1	0.0	0.1	0.1	0.1	1.00	0.99
47A-GW6	1	-0.4	0.4	0.5	0.3	0.97	0.84
47A-GW3	1	-0.2	0.5	0.6	0.5	0.91	0.78
49-GW14	1	0.0	0.5	0.6	0.6	0.90	0.81
49L-GW3	1	-0.5	1.0	1.2	1.1	0.92	0.75
49L-GW4	1	-0.7	0.8	0.9	0.5	0.95	0.67
49-GW11	1	0.7	1.3	1.8	1.7	0.77	0.50
49-GW13	1	-3.6	3.6	4.1	2.0	0.68	-1.35
49-GW17	1	0.4	1.0	1.1	1.1	0.72	-1.48
49-GW19	1	0.3	0.4	0.6	0.6	0.97	0.89
49-GW12	1	-0.7	0.7	0.9	0.6	0.90	0.56
49-GW21	1	0.7	0.7	0.9	0.5	0.91	0.59
49-GW22	1	-0.1	0.6	0.6	0.6	0.72	-25.57
L-1138	1	0.6	0.7	0.8	0.4	0.89	0.11
KIRKE_MW1	1	-1.1	1.2	1.3	0.6	0.90	0.10
KIRKE_MW2	1	-0.4	0.6	0.7	0.6	0.87	0.63
KIRKE_MW3	1	-0.1	0.5	0.6	0.6	0.89	0.76
HF1	1	-1.5	1.6	2.0	1.4	0.82	0.21

Name	Layer	ME[1] (ft)	MAE[2] (ft)	RMSE[3] (ft)	STD[4]	R[5]	R2[6]
C-1078	1	2.0	2.2	2.4	1.4	0.84	-0.13
C-984	1	1.9	1.9	2.1	1.0	0.89	-2.71
C-492	3	0.1	0.4	0.5	0.5	0.96	0.89
L-5667	2	0.9	0.9	1.0	0.5	0.91	0.36
49-GW16	3	-4.8	4.8	5.1	1.7	0.96	-2.34
L1691	3	-6.9	6.9	7.3	2.3	0.96	-3.21
L-2550	3	-0.5	0.9	1.1	1.0	0.83	0.61
C-1279	3	-5.1	5.1	5.3	1.6	0.96	-2.59
FP11-GW1	3	-0.7	0.8	1.0	0.8	0.88	0.59
L-738	3	-5.4	5.4	5.8	2.1	0.93	-2.33
L-5673	5	-8.3	8.3	8.7	2.7	0.98	-2.70
L2192	5	5.2	5.4	6.9	4.6	0.34	-46.64
L5745R	5	-7.8	7.8	8.1	2.5	0.89	-4.11
L-731	5	2.6	3.2	3.6	2.6	0.90	0.62
HF6	3	-3.1	3.2	4.4	3.1	0.65	-0.23
C-981	2	1.0	1.1	1.3	0.7	0.92	-0.41
C-1244	3	-3.3	3.5	4.9	3.7	0.69	-0.06
C-1245	3	-3.2	3.6	5.1	3.9	0.66	-0.04
SGT5W1	1	0.2	0.2	0.3	0.2	0.94	0.68
SGT5W2	1	0.0	0.2	0.2	0.2	0.93	0.86
SGT5W3	3	-0.4	0.5	0.5	0.4	0.89	0.07
C-1059	2	-0.3	0.6	0.7	0.6	0.83	0.58
C-1061	1	7.4	7.4	7.6	1.7	0.52	-155.14
SGT3W7	1	-0.1	0.6	0.7	0.7	0.93	0.81
C-503	1	0.4	0.6	0.8	0.6	0.92	0.65
SGT1W2	1	-1.3	1.4	1.5	0.7	0.92	0.03
SGT1W4	1	-0.6	0.8	0.9	0.7	0.94	0.77
SGT1W5	2	-0.5	0.7	0.8	0.6	0.94	0.76
SGT2W1	1	0.4	0.7	1.0	0.9	0.90	0.71
SGT2W2	1	-1.2	1.3	1.6	1.0	0.87	0.35
SGT2W3	1	-2.5	2.6	2.8	1.3	0.75	-2.12
SGT2W4	1	-0.3	0.7	0.9	0.8	0.91	0.81
SGT2W5	1	-0.2	0.6	0.8	0.8	0.90	0.78
SGT2W6	1	-0.2	0.8	1.0	0.9	0.86	0.65
SGT3W1	1	-1.7	1.7	1.9	0.8	0.89	-0.33
SGT3W2	1	-1.6	1.7	1.8	0.8	0.88	-0.40
SGT3W4	1	-0.4	0.8	1.0	0.9	0.93	0.81
SGT3W5	1	-0.2	0.7	0.9	0.9	0.89	0.73
SGT3W6	1	-0.1	0.7	0.9	0.9	0.90	0.74
SGT3W3	1	-2.0	2.0	2.3	1.1	0.79	-1.38
SGT4W1	1	-0.3	0.6	0.7	0.7	0.91	0.72
SGT4W2	1	-0.4	0.6	0.7	0.6	0.91	0.73
SGT4W3	1	-0.3	0.5	0.6	0.5	0.91	0.75
SGT4W4	1	0.3	0.6	0.8	0.7	0.87	0.66
SGT4W5	1	-0.6	0.8	1.0	0.7	0.93	0.74
SGT4W6	1	-0.5	0.9	1.0	0.8	0.91	0.74
C-1274	3	-0.6	0.7	0.9	0.7	0.74	-0.71

Name	Layer	ME[1] (ft)	MAE[2] (ft)	RMSE[3] (ft)	STD[4]	R[5]	R2[6]
C-489	3	-2.6	2.7	3.2	1.9	0.73	-0.52
C-968	1	1.1	1.1	1.3	0.7	0.96	0.56
SGT1W1	1	-1.1	1.2	1.4	0.8	0.91	0.21
C-976	1	-0.8	0.8	0.9	0.5	0.95	0.57
C-1276	1	-0.2	0.4	0.5	0.4	0.93	0.82
C-1004R	3	-3.6	3.6	4.0	1.8	0.94	-1.23
C-496	3	1.3	1.3	1.6	0.8	0.86	-0.31
C-953R	2	-0.2	0.6	0.8	0.8	0.90	0.65
C-1063	3	0.5	0.6	0.7	0.5	0.97	0.83
C-528	3	2.2	2.2	2.4	0.8	0.63	-23.01
C-1277	4	-0.8	0.9	1.1	0.7	0.97	0.81
C-1281	3	-1.1	1.1	1.2	0.4	0.95	0.00
C-1275	3	-0.2	0.4	0.5	0.4	0.94	0.86
C-988	5	0.7	0.8	1.0	0.7	0.96	0.85
C-1273	3	-0.7	0.7	1.0	0.6	0.82	-0.34
C-977	5	-0.6	0.7	0.9	0.6	0.92	0.63
C-1064	3	0.5	0.5	0.6	0.3	0.97	0.77
C-982	5	4.1	4.2	5.3	3.3	0.72	-1.04
C-985	5	-2.1	2.5	3.3	2.5	0.79	0.31
C-951R	5	-3.1	3.1	3.2	0.9	0.94	-1.00
C-1224	5	-0.4	0.6	0.8	0.7	0.80	0.53
C-1100	1	-2.5	2.5	2.7	0.8	0.73	-36.26
C-1068R	5	-1.7	1.7	1.9	0.9	0.85	-1.20
C-982	5	4.1	4.2	5.3	3.3	0.72	-1.04
C-516	3	3.8	3.8	3.9	0.8	0.84	-8.92
C-391	3	1.9	2.1	2.4	1.4	0.65	-0.81
C-392	2	3.3	4.7	4.9	3.6	-0.31	-3.25
C-526	3	3.1	3.1	3.2	0.8	0.26	-32.08
SGT5W3SW	3	-0.4	0.5	0.5	0.4	0.89	0.22
SGT5W2SW	1	0.1	0.2	0.3	0.3	0.89	0.74
SGT5W1SW	1	0.3	0.3	0.3	0.2	0.95	0.74

[1] ME = Mean Error. Mean Error is calculated as observed minus simulated.
[2]MAE = Mean of the Absolute Errors.
[3]RMSE = Root Mean Square Error.
[4]STD = Standard Deviation of the Residuals.
[5]R = Correlation Coefficient.
[6]R2 = The Nash-Sutcliffe coefficient.

Table 11-5. Simulation Statistics for Surface Water Stage Calibration Points within the Model Domain for the Simulation Period of January 1, 2017 through December 31, 2020.

Name	ME[1] (ft)	MAE[2] (ft)	RMSE[3] (ft)	STD[4]	R[5]	R2[6]
CRKSWPS	0.3	0.9	1.0	1.0	0.82	0.51
BRDROOK	0.6	0.7	0.8	0.5	0.95	0.75
Cork3_H	0.1	1.0	1.2	1.2	0.80	0.31
Cork2_H	-0.5	1.2	1.5	1.4	0.57	-0.53

Name	ME[1] (ft)	MAE[2] (ft)	RMSE[3] (ft)	STD[4]	R[5]	R2[6]
Cork1_H	-0.6	1.0	1.2	1.0	0.87	0.40
COCO4_H	0.1	0.7	0.9	0.9	0.74	0.37
COCO4_T	-0.4	0.8	1.0	1.0	0.88	0.45
CUR1_H	-0.3	0.9	1.1	1.0	0.88	0.42
CUR1_T	0.2	0.5	0.6	0.6	0.85	0.20
COCO3_H	0.0	0.7	0.9	0.9	0.70	0.38
COCO3_T	0.2	0.6	0.8	0.8	0.65	0.16
COCO2_H	0.4	0.8	1.0	1.0	0.47	-0.41
COCO2_T	0.3	0.6	0.8	0.7	0.27	-0.60
COCO1_H	0.6	0.8	0.9	0.7	0.47	-1.02
COCO1_T	-0.3	0.3	0.4	0.3	0.92	0.73
COCOH.PR	-0.1	0.5	0.5	0.5	0.26	0.03
KEHL_H	0.8	0.9	1.3	1.0	0.92	0.61
KEHL_T	0.7	0.8	1.2	1.0	0.94	0.79
Imperia1_H	-0.3	1.2	1.3	1.3	0.94	0.76
Lake Trafford	-0.7	0.7	0.9	0.6	0.78	0.10
Keais846	0.1	0.5	0.6	0.6	0.84	0.64
GG7_H	0.0	0.1	0.2	0.2	0.98	0.95
GG6_H	0.1	0.1	0.3	0.2	0.96	0.91
GOLDW5_H	1.2	1.2	1.3	0.6	0.36	-11.42
GOLDW5_T	0.7	0.8	1.0	0.7	0.80	-0.31
GG4_H	0.7	0.8	0.9	0.5	0.86	-0.09
CG4_T	-0.6	0.7	0.9	0.7	0.79	0.35
MIL3_H	0.7	0.8	0.9	0.5	0.86	-0.09
MIL3_T	-0.6	0.9	1.0	0.8	0.81	0.49
CYP1_H	0.6	0.7	0.8	0.5	0.85	0.03
GG3_H	-0.8	0.8	1.0	0.6	0.87	0.28
GG3_T	-0.3	0.3	0.5	0.4	0.93	0.60
GG2_H	0.0	0.1	0.2	0.2	0.95	0.89
GG2_T	0.0	0.2	0.3	0.3	0.93	0.85
GG1_H	0.0	0.1	0.2	0.2	0.97	0.95
GG1_T	0.1	0.3	0.4	0.4	0.90	0.79
CR951N_H	-0.8	1.2	1.6	1.3	0.57	0.08
CR951S_H	1.1	1.2	1.4	0.9	0.68	-0.48
CR951S_T	-0.2	0.3	0.4	0.4	0.92	0.62
I75W3_H	0.1	0.3	0.5	0.5	0.59	0.31
D2-8_H	-0.1	0.3	0.5	0.5	0.57	0.23
I75W1_H	0.0	0.4	0.6	0.6	0.50	0.18
I75W1_T	-0.1	0.1	0.3	0.3	0.93	0.84
AR_H	2.8	2.8	3.0	1.0	0.40	-10.42
AR_T	-0.1	0.1	0.3	0.3	0.93	0.83
GORDON 2_H	-1.2	1.2	1.4	0.7	0.58	-2.11
GORDON 2_T	0.1	0.4	0.5	0.5	0.87	0.72
FU7_H	0.4	1.1	1.5	1.4	-0.08	-1.79
FU-6_H	0.2	0.2	0.5	0.4	0.80	-0.06
FU-6_T	0.8	0.8	1.2	0.9	0.81	-1.20

Name	ME[1] (ft)	MAE[2] (ft)	RMSE[3] (ft)	STD[4]	R[5]	R2[6]
FU5_H	0.8	0.8	1.3	1.0	0.83	-1.07
FU5_T	7.6	7.6	7.8	1.6	0.42	-18.16
FU4_H	0.0	0.2	0.5	0.5	0.97	0.94
FU4_T	0.1	0.6	0.9	0.9	0.69	0.39
FAKI75	0.0	0.5	0.7	0.7	0.70	0.48
S487_H	3.4	3.5	3.7	1.4	0.47	-6.26
LUCKLK_H	-1.3	1.4	1.7	1.1	0.51	-0.95
MLRI75_H	-1.0	1.0	1.1	0.5	0.90	-0.07
FAKA_H	0.0	0.3	0.5	0.5	0.74	0.52
FAKA_T	0.0	0.1	0.2	0.2	0.98	0.95
HEN84	0.2	0.7	0.9	0.8	0.94	0.83
HC2_H	1.1	1.2	1.4	0.9	0.86	0.07
HC2_T	1.1	1.1	1.2	0.6	0.83	-0.33
HENDTAMI_H	-0.1	0.5	0.7	0.7	0.84	0.68
HENDTAMI_T	-0.1	0.6	0.7	0.7	0.61	0.05
HC1_H	-0.1	0.5	0.7	0.7	0.84	0.68
HC1_T	-0.1	0.6	0.7	0.7	0.61	0.04
TAMIATOM	0.5	0.7	0.9	0.7	0.86	0.50
TAMIBR40	-0.5	0.5	0.6	0.3	0.93	0.54
TAMIBR66	0.3	0.4	0.5	0.4	0.00	-5.11E+10 [7]
TAMIBR45	0.6	0.8	0.9	0.7	0.34	-0.93
TAMIBR71	0.0	0.4	0.5	0.5	0.72	0.50
TMBR37	-0.1	0.4	0.5	0.5	0.91	0.80
TMBR52	-0.4	0.4	0.5	0.3	0.93	0.36
TMBR55	-0.1	0.4	0.5	0.5	0.58	0.31
SR29OKA	-1.7	1.7	2.0	0.9	0.88	-0.11
BARW6A	-0.3	0.9	1.1	1.1	0.66	-0.18
BARW4	-0.4	1.0	1.2	1.1	0.72	0.32
MMNP	0.0	0.2	0.3	0.3	0.96	0.91

[1] ME = Mean Error. Mean Error is calculated as observed minus simulated.
[2]MAE = Mean of the Absolute Errors.
[3]RMSE = Root Mean Square Error.
[4]STD = Standard Deviation of the Residuals.
[5]R = Correlation Coefficient.
[6]R2 = The Nash-Sutcliffe coefficient.
[7] Small number of observations causes low R2

Table 11-6. Simulation Statistics for Surface Water Flow Calibration Points within the Model Domain for the Simulation Period of January 1, 2017 through December 31, 2020.

Name	ME[1] (cfs)	MAE[2] (cfs)	RMSE[3] (cfs)	STD[4]	R[5]	R2[6]
COCO4_Q	5	11	24	24	0.74	0.13
CUR1_Q	-9	13	22	20	0.91	0.76
COCO3_Q	-2	14	44	44	0.88	0.65
COCO2_Q	12	29	62	60	0.90	0.79
COCO1_Q	6	22	54	54	0.92	0.84

Name	ME[1] (cfs)	MAE[2] (cfs)	RMSE[3] (cfs)	STD[4]	R[5]	R2[6]
KEHL_Q	-59	101	360	355	-0.64	-1.71
Imperia1_Q	31	45	89	83	0.92	0.83
GOLDW5_Q	-16	18	30	25	0.48	-2.03
GG4_Q	-91	92	136	101	0.47	-29.40
MIL3_Q	38	40	97	90	0.23	-0.14
GG3_Q	-73	91	194	180	0.93	0.52
GG2_Q	-86	134	272	258	0.89	0.57
GG1_Q	-50	98	233	228	0.90	0.74
CR951S_Q	-14	17	52	50	0.47	-2.61
I75W1_Q	-19	27	82	79	0.40	-2.20
FU-6_Q	38	43	162	157	0.05	-0.06
FAKA_Q	200	233	333	266	0.84	0.52
HENDTAMI_Q	-62	62	94	72	0.72	-13.57
HC1_Q	-49	49	72	53	0.86	-1.56
Barron293_Q	-135	135	156	79	0.85	-15.45

[1] ME = Mean Error. Mean Error is calculated as observed minus simulated.
[2]MAE = Mean of the Absolute Errors.
[3]RMSE = Root Mean Square Error.
[4]STD = Standard Deviation of the Residuals.
[5]R = Correlation Coefficient.
[6]R2 = The Nash-Sutcliffe coefficient.

11.5 Basin Water Balance

This section shows simulated water balances for the calibration period for six of the project area basins (as delineated by the AHED Sub-Watersheds spatial dataset) shown in Figure 11-66. The water balance components were summarized for seven periods starting in June 1, 2017 until October 31, 2020 (four wet seasons and three dry seasons), shown in Table 11-7. The terms in the water balance tables are described in Table 11-8 and are illustrated in Figure 11-67. The values provided in the water balance tables are in both depths averaged over the basin areas and in volumes.

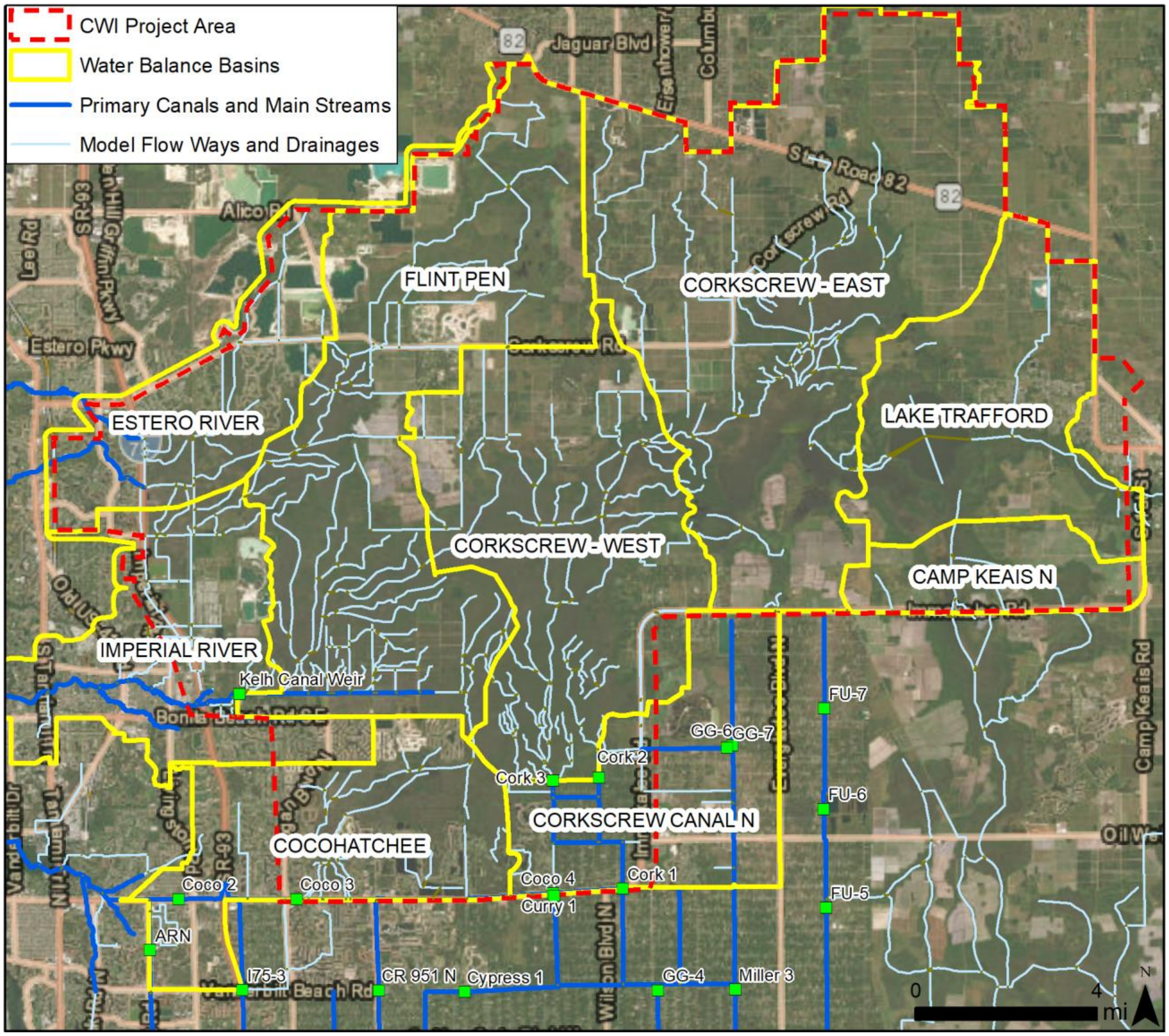

Figure 11-66. Water Balance Basins (AHED Sub-watersheds)

Table 11-7. Water Balance Seasonal Periods (For Water Balance Tables)

Season ID	Period
1	June 1 to October 31, 2017
2	November 1, 2017 to May 31, 2018
3	June 1 to October 31, 2018
4	November 1, 2018 to May 31, 2019
5	June 1 to October 31, 2019
6	November 1, 2019 to May 31, 2020
7	June 1 to October 31, 2020

Table 11-8. Water Balance Table Acronyms and Descriptions

Water Balance Table Acronym		Description (sign convention)[1]
Inflows (positive)	Rain	Total rainfall for water balance period (negative)
	OL Bnd	Overland flow basin boundary inflow
	SZ Bnd	Saturated Zone basin boundary inflow
	Irrig.	Irrigation
	MH to SZ	Surface water (MIKE HYDRO) recharge to groundwater
Outflows (negative)	ET	Total actual evapotranspiration calculated by the model
	OL Bnd	Overland flow basin boundary outflow
	SZ Bnd	Saturated Zone basin boundary outflow
	Pumping	Total groundwater pumping
	OL to MH[2]	Overland flow to MIKE HYDRO, combined term: net inflow if positive, net outflow if negative.
	SZ to MH	Baseflow to surface water (MIKE HYDRO)
	PD to MH	Ponded drainage (urban areas) to MIKE HYDRO
	SZ D to MH	Groundwater drainage (farm areas) to MIKE HYDRO
Change in Storage	OL dS	Change in overland storage
	SZ dS	Change in groundwater storage
	PD dS	Change in drainage storage
Totals	Total In	Total inflows (positive)
	Total Out	Total outflows (negative)
	dS	Total change in storage, positive increases, negative decreases
	Error[3]	Total In + Total Out - dS

[1] The inflows and outflow signs have been reversed from the MIKE SHE water balance sign convention
[2] This term combines both the inflows and outflows, whereas the baseflows are separated.
[3] May be larger than the numerical error calculated by MIKE SHE due to smaller terms that were excluded.

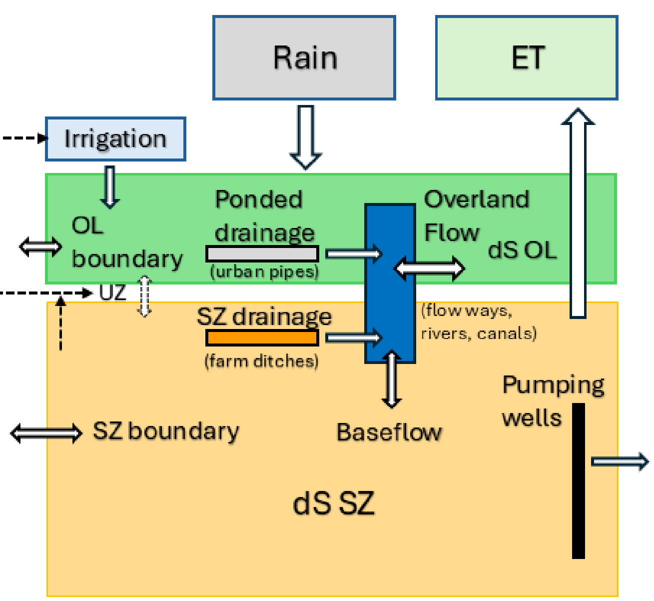

Figure 11-67. Water Balance Components

Note that exchanges between overland, unsaturated zone and saturated zone or in between groundwater layers are not included separately in the water balance extraction that is shown the tables below. Those terms can be extrated if necessary in more detailed water balance extractions.

A plot of the monthly rainfall depths for the calibration period (January 1, 2017 – December 31, 2020) averaged over the Corkscrew West and Flint Pen basins is shown in Figure 11-68.

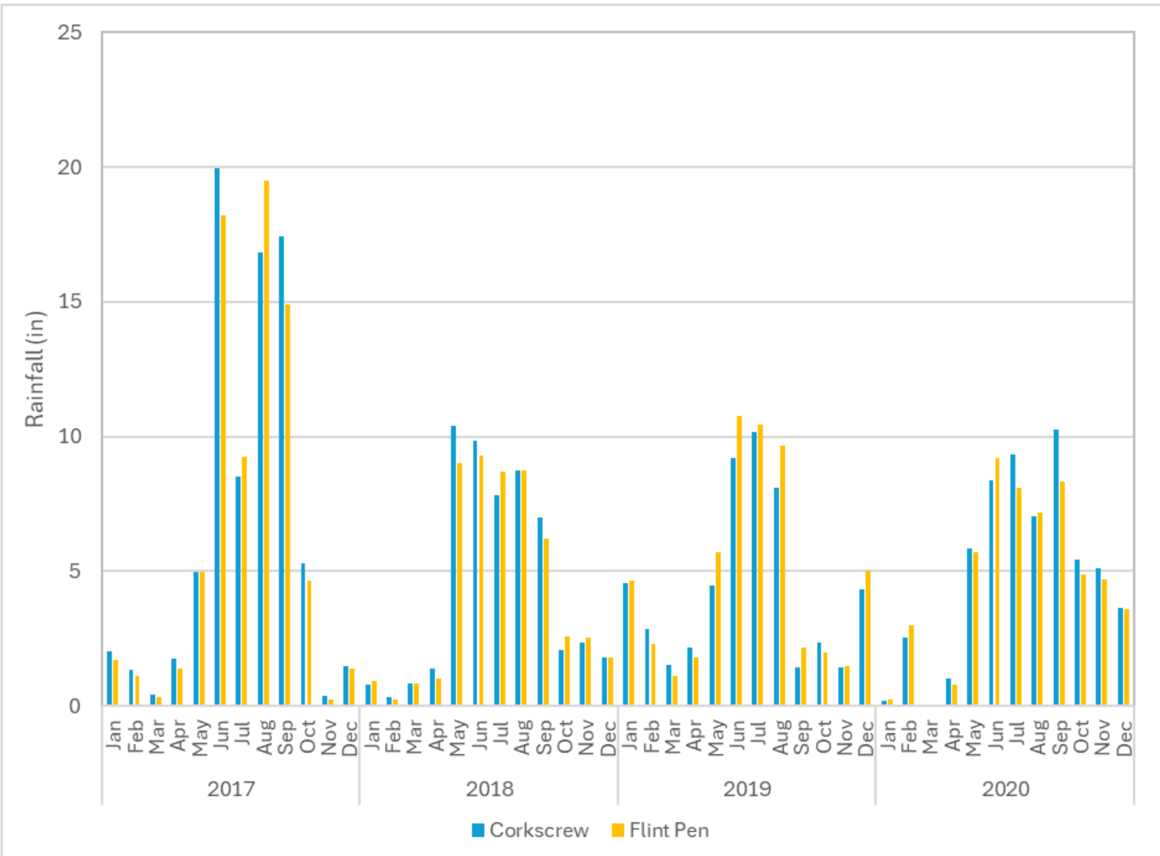

Figure 11-68. Monthly Rainfall for the Simulation Period (January 1, 2017 – December 31, 2020) in Corkscrew and Flint Pen Basins.

Table 11-9 and Table 11-10 show the water balances for the Corkscrew East sub-watershed as depths and volumes, respectively. Table 11-11 and Table 11-12 show the water balances for the Corkscrew West sub-watershed as depths and volumes, respectively. Table 11-13 and Table 11-14 show the water balances for the Flint Pen sub-watershed as depths and volumes, respectively. Table 11-15 and Table 11-16 show the water balances for the Imperial River sub-watershed as depths and volumes, respectively. Table 11-17 and Table 11-18 show the water balances for the Corkscrew Canal N sub-watershed as depths and volumes, respectively. Table 11-19 and Table 11-20 show the water balances for the Cocohatchee sub-watershed as depths and volumes, respectively. Table 11-21 and Table 11-22 show the water balances for the Lake Trafford sub-watershed as depths and volumes, respectively. Table 11-23 and Table 11-24 show the water balances for the Camp Keais N sub-watershed as depths and volumes, respectively. Table 11-25 and Table 11-26 show the water balances for the Estero sub-watershed as depths and volumes, respectively. Note that portions of Estero and Imperial are outside the model domain.

Table 11-9. Corkscrew East Basin Water Balance Depth (inches), Basin Area 48,382 Acres

Season[1]	Inflows					Outflows								Storage			Total			
	Rain	OL Bnd	SZ Bnd	Irrig	MH to SZ	ET	OL Bnd	SZ Bnd	Pump	OL to MH	SZ to MH	PD to MH	SZ D to MH	OL dS	SZ dS	PD dS	Total In	Total Out	dS	Error
1	67.2	2.4	1.5	0.8	0.2	-24.2	-5.7	-2.5	-0.4	-11.4	-1.6	-0.6	-6.3	3.8	14.2	0.0	72.1	-52.6	17.9	1.5
2	15.9	0.1	2.8	4.9	0.9	-23.8	-0.5	-3.3	-6.1	0.5	-1.1	-0.1	-0.8	-3.5	-6.8	0.0	24.6	-35.2	-10.3	-0.3
3	35.5	0.2	1.3	1.1	0.2	-23.4	-1.2	-2.2	-1.0	-2.1	-1.4	-0.1	-2.0	1.0	3.4	0.0	38.3	-33.4	4.4	0.4
4	20.6	0.0	2.4	3.6	0.5	-24.0	-0.1	-3.4	-4.7	0.8	-1.1	0.0	-0.6	-1.1	-5.0	0.0	27.1	-33.2	-6.1	0.0
5	30.7	0.2	1.6	1.7	0.3	-20.7	-1.0	-2.1	-2.3	-1.6	-1.1	-0.1	-1.5	0.6	2.9	0.0	34.4	-30.5	3.5	0.4
6	15.4	0.1	2.5	5.9	0.9	-22.7	-0.1	-3.5	-5.6	0.6	-0.8	0.0	-0.3	-0.7	-6.8	0.0	24.9	-32.4	-7.6	0.0
7	40.6	0.2	1.4	2.1	0.3	-21.3	-1.0	-2.0	-1.6	-3.0	-1.1	-0.1	-2.0	1.8	10.3	0.0	44.6	-32.1	12.0	0.4

[1]Wet periods are shaded in blue, dry periods are shaded in orange

Table 11-10. Corkscrew East Basin Water Balance Volume (acre-ft), Basin Area 48,382 Acres

Season[1]	Inflows					Outflows								Storage			Total			
	Rain	OL Bnd	SZ Bnd	Irrig	MH to SZ	ET	OL Bnd	SZ Bnd	Pump	OL to MH	SZ to MH	PD to MH	SZ D to MH	OL dS	SZ dS	PD dS	Total In	Total Out	dS	Error
1	271,057	9,688	6,200	3,066	754	-97,512	-23,102	-9,899	-1,723	-46,019	-6,250	-2,487	-25,201	15,152	57,158	39	290,765	-212,192	72,349	6,224
2	64,095	270	11,312	19,686	3,799	-95,907	-2,012	-13,179	-24,770	1,998	-4,294	-227	-3,388	-14,299	-27,254	-27	99,162	-141,779	-41,580	-1,037
3	143,228	735	5,262	4,296	705	-94,480	-4,983	-8,989	-4,189	-8,315	-5,607	-278	-8,020	4,182	13,657	7	154,227	-134,859	17,846	1,522
4	83,135	129	9,517	14,406	2,083	-96,586	-573	-13,816	-18,905	3,121	-4,569	-137	-2,536	-4,286	-20,329	-10	109,269	-134,001	-24,625	-107
5	123,672	718	6,458	6,797	1,072	-83,504	-4,025	-8,554	-9,437	-6,462	-4,598	-229	-6,195	2,370	11,867	5	138,718	-123,004	14,241	1,472
6	62,251	420	10,101	23,649	3,778	-91,560	-413	-13,957	-22,758	2,495	-3,047	-95	-1,289	-2,998	-27,451	-6	100,198	-130,624	-30,456	29
7	163,681	864	5,606	8,511	1,131	-85,685	-4,007	-8,231	-6,613	-12,144	-4,361	-217	-8,246	7,144	41,356	4	179,793	-129,503	48,504	1,786

[1]Wet periods are shaded in blue, dry periods are shaded in orange

Table 11-11. Corkscrew West Basin Water Balance Depth (inches), Basin Area 28,437 Acres

Season[1]	Inflows					Outflows								Storage			Total			
	Rain	OL Bnd	SZ Bnd	Irrig	MH to SZ	ET	OL Bnd	SZ Bnd	Pump	OL to MH	SZ to MH	PD to MH	SZ D to MH	OL dS	SZ dS	PD dS	Total In	Total Out	dS	Error
1	69.5	8.9	2.5	0.5	3.5	-21.1	-13.2	-3.3	-0.4	-22.1	-2.0	-2.5	-3.8	2.6	13.6	0.1	85.0	-68.3	16.2	0.4
2	15.1	0.8	3.2	3.4	3.2	-23.7	-1.1	-4.9	-4.5	3.1	-0.9	-0.3	-3.0	-2.5	-6.5	-0.1	25.8	-35.3	-9.1	-0.4
3	35.2	2.1	2.0	0.8	2.1	-20.7	-1.6	-3.3	-0.6	-5.5	-2.5	-0.5	-2.8	0.5	4.3	0.0	42.3	-37.5	4.8	0.0
4	18.0	0.2	2.8	2.8	2.0	-24.8	-1.1	-4.8	-3.4	5.1	-1.5	-0.2	-3.1	-0.6	-7.2	0.0	25.8	-33.7	-7.8	-0.1
5	32.3	1.7	2.1	1.1	2.1	-18.4	-1.6	-3.2	-0.8	-3.8	-2.1	-0.4	-2.7	0.2	6.0	0.0	39.2	-33.1	6.2	0.0
6	15.1	0.2	2.9	3.7	1.9	-22.8	-1.1	-4.7	-3.6	6.0	-1.0	-0.1	-2.9	0.0	-6.6	0.0	23.7	-30.3	-6.6	0.0
7	40.1	1.7	1.9	1.2	1.7	-18.9	-1.8	-3.1	-0.8	-5.6	-2.2	-0.6	-2.8	1.4	9.1	0.0	46.5	-35.8	10.5	0.2

[1]Wet periods are shaded in blue, dry periods are shaded in orange

Table 11-12. Corkscrew West Basin Water Balance Volume (acre-ft), Basin Area 28,437 Acres

Season[1]	Inflows					Outflows								Storage			Total			
	Rain	OL Bnd	SZ Bnd	Irrig	MH to SZ	ET	OL Bnd	SZ Bnd	Pump	OL to MH	SZ to MH	PD to MH	SZ D to MH	OL dS	SZ dS	PD dS	Total In	Total Out	dS	Error
1	164,780	21,178	5,874	1,257	8,391	-50,105	-31,168	-7,796	-890	-52,303	-4,658	-6,018	-9,017	6,157	32,145	170	201,481	-161,956	38,472	1,053
2	35,809	1,981	7,681	7,973	7,667	-56,050	-2,554	-11,599	-10,746	7,299	-2,218	-724	-7,135	-5,965	-15,459	-169	61,112	-83,727	-21,593	-1,022
3	83,512	4,929	4,816	2,001	5,021	-49,001	-3,807	-7,810	-1,352	-13,074	-5,999	-1,199	-6,735	1,279	10,085	25	100,279	-88,976	11,388	-86
4	42,640	539	6,617	6,579	4,805	-58,822	-2,498	-11,328	-8,078	12,005	-3,501	-409	-7,256	-1,482	-16,988	-29	61,180	-79,887	-18,499	-208
5	76,564	3,961	4,992	2,507	4,887	-43,700	-3,679	-7,571	-1,963	-9,026	-4,982	-1,006	-6,434	440	14,127	9	92,910	-78,361	14,577	-27
6	35,749	400	6,813	8,878	4,409	-54,089	-2,521	-11,224	-8,591	14,144	-2,457	-293	-6,809	-49	-15,564	0	56,249	-71,841	-15,612	21
7	94,931	3,977	4,387	2,749	4,040	-44,719	-4,199	-7,445	-1,823	-13,194	-5,331	-1,449	-6,653	3,313	21,521	45	110,083	-84,814	24,879	390

[1]Wet periods are shaded in blue, dry periods are shaded in orange

Table 11-13. Flint Pen Basin Water Balance Depth (inches), Basin Area 37,507 Acres

[1]Season	Inflows					Outflows								Storage			Total			
	Rain	OL Bnd	SZ Bnd	Irrig	MH to SZ	ET	OL Bnd	SZ Bnd	Pump	OL to MH	SZ to MH	PD to MH	SZ D to MH	OL dS	SZ dS	PD dS	Total In	Total Out	dS	Error
1	66.5	6.7	1.8	0.4	1.2	-20.6	-2.5	-3.2	-1.7	-24.5	-5.7	-0.7	-1.6	2.2	13.5	0.0	76.6	-60.4	15.7	0.4
2	13.7	0.7	3.3	2.5	1.7	-21.1	0.0	-3.7	-5.0	-0.8	-0.8	-0.1	-0.5	-2.1	-7.5	0.0	21.9	-31.9	-9.6	-0.3
3	35.5	1.0	1.7	0.5	1.2	-19.9	-0.2	-2.8	-1.8	-4.5	-4.0	-0.1	-0.9	0.5	5.1	0.0	39.9	-34.3	5.6	0.0
4	19.9	0.8	3.0	1.7	2.2	-23.4	0.0	-3.3	-4.8	-1.2	-0.8	-0.1	-0.5	-0.4	-6.1	0.0	27.6	-34.1	-6.5	0.0
5	35.0	1.0	1.7	0.5	1.1	-17.8	-0.4	-2.8	-2.1	-6.0	-3.7	-0.2	-1.0	0.4	5.0	0.0	39.4	-34.0	5.4	0.0
6	16.1	0.7	3.1	2.7	1.8	-21.0	0.0	-3.3	-5.5	-1.0	-0.7	0.0	-0.4	-0.4	-7.2	0.0	24.3	-31.9	-7.6	0.0
7	37.7	1.1	1.6	0.9	1.4	-18.3	-0.2	-2.5	-2.3	-4.7	-3.8	-0.2	-0.8	0.7	9.3	0.0	42.7	-32.7	9.9	0.1

[1]Wet periods are shaded in blue, dry periods are shaded in orange

Table 11-14. Flint Pen Basin Water Balance Volume (acre-ft), Basin Area 37,507 Acres

[1]Season	Inflows					Outflows								Storage			Total			
	Rain	OL Bnd	SZ Bnd	Irrig	MH to SZ	ET	OL Bnd	SZ Bnd	Pump	OL to MH	SZ to MH	PD to MH	SZ D to MH	OL dS	SZ dS	PD dS	Total In	Total Out	dS	Error
1	207,875	20,947	5,555	1,163	3,754	-64,446	-7,709	-9,887	-5,212	-76,632	-17,790	-2,266	-4,981	6,877	42,192	58	239,295	-188,921	49,127	1,247
2	42,751	2,310	10,198	7,958	5,369	-65,823	-65	-11,523	-15,695	-2,443	-2,544	-184	-1,473	-6,597	-23,439	-55	68,587	-99,750	-30,092	-1,071
3	110,954	3,178	5,238	1,669	3,632	-62,213	-518	-8,863	-5,547	-14,155	-12,648	-466	-2,769	1,482	16,079	4	124,672	-107,179	17,564	-72
4	62,141	2,477	9,351	5,355	6,832	-73,083	-141	-10,285	-14,881	-3,824	-2,544	-240	-1,544	-1,327	-18,927	-2	86,157	-106,540	-20,256	-127
5	109,413	3,164	5,359	1,610	3,574	-55,732	-1,231	-8,746	-6,483	-18,782	-11,545	-613	-3,141	1,140	15,666	0	123,120	-106,273	16,806	41
6	50,406	2,164	9,662	8,303	5,502	-65,540	-66	-10,372	-17,266	-3,003	-2,080	-146	-1,355	-1,322	-22,503	8	76,037	-99,827	-23,818	27
7	117,780	3,423	5,156	2,769	4,342	-57,241	-531	-7,671	-7,284	-14,609	-11,875	-499	-2,537	2,060	29,009	-4	133,470	-102,246	31,065	158

[1]Wet periods are shaded in blue, dry periods are shaded in orange

Table 11-15. Imperial River Basin Water Balance Depth (inches), Basin Area 17,902 Acres[2]

Season[1]	Inflows					Outflows								Storage			Total			
	Rain	OL Bnd	SZ Bnd	Irrig	MH to SZ	ET	OL Bnd	SZ Bnd	Pump	OL to MH	SZ to MH	PD to MH	SZ D to MH	OL dS	SZ dS	PD dS	Total In	Total Out	dS	Error
1	73.6	3.5	35.0	3.2	0.2	-20.5	-1.0	-33.3	-0.9	-17.2	-6.4	-18.5	-1.5	2.5	13.2	0.3	115.5	-99.4	16.0	0.2
2	13.1	0.2	44.0	12.7	0.2	-23.8	-0.1	-42.9	-3.7	-1.7	-4.6	-3.7	-0.1	-2.3	-7.7	-0.3	70.2	-80.6	-10.2	-0.2
3	31.9	0.3	33.1	5.3	0.2	-19.6	-0.2	-31.1	-1.3	-3.7	-4.4	-5.7	-0.1	0.8	3.8	0.1	70.8	-66.2	4.6	0.0
4	16.7	0.3	44.7	11.6	0.3	-24.0	-0.1	-43.1	-3.3	-1.8	-4.6	-3.5	0.0	-0.7	-6.0	-0.1	73.6	-80.4	-6.8	-0.1
5	35.8	0.6	35.7	4.4	0.2	-17.8	-0.4	-33.7	-1.4	-5.0	-4.8	-6.7	-0.4	0.7	5.5	0.1	76.7	-70.4	6.2	0.1
6	16.4	0.3	45.2	12.1	0.2	-23.4	-0.2	-43.6	-3.4	-1.7	-4.4	-3.3	0.0	-0.8	-5.0	0.0	74.2	-80.1	-5.8	-0.1
7	39.0	0.5	34.8	4.9	0.3	-18.4	-0.4	-32.8	-1.4	-5.1	-5.0	-7.3	-0.3	1.3	7.3	0.1	79.5	-70.7	8.7	0.1

[1]Wet periods are shaded in blue, dry periods are shaded in orange
[2]Portions of the basin are outside the model domain, area shown is the area inside the model domain.

Table 11-16. Imperial River Basin Water Balance Volume (acre-ft), Basin Area 17,902 Acres

Season[1]	Inflows					Outflows								Storage			Total			
	Rain	OL Bnd	SZ Bnd	Irrig	MH to SZ	ET	OL Bnd	SZ Bnd	Pump	OL to MH	SZ to MH	PD to MH	SZ D to MH	OL dS	SZ dS	PD dS	Total In	Total Out	dS	Error
1	109,847	5,171	52,254	4,732	349	-30,650	-1,464	-49,690	-1,313	-25,689	-9,542	-27,587	-2,302	3,690	19,677	436	172,354	-148,236	23,804	313
2	19,552	372	65,653	18,887	304	-35,463	-144	-64,062	-5,567	-2,603	-6,808	-5,480	-115	-3,387	-11,467	-382	104,768	-120,241	-15,237	-236
3	47,541	509	49,327	7,877	368	-29,198	-339	-46,357	-2,003	-5,519	-6,540	-8,508	-224	1,140	5,682	98	105,622	-98,687	6,920	14
4	24,902	399	66,751	17,305	391	-35,747	-190	-64,314	-4,970	-2,644	-6,874	-5,224	-17	-1,110	-8,926	-113	109,748	-119,980	-10,148	-84
5	53,391	827	53,319	6,592	329	-26,601	-579	-50,345	-2,089	-7,529	-7,172	-10,066	-663	1,014	8,197	111	114,457	-105,044	9,322	91
6	24,518	391	67,444	18,075	334	-34,927	-250	-65,088	-5,142	-2,487	-6,592	-4,946	-45	-1,121	-7,477	-40	110,762	-119,476	-8,638	-75
7	58,249	731	51,903	7,279	400	-27,448	-574	-48,901	-2,068	-7,682	-7,439	-10,860	-508	1,984	10,853	140	118,563	-105,481	12,977	104

[1]Wet periods are shaded in blue, dry periods are shaded in orange

Table 11-17. Corkscrew Canal N Basin Water Balance Depth (inches), Basin Area 15,997 Acres

Season[1]	Inflows					Outflows								Storage			Total			
	Rain	OL Bnd	SZ Bnd	Irrig	MH to SZ	ET	OL Bnd	SZ Bnd	Pump	OL to MH	SZ to MH	PD to MH	SZ D to MH	OL dS	SZ dS	PD dS	Total In	Total Out	dS	Error
1	77.5	17.3	5.4	2.6	0.3	-20.9	-2.0	-4.7	-1.9	-19.1	-4.4	-27.9	-0.9	4.9	15.8	0.4	103.1	-81.9	21.0	0.2
2	12.9	0.1	5.6	11.8	0.4	-24.0	-0.1	-6.1	-9.4	-0.5	-2.3	-2.6	-0.2	-3.9	-9.9	-0.3	30.9	-45.1	-14.1	-0.2
3	38.7	0.5	4.7	4.3	0.3	-20.3	-0.2	-4.4	-3.4	-1.9	-3.0	-6.8	-0.2	1.8	6.1	0.2	48.5	-40.4	8.1	0.0
4	15.3	0.4	5.6	11.1	1.3	-24.0	0.0	-6.8	-9.1	0.4	-1.7	-2.3	-0.1	-1.9	-7.9	-0.2	33.7	-43.7	-9.9	0.0
5	36.7	0.7	4.8	3.8	0.5	-18.0	-0.4	-4.6	-3.2	-2.0	-2.6	-6.2	-0.2	1.6	7.5	0.1	46.5	-37.3	9.2	0.0
6	16.7	0.3	5.5	11.4	1.3	-23.6	0.0	-6.8	-9.5	0.3	-1.7	-2.4	-0.1	-1.7	-6.7	-0.1	35.3	-43.8	-8.5	0.0
7	37.6	0.7	4.5	4.2	0.7	-18.5	-0.1	-4.6	-3.4	-1.4	-2.2	-5.8	-0.2	2.4	8.7	0.3	47.7	-36.3	11.4	0.0

[1]Wet periods are shaded in blue, dry periods are shaded in orange

Table 11-18. Corkscrew Canal N Basin Water Balance Volume (acre-ft), Basin Area 15,997 Acres

Season[1]	Inflows					Outflows								Storage			Total			
	Rain	OL Bnd	SZ Bnd	Irrig	MH to SZ	ET	OL Bnd	SZ Bnd	Pump	OL to MH	SZ to MH	PD to MH	SZ D to MH	OL dS	SZ dS	PD dS	Total In	Total Out	dS	Error
1	103,334	23,052	7,229	3,484	392	-27,923	-2,622	-6,332	-2,584	-25,438	-5,859	-37,184	-1,237	6,512	21,031	472	137,491	-109,178	28,015	297
2	17,173	189	7,509	15,738	557	-31,930	-142	-8,101	-12,531	-721	-3,072	-3,483	-201	-5,209	-13,190	-365	41,167	-60,181	-18,764	-250
3	51,548	643	6,259	5,708	463	-27,085	-318	-5,919	-4,529	-2,525	-4,032	-9,130	-262	2,382	8,174	246	64,621	-53,801	10,802	18
4	20,370	548	7,480	14,808	1,782	-32,033	-16	-9,098	-12,115	524	-2,324	-3,117	-104	-2,525	-10,516	-215	44,987	-58,283	-13,256	-40
5	48,871	922	6,410	5,114	703	-24,021	-492	-6,070	-4,330	-2,723	-3,427	-8,332	-306	2,108	10,035	153	62,021	-49,701	12,296	24
6	22,241	437	7,388	15,255	1,713	-31,498	-24	-9,074	-12,692	347	-2,231	-3,152	-104	-2,301	-8,901	-175	47,034	-58,428	-11,378	-16
7	50,173	967	5,942	5,632	895	-24,652	-195	-6,123	-4,560	-1,873	-2,907	-7,773	-281	3,190	11,612	376	63,609	-48,365	15,178	66

[1]Wet periods are shaded in blue, dry periods are shaded in orange

Table 11-19. Cocohatchee Basin Water Balance Depth (inches), Basin Area 17,629 acres

Season[1]	Inflows					Outflows								Storage			Total			
	Rain	OL Bnd	SZ Bnd	Irrig	MH to SZ	ET	OL Bnd	SZ Bnd	Pump	OL to MH	SZ to MH	PD to MH	SZ D to MH	OL dS	SZ dS	PD dS	Total In	Total Out	dS	Error
1	79.7	0.8	5.0	3.6	2.9	-20.3	-11.3	-11.0	-1.2	-1.9	-5.3	-24.4	0.0	2.5	13.2	0.8	91.9	-75.3	16.5	0.1
2	13.1	0.1	3.5	10.2	2.0	-22.4	0.0	-9.9	-3.3	1.6	-1.4	-3.5	0.0	-2.0	-7.4	-0.5	28.9	-38.9	-9.9	-0.1
3	37.6	0.2	4.4	4.6	2.0	-19.4	-0.3	-7.8	-1.3	-3.3	-3.3	-8.7	0.0	0.8	4.0	0.1	48.9	-44.0	4.9	0.0
4	15.6	0.0	3.6	9.4	2.5	-22.7	-0.4	-9.3	-2.9	1.4	-1.1	-3.0	0.0	-0.8	-6.0	-0.1	31.1	-38.0	-6.9	0.0
5	40.7	0.3	4.0	4.1	2.6	-17.6	-0.4	-8.7	-1.9	-3.7	-3.6	-9.0	0.0	0.7	5.8	0.3	51.7	-44.9	6.8	0.0
6	18.4	0.0	3.3	9.7	2.4	-22.3	-0.3	-10.1	-3.4	1.3	-1.1	-2.8	0.0	-0.6	-4.1	-0.2	33.8	-38.7	-4.9	0.0
7	37.1	0.1	3.2	4.5	2.2	-18.2	-0.4	-7.9	-1.7	-2.3	-2.3	-7.0	0.0	1.1	6.0	0.3	47.2	-39.8	7.4	0.0

[1]Wet periods are shaded in blue, dry periods are shaded in orange

Table 11-20. Cocohatchee Basin Water Balance Volume (acre-ft), Basin Area 17,629 acres

Season[1]	Inflows					Outflows								Storage			Total			
	Rain	OL Bnd	SZ Bnd	Irrig	MH to SZ	ET	OL Bnd	SZ Bnd	Pump	OL to MH	SZ to MH	PD to MH	SZ D to MH	OL dS	SZ dS	PD dS	Total In	Total Out	dS	Error
1	117,097	1,161	7,354	5,253	4,199	-29,788	-16,570	-16,091	-1,811	-2,785	-7,770	-35,825	0	3,611	19,439	1,165	135,065	-110,641	24,215	209
2	19,220	98	5,130	14,971	2,978	-32,956	-49	-14,517	-4,874	2,408	-2,052	-5,153	0	-2,998	-10,817	-768	42,398	-57,193	-14,584	-211
3	55,233	290	6,524	6,799	2,970	-28,437	-371	-11,471	-1,939	-4,808	-4,777	-12,818	0	1,120	5,946	187	71,815	-64,622	7,253	-60
4	22,929	9	5,217	13,777	3,693	-33,416	-541	-13,651	-4,200	2,079	-1,669	-4,469	0	-1,216	-8,776	-196	45,625	-55,866	-10,188	-53
5	59,827	459	5,808	6,076	3,752	-25,922	-638	-12,729	-2,785	-5,396	-5,238	-13,278	0	1,059	8,491	369	75,923	-65,987	9,918	18
6	27,050	16	4,875	14,182	3,458	-32,810	-450	-14,799	-4,950	1,903	-1,644	-4,087	0	-850	-6,093	-295	49,581	-56,837	-7,237	-19
7	54,537	150	4,758	6,672	3,201	-26,672	-589	-11,534	-2,551	-3,396	-3,342	-10,357	0	1,686	8,778	407	69,318	-58,441	10,871	6

[1]Wet periods are shaded in blue, dry periods are shaded in orange

Table 11-21. Lake Trafford Basin Water Balance Depth (inches), Basin Area 18,556 acres

[1]Season	Inflows					Outflows								Storage			Total			
	Rain	OL Bnd	SZ Bnd	Irrig	MH to SZ	ET	OL Bnd	SZ Bnd	Pump	OL to MH	SZ to MH	PD to MH	SZ D to MH	OL dS	SZ dS	PD dS	Total In	Total Out	dS	Error
1	66.9	1.5	3.4	2.6	0.1	-23.6	-5.0	-3.1	-1.7	-14.6	-0.2	-3.5	-6.1	2.8	12.9	0.1	74.6	-57.9	15.8	0.9
2	13.1	0.0	4.0	7.0	0.3	-24.8	-0.1	-5.3	-5.1	1.4	-0.1	-0.7	-1.5	-2.6	-8.7	-0.1	24.5	-36.2	-11.4	-0.3
3	32.3	0.1	3.4	3.8	0.1	-22.9	-0.4	-2.6	-2.3	-2.9	-0.2	-1.1	-2.0	0.9	4.2	0.1	39.6	-34.3	5.2	0.2
4	20.5	0.1	3.9	6.4	0.1	-24.7	-0.1	-5.2	-4.6	1.1	-0.2	-0.6	-1.3	-0.7	-3.7	0.0	31.0	-35.5	-4.4	-0.1
5	28.8	0.2	3.2	3.6	0.1	-20.1	-0.4	-3.1	-2.4	-2.9	-0.2	-1.0	-1.8	0.6	3.1	0.0	35.8	-31.9	3.7	0.1
6	15.4	0.0	3.6	7.8	0.3	-23.9	0.0	-5.2	-5.3	2.3	-0.1	-0.5	-1.0	-0.9	-5.7	0.0	27.0	-33.7	-6.6	0.0
7	36.5	0.2	2.8	4.0	0.1	-20.9	-0.6	-2.7	-2.4	-4.3	-0.3	-1.2	-2.0	1.6	7.6	0.1	43.6	-34.3	9.2	0.1

[1]Wet periods are shaded in blue, dry periods are shaded in orange

Table 11-22. Lake Trafford Basin Water Balance Volume (acre-ft), Basin Area 18,556 acres

[1]Season	Inflows					Outflows								Storage			Total			
	Rain	OL Bnd	SZ Bnd	Irrig	MH to SZ	ET	OL Bnd	SZ Bnd	Pump	OL to MH	SZ to MH	PD to MH	SZ D to MH	OL dS	SZ dS	PD dS	Total In	Total Out	dS	Error
1	103,446	2,379	5,289	4,075	169	-36,464	-7,781	-4,776	-2,672	-22,563	-333	-5,444	-9,488	4,283	20,003	193	115,357	-89,521	24,478	1,358
2	20,326	62	6,238	10,874	389	-38,334	-164	-8,144	-7,961	2,212	-227	-1,040	-2,325	-3,971	-13,484	-161	37,889	-55,984	-17,616	-478
3	49,924	223	5,186	5,864	105	-35,364	-558	-4,028	-3,514	-4,423	-361	-1,745	-3,050	1,437	6,496	77	61,302	-53,044	8,010	249
4	31,703	80	6,063	9,956	167	-38,154	-115	-7,999	-7,181	1,743	-262	-961	-1,952	-1,070	-5,685	-44	47,968	-54,881	-6,799	-113
5	44,490	242	4,936	5,574	86	-31,111	-643	-4,763	-3,663	-4,537	-287	-1,588	-2,780	911	4,807	37	55,328	-49,370	5,755	203
6	23,749	45	5,490	11,986	478	-36,978	-65	-8,006	-8,160	3,600	-139	-746	-1,558	-1,406	-8,764	-74	41,747	-52,051	-10,243	-60
7	56,456	333	4,404	6,126	161	-32,264	-986	-4,185	-3,765	-6,577	-402	-1,801	-3,098	2,434	11,706	103	67,480	-53,077	14,242	160

[1]Wet periods are shaded in blue, dry periods are shaded in orange

Table 11-23. Camp Keais N Basin Water Balance Depth (inches), Basin Area 7,003 acres

Season[1]	Inflows					Outflows								Storage			Total			
	Rain	OL Bnd	SZ Bnd	Irrig	MH to SZ	ET	OL Bnd	SZ Bnd	Pump	OL to MH	SZ to MH	PD to MH	SZ D to MH	OL dS	SZ dS	PD dS	Total In	Total Out	dS	Error
1	62.1	5.5	4.7	1.7	0.6	-22.9	-1.3	-4.6	-0.9	-25.1	-0.5	0.0	-3.7	1.3	14.0	0.0	74.6	-59.0	15.3	0.3
2	14.1	0.1	7.0	6.9	1.1	-23.4	-0.1	-9.3	-5.4	-1.7	-0.1	0.0	-0.2	-1.3	-9.5	0.0	29.2	-40.2	-10.8	-0.2
3	31.1	0.6	4.6	3.6	0.7	-22.3	-0.1	-5.2	-1.9	-3.8	-0.4	0.0	-0.6	0.1	6.1	0.0	40.6	-34.3	6.3	0.0
4	20.9	0.1	7.1	5.6	1.4	-24.3	-0.1	-10.1	-5.0	-1.2	-0.1	0.0	-0.3	-0.1	-5.8	0.0	35.1	-41.0	-5.9	0.0
5	29.8	0.6	4.4	3.1	0.6	-19.6	-0.1	-5.0	-2.3	-4.9	-0.3	0.0	-0.5	0.1	5.6	0.0	38.5	-32.8	5.7	0.0
6	15.1	0.0	7.4	7.4	1.0	-22.7	0.0	-8.9	-5.8	-0.6	-0.1	0.0	-0.8	-0.1	-7.9	0.0	31.0	-39.0	-8.0	0.0
7	38.7	1.1	4.3	3.3	0.7	-20.3	-0.3	-5.3	-2.1	-7.7	-0.6	0.0	-1.2	0.5	10.0	0.0	48.0	-37.4	10.6	0.1

[1]Wet periods are shaded in blue, dry periods are shaded in orange

Table 11-24. Camp Keais N Basin Water Balance Volume (acre-ft), Basin Area 7,003 acres

Season[1]	Inflows					Outflows								Storage			Total			
	Rain	OL Bnd	SZ Bnd	Irrig	MH to SZ	ET	OL Bnd	SZ Bnd	Pump	OL to MH	SZ to MH	PD to MH	SZ D to MH	OL dS	SZ dS	PD dS	Total In	Total Out	dS	Error
1	36,246	3,191	2,718	1,017	372	-13,377	-773	-2,691	-501	-14,641	-275	0	-2,186	764	8,178	0	43,544	-34,444	8,941	159
2	8,215	85	4,107	4,012	620	-13,643	-35	-5,437	-3,163	-1,000	-86	0	-98	-749	-5,531	0	17,040	-23,462	-6,280	-142
3	18,150	341	2,672	2,118	394	-13,035	-85	-3,038	-1,100	-2,217	-219	0	-346	61	3,587	0	23,675	-20,041	3,648	-14
4	12,195	71	4,144	3,262	832	-14,152	-52	-5,889	-2,907	-704	-74	0	-177	-76	-3,373	0	20,504	-23,954	-3,449	-1
5	17,412	358	2,549	1,800	333	-11,461	-85	-2,931	-1,320	-2,858	-204	0	-268	74	3,251	0	22,452	-19,126	3,325	1
6	8,838	21	4,303	4,326	603	-13,252	-24	-5,167	-3,413	-368	-49	0	-469	-59	-4,593	0	18,092	-22,741	-4,652	3
7	22,596	614	2,490	1,902	397	-11,843	-159	-3,118	-1,204	-4,473	-323	0	-688	296	5,862	0	27,999	-21,808	6,158	33

[1]Wet periods are shaded in blue, dry periods are shaded in orange

Table 11-25. Estero Basin Water Balance Depth (inches), Basin Area 14,001 acres[2]

Season[1]	Inflows					Outflows								Storage			Total			
	Rain	OL Bnd	SZ Bnd	Irrig	MH to SZ	ET	OL Bnd	SZ Bnd	Pump	OL to MH	SZ to MH	PD to MH	SZ D to MH	OL dS	SZ dS	PD dS	Total In	Total Out	dS	Error
1	69.9	1.9	3.1	1.5	0.5	-20.6	-4.7	-2.4	-3.1	-16.0	-2.9	-9.5	-0.2	4.4	12.2	0.4	76.8	-59.5	16.9	0.4
2	13.0	0.0	2.8	6.6	1.0	-22.5	-0.1	-3.8	-5.5	0.5	-1.3	-1.3	0.0	-3.9	-5.9	-0.4	23.5	-34.0	-10.1	-0.3
3	32.4	0.2	2.3	2.3	0.5	-19.8	-0.4	-2.6	-3.3	-2.1	-2.4	-3.1	0.0	1.0	2.8	0.2	37.6	-33.6	4.0	0.0
4	20.6	0.1	2.4	5.5	1.1	-24.0	-0.1	-3.4	-4.0	0.3	-1.4	-1.6	0.0	-1.0	-3.1	-0.1	29.8	-34.1	-4.3	-0.1
5	35.0	0.2	2.3	1.9	0.4	-18.0	-0.9	-2.3	-3.2	-4.0	-2.6	-3.8	-0.1	1.3	3.6	0.1	40.0	-34.9	5.0	0.1
6	17.1	0.0	2.3	6.0	1.0	-23.1	-0.1	-3.8	-4.4	0.3	-1.5	-1.2	0.0	-1.5	-5.6	-0.2	26.4	-33.9	-7.3	-0.1
7	39.9	0.2	2.0	2.1	0.5	-18.6	-0.8	-2.6	-2.4	-4.0	-2.6	-3.9	0.0	2.4	7.0	0.3	44.7	-34.8	9.7	0.2

[1]Wet periods are shaded in blue, dry periods are shaded in orange

[2]Portions of the basin are outside the model domain, area shown is the area inside the model domain.

Table 11-26. Estero Basin Water Balance Volume (acre-ft), Basin Area 14,001 acres

Season[1]	Inflows					Outflows								Storage			Total			
	Rain	OL Bnd	SZ Bnd	Irrig	MH to SZ	ET	OL Bnd	SZ Bnd	Pump	OL to MH	SZ to MH	PD to MH	SZ D to MH	OL dS	SZ dS	PD dS	Total In	Total Out	dS	Error
1	81,510	2,258	3,571	1,728	572	-24,079	-5,437	-2,760	-3,656	-18,683	-3,435	-11,100	-242	5,076	14,223	467	89,639	-69,392	19,766	481
2	15,213	37	3,320	7,744	1,150	-26,199	-89	-4,450	-6,450	545	-1,491	-1,516	-31	-4,502	-6,903	-426	27,465	-39,681	-11,830	-385
3	37,827	200	2,641	2,697	556	-23,068	-442	-3,025	-3,856	-2,446	-2,795	-3,576	-31	1,121	3,299	237	43,921	-39,239	4,657	24
4	24,079	90	2,836	6,432	1,332	-27,961	-143	-3,952	-4,628	348	-1,638	-1,831	-15	-1,211	-3,616	-154	34,769	-39,820	-4,981	-70
5	40,884	287	2,695	2,253	510	-21,015	-1,090	-2,728	-3,697	-4,616	-3,021	-4,483	-66	1,520	4,150	161	46,629	-40,715	5,831	83
6	19,915	45	2,726	7,029	1,134	-26,948	-115	-4,429	-5,189	330	-1,714	-1,410	-26	-1,780	-6,569	-210	30,849	-39,501	-8,560	-92
7	46,604	250	2,277	2,425	558	-21,654	-889	-3,020	-2,785	-4,626	-3,030	-4,568	-53	2,843	8,165	295	52,113	-40,624	11,303	186

[1]Wet periods are shaded in blue, dry periods are shaded in orange

11.6 Water Depths and Hydroperiod Maps

This section shows a preview of some of the types of performance measures (PMs) to be analyzed during the project alternative analyses. The PMs, developed in collaboration with Audubon, are described in *Deliverable 3.2: Final Project Performance Measures and Metrics Technical Memorandum, March 13, 2025*. In addition, CWI project TWG ecologist, Mike Duever, provided a document titled Recommendations for Corkscrew Watershed Initiative Model Hydrologic Metrics for Evaluating Scenario Benefits dated September 9, 2024, which describes the connection between the water level/depths and hydroperiod metrics and ecological needs. A PM model output tool is being developed to include the specific measures that will be quantified to be implemented for the Existing Conditions Model Report. The tool will customize and expand the number of simulation years to be included in the calculations and provide summary statistics for the spatial data.

Three maps are shown below for the CWI project area, including wet and dry season water depths and hydroperiod. The depths presented were calculated by subtracting the simulated water table from the corrected LiDAR averaged over the model 500-ft cells. The hydroperiod map was calculated by converting the simulated water table to depths above ground based on the corrected LiDAR averaged to a higher resolution of 10-ft. The higher resolution topography will be used subsequently for the depth calculations in the PM tool being developed. The maps also include the ecological indicator points that were defined by the TWG for PM analysis. These indicator points represent different habitats and ecosystems and will be presented with more meaningful descriptions relation to the types of habitat and vegetation in the subsequent deliverables.

Figure 11-69 shows the hydroperiod in months calculated for the water year June 1, 2018 to May 31, 2019, which is an average year within the calibration period.

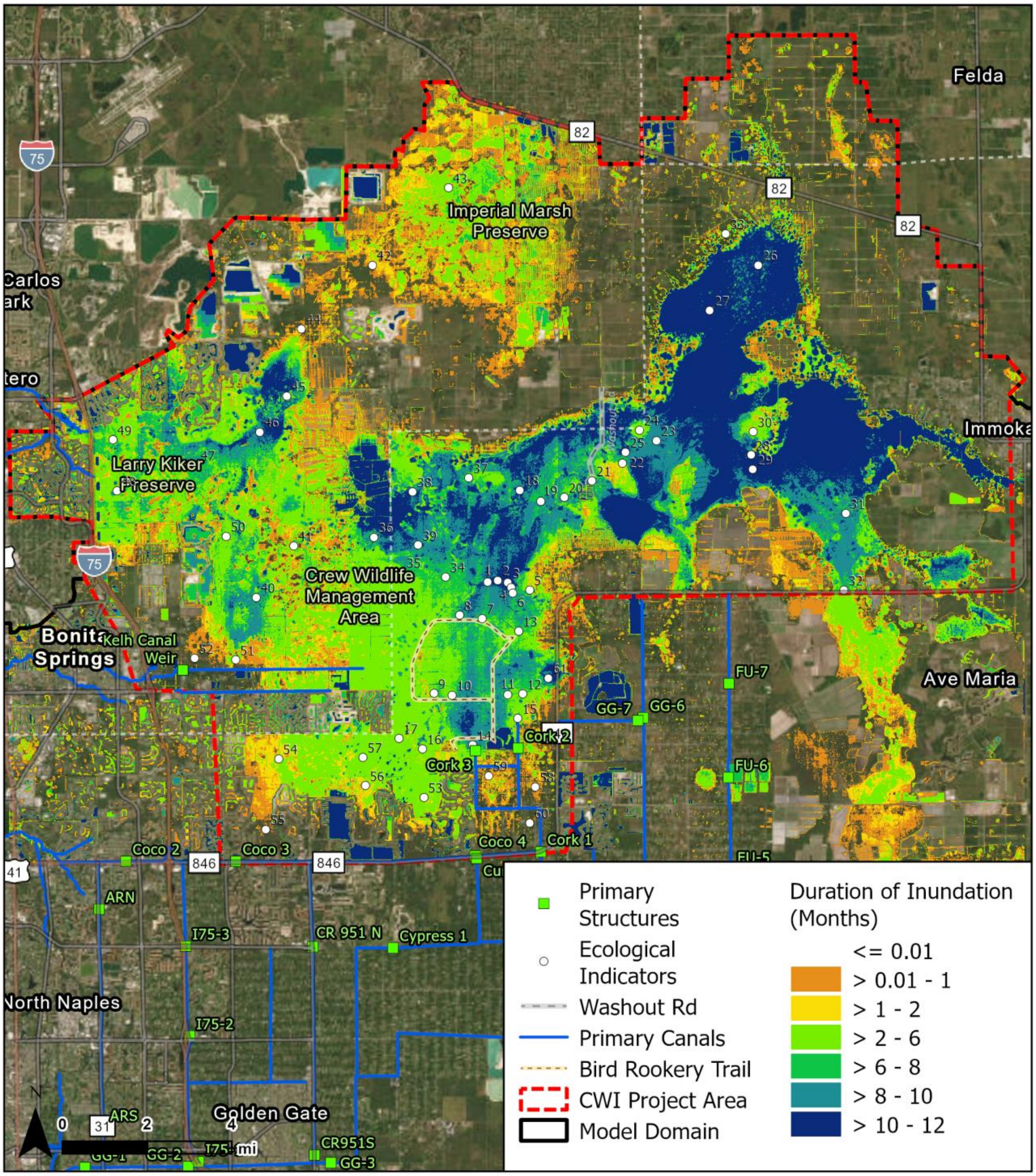

Figure 11-69. Hydroperiod for Water Year June 1, 2018 – May 31, 2019 for CWI Project Area.

Figure 11-70 shows the average wet season water depth above ground from July 1 to September 30, 2018. This metric measures the ability for aquatic communities to develop their populations through the wet season. More details are provided in the document provided by Duever, 2024 mentioned above.

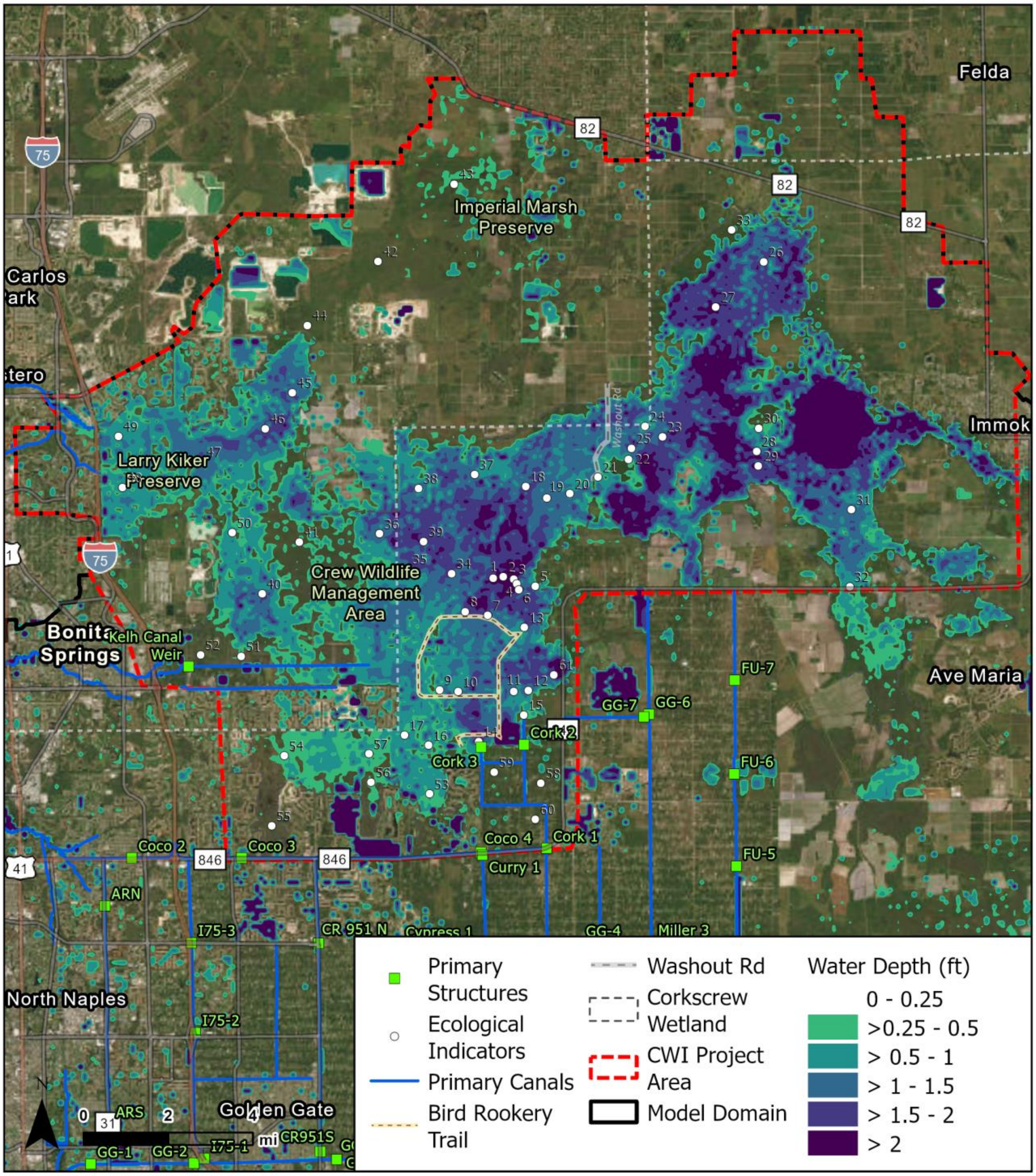

Figure 11-70. Average Wet Season (July 1, 2018 – September 30, 2018) Above Ground Water Depth Relative to Corrected LiDAR Elevation

Figure 11-71 shows the minimum dry season water depth from November 1, 2018 to May 31, 2019. Positive values are above ground and negative values are below ground. The minimum water depth metric provides a measure to determine condtions such as the ability of plant communities to germinate, predator foraging sites, aeration of wetland substrates, and fire conditions. More details are provided in the document provided by Duever, 2024 mentioned above.

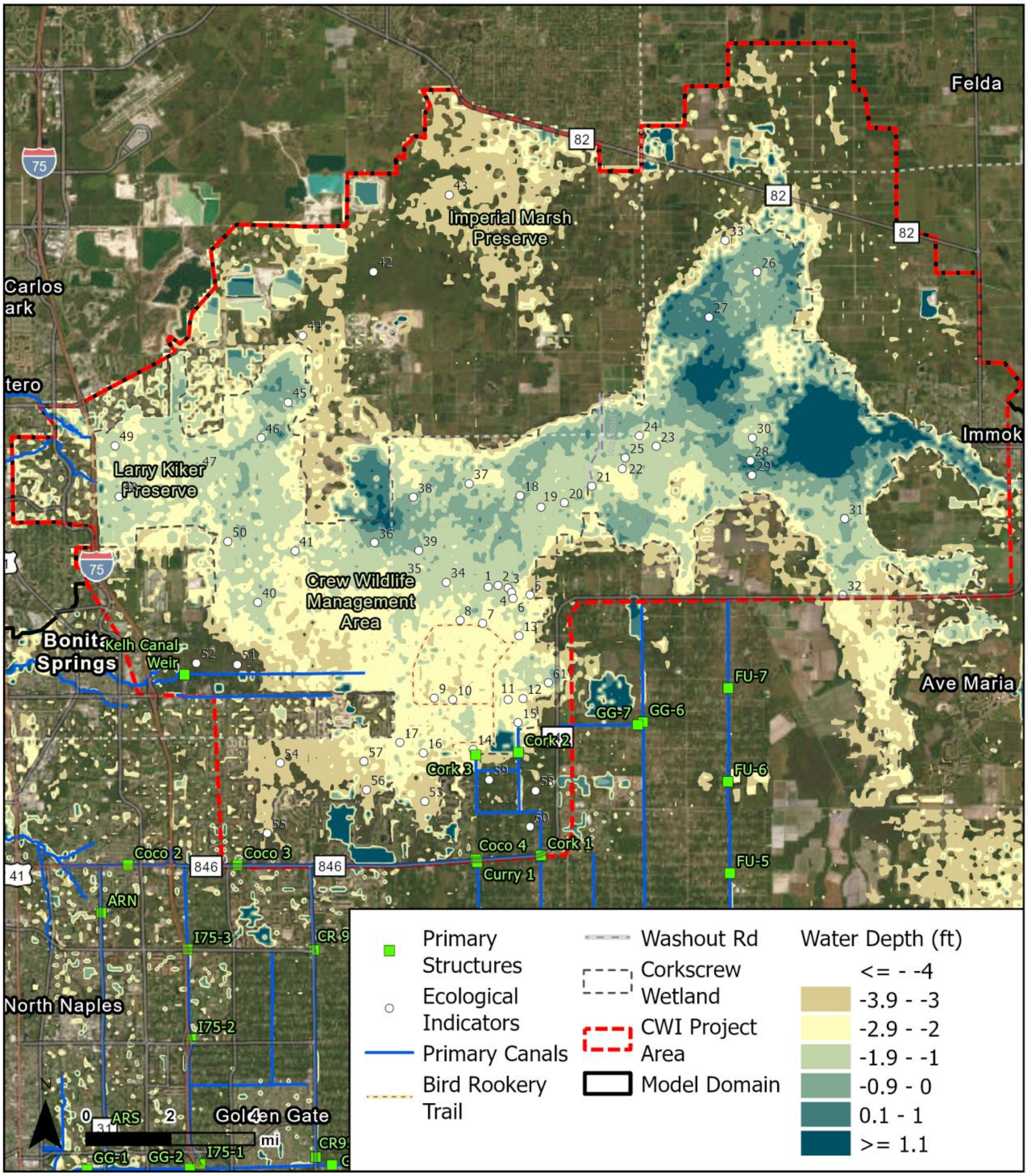

Figure 11-71. Minimum Dry Season (November 1, 2018 to May 31, 2019) Water Depth Relative to Corrected LiDAR Elevation

12.0 Model Limitations and Recommendations

12.1 General Modeling Tool Limitations

The BCB model is a comprehensive regional model that includes dynamically integrated and physical based hydrologic and hydraulic processes. The CWI model refinement process documented in this report has incorporated hydraulic details to capture interactions between Corkscrew, adjacent basins, and the primary drainage system. Nevertheless, there are limitations to the tool which need to be considered when using it to evaluate the CWI project performance measures. Some of these limitations are listed below:

- The MIKE SHE model resolution of 500 x 500 feet grid cell limits the ability of the model to capture the fine topographic and land use details. This impacts the ability to output detailed flood maps, capture detailed water level gradients, and generalizes the different hydrological processes.
- Land use / vegetation types in the model are lumped into general categories. Specific wetland vegetation data is limited for input evapotranspiration parameters. Several wetland categories are assumed to have similar parameters, which limits the ability of the model to evaluate the ET response of different types of wetland vegetation.
- Water use inputs are based on reported monthly volumes and DSS estimates and thus, information that may impact the model results could be missing. In evaluating the impact of the project on water use this should be considered by performing uncertainty analysis on pumping volumes.
- Some hydrological processes in the model are simplified or generalized. For example, soil dynamics, crop cycles, irrigation demand and drainage can impact how adjacent farms interact with Corkscrew.
- Readily available secondary and tertiary system structure information is limited, for example Collier County stormwater data includes many structure locations and sizes but does not include key pieces of information, such as invert elevations. Investigating and extracting this type of information from ERP permit reports is time consuming. Due to scope and schedule limitations, this effort was limited to selected areas. Moreover, this information is generally conceptualized in the model, for example secondary and tertiary system outlets and storage features are lumped together in most cases.
- Sheet flow blockages by roads and levees are conceptually represented and approximated using a combination of the overland flow SFAs, which are limited by the model resolution and apply an infinite vertical wall between the boundaries, and MIKE HYDRO culverts and weirs. While the weirs to represent the top of the roads and levees allow flow to cross the SFA wall if overtopped, the length of the weirs are limited by the 1D cross sections widths. Moreover, since flow can cross the SFA wall via the groundwater component, in areas where the topography was raised in Corkscrew, flow can occur above the real topography through the conceptualized vegetation zone. While this flow is small compared to the surface water flows, the Sheet Pile module in the Saturated Zone component, which restricts flow across cells, can be activated in the baseline and alternatives' models to overcome this limitation. Nevertheless, it will be limited by the model resolution, which is adequate for regional scale planning purposes. For design of levees a sub-model of higher resolution should be used.

12.2 Recommendations for Future Calibration Improvements

The comparison between simulated and observed data shows that the CWI RM performs well in Corkscrew and reasonably well in the downstream surface water stations. Nevertheless, there are inaccuracies that may impact the evaluation of performance measures, as follows:

- Groundwater layer heads are generally higher than observed in the lower aquifers (i.e., the Lower Tamiami and Sandstone aquifers). The CWI refinement effort focused more on the surficial aquifer. Thus, calibration and sensitivity analyses of groundwater abstractions in the lower aquifers is necessary to improve the model inaccuracy.
- The Bird Rookery station (BRDROOK) wet season levels are lower and show a more rapid recession than observed. This could be due to the MIKE HYDRO branch in the model having a higher capacity or lower resistance than the real swale where the station is located. It may also be that the model represents less obstructions or constrictions between the station location and the CORK3 gate. While some attempts to improve the stages were conducted by adding more resistance to the channel, structures and conductances, further information and calibration is necessary to improve the constrictions between CORK3 and the BRDROOK station. For example, there are uncertainties in the culvert inverts along and under Shady Hollow which may impact stages.
- CORK2_H and CORK3_H stages could be further improved with better quality operational data. Note that the CWI RM uses the available recorded gate levels during the calibration period. Analysis of the stage and gate level data shows that there are operational uncertainties in the data. For example, there are extended periods in summer months when the CORK2 gates are closed after several inches of rainfall have accumulated in Corkscrew and the observed stages in CORK1 and CORK2 are similar suggesting that gates were likely open. Conversely, there are some periods where small gate openings allow some flow to drain during dry periods where the data shows that levels should be closer to the water table. Some of these uncertainties can be reduced by updating the calibration period to more recent years since more data is now available.
- Stages and flow in the Corkscrew Canal N Basin: CORK1, CORK2, CORK3, COCO4, COCO3, and Curry1 are affected by the operational data uncertainties in these structures, simulated flow from the tributaries contributing to the basin, including the developments north of the Cocohatchee Canal, simulated head losses dependent on uncontrolled factors, such as channel cross sectional geometry and resistance, and other unknown flows. In general, stages in the basin perform well during average and low flows, but there are some periods during early and late summers where simulated stages are either higher (late summer of 2017, which is the wettest condition in the calibration period) or lower than observed (early summer 2017, September and October 2018, and late 2020). In some of the periods where the simulated stages in COCO3 are lower than observed (September/October 2018), they are higher than observed in the east side of COCO4, CORK1, CORK2, and CORK3. This could be due to more flow going towards CORK1 instead of COCO4, but also the gates are fully closed in COCO4 in October causing the high simulated stages east of the structure. The flow distribution between COCO4 (going west to COCO3) and CORK1 (going south) depends on the representation of the flow rating through these structures, the head losses in the channel between them, and the downstream conditions. Although gate level data is available, flow data is not available for CORK1 for the calibration period. As previously stated, updating the model calibration to more recent years would take advantage of more data availability.

- Kehl Canal/Imperial River flow and stage calibration improved substantially but could be further optimized to better capture the rise and recessions in the hydrographs. The 3D concept of wetland flow in combination with the adjustment of various parameters and the redefinition of flow ways and connections proved to be effective in increasing the simulated groundwater heads and flows. However, more data and calibration is required to improve on the concept, e.g., varying vegetation heights and resistance spatially, which would require more detailed vegetation mapping. In addition, the urban portions of the Imperial River basin should be investigated further to ensure the hydraulic connections and storage features are represented adequately.
- Groundwater levels in the farm areas north of Corkscrew are generally lower than observed. Further optimization of conductivities and other parameters, water management refinement, and the application of the wetland conceptualization concepts that were applied to Corkscrew to the AGIs and wetland areas adjacent to the farm fields, may help to improve the calibration in these areas. Moreover, some of these areas are undergoing land use changes to residential developments. Thus, updating the land use and the calibration period will be important for future model improvements.

12.3 Data Recommendations for Future Model Improvements

Some examples of data that could benefit future modeling tools and project evaluations that are beyond the scope of this current planning study are listed below.

- Spatially distributed surveys to correct the LiDAR with ground truth elevations. Survey should include wetland vegetation types and water depths in order to establish correlations to errors in the LiDAR data. Development of machine learning based methodologies could be used to apply this information for large areas at a fine resolution.
- Frequent and spatially distributed surface water and groundwater measurements, flow measurements, structure rating developments and calibration. Even though more stations have been added in recent years after the calibration period, there are still large portions of Corkscrew without monitoring. For example, the southern portions of Corkscrew between COCO4 and COCO3 would be useful to monitor to better assess the uncontrolled flow into this portion of the Cocohatchee Canal. In addition, the Cork3 structure tailwater remains to be unmonitored, which is a limitation in developing calibrated and verified flow ratings.
- Groundwater withdrawals uncertainty analysis and investigation of data quality.
- Survey of staff gauge datums. Errors have been reported in some stations, which impact analyses, such as assessing vertical head losses in the aquifer systems.

13.0 References

AIM Engineering and Surveying, Inc. 2020. Southern Lee County Flood Mitigation Plan. Submitted to Lee County. August, 2020.

AIM Engineering and Surveying, Inc. 2022. Survey Report: (BCB) Corkscrew Swamp Transect / Topographic Survey (Phases 1-3). Prepared from SFWMD. May, 2022.

Bandara, U., Earle, R., Butler, D., Assegid, Y., and Parrish D.M. 2020. Model Documentation Report for the Lower West Coast Surficial and Intermediate Aquifer Systems Model (LWCSIM). SFWMD Report. November, 2020.

CDM, 1996. Collier County Water Master Plan Update.

Clem, S.E. and Duever, M.J. 2019. Hydrologic Changes over 60 Years (1959-2019) in an Old-Growth Bald Cypress Swamp on a Rapidly Developing Landscape. Wetland Science & Practice, October 2019.

Clem, S.E. and Cornell, B. 2021. Investigation of Observed Drier Conditions in Long-Term Data at Lettuce Lake by National Audubon Society's Corkscrew Swamp Sanctuary. Prepared by Audubon Florida for South Florida Water Management District, February 2021.

Coastal and Heartland National Estuary Partnership (CHNEP) and Lago Consulting and Services. 2021. South Lee County Watershed Initiative. Final Report.

Digital Aerial Solutions. 2018. LiDAR Project Report LiDAR Collection, Processing, and QA/QC, FL_Southwest_2018_D18. Prepared for USGS. Retrieved 8/28/24 from gisftpdata.leegov.com/LiDAR/LiDAR2018/18012_FL_SW_2018_D18_Report.pdf.

Geddes, E., E. Richardson, and A. Dodd. 2015. Hydrogeologic Unit Mapping Update for the Lower West Coast Water Supply Planning Area. Technical Publication WS-35. South Florida Water Management District, West Palm Beach, FL. August 2015.

Hazen and Sawyer. 2025. Big Cypress Basin Model Update. Task 4: Model Calibration. Submitted to SFWMD, March 18, 2024 with addendum on March 27, 2025.

Lal, A.M.W., Moustafa, M.Z., and Wilcox, W.M. 2015. The use of discharge perturbations to understand in situ vegetation resistance in wetlands. Water Resour. Res., 51, 2477–2497, doi:10.1002/2014WR015472.

Lightbody, A.F., Avener, M.E., and Nepf, H.M. 2008. Observations of short-circuiting flow paths within a free-surface wetland in Augusta, Georgia, U.S.A. Limnol. Oceanogr., 53(3), 1040–1053. doi.org/10.4319/lo.2008.53.3.1040.

MWH and ADA Engineering. 2015. STA 1W Expansion #1 Stormwater Treatment Area Preliminary Design. Deliverable 4.1.1.2 – Final Calibration Refinement For Normal Conditions Technical Memorandum. Submitted to SFWMD, September 2014 (Revised June 2015).

Parsons and Interflow Engineering. 2017. Flood Protection Level of Service for Big Cypress Basin: Current and Future Service in Golden Gate, Cocohatchee, Henderson-Belle Meade, and Faka Union Watersheds. Deliverable 2-5 Model Re-Calibration. Submitted to SFWMD April 2017.

Rakib, Z. and Zeng, J. 2019. Flow Rating Development For CORK3 Structure with CFD. Prepared By Zubayed Rakib and Jie Zeng, Applied Hydraulics Section, Hydrology and Hydraulics Bureau, South Florida Water Management District. June 2019.

Rakib, Z. and Zeng, J. 2020a. Flow Rating Development For CORK2 Structure with CFD. Prepared By Zubayed Rakib and Jie Zeng, Applied Hydraulics Section, Hydrology and Hydraulics Bureau, South Florida Water Management District. November 2017 (Updated June 2020).

Rakib, Z. and Zeng, J. 2020b. Flow Rating Development For CORK1 Structure with CFD. Prepared By Zubayed Rakib and Jie Zeng, Applied Hydraulics Section, Hydrology and Hydraulics Bureau, South Florida Water Management District. August 2017 (Updated June 2020).

Rakib, Z. and Zeng, J. 2020c. Flow Rating Development For COCO3 Structure with CFD. Prepared By Zubayed Rakib and Jie Zeng, Applied Hydraulics Section, Hydrology and Hydraulics Bureau, South Florida Water Management District. October 2017 (Updated July 2020).

Rakib, Z. and Zeng, J. 2020d. Flow Rating Development For COCO4 Structure with CFD. Prepared By Zubayed Rakib and Jie Zeng, Applied Hydraulics Section, Hydrology and Hydraulics Bureau, South Florida Water Management District. June 2018 (Updated July 2020).

Rakib, Z. and Zeng, J. 2020e. Flow Rating Development For Spillway CUR1 with CFD. Prepared By Zubayed Rakib and Jie Zeng, Applied Hydraulics Section, Hydrology and Hydraulics Bureau, South Florida Water Management District. December 2020.

SFWMD. 2015. Atlas of Flow Computations at Hydraulic Structures In the South Florida Water Management District. Technical Publication: HHB Report #2015-001. Prepared by the Hydraulic Design Unit. October 2015.

SFWMD. 2020. Water Control Operations Atlas: Big Cypress Basin System Part 2: Structure Description. Prepared by: South Florida Water Management District Hydrology and Hydraulics Bureau and Big Cypress Basin Service Center. May 23, 2020. Zumbro, J., Coonts, S., and Bouchier A., 2023. Hydrostratigraphy and Aquifer Hydraulic Properties Update for the Surficial and Intermediate Aquifer Systems, Lower West Coast Planning Area. SFWMD Technical Publication WS-62. Hydrogeology Unit, Resource Evaluation Section, Water Supply Bureau. July 2023.

SFWMD. 2022. Lower West Coast Water Supply Plan Update, Appendix A. December, 2022.

SFWMD. 2025. South Florida Water Management District 2023 Estimated Water Use Report. Prepared by: Water Supply Bureau of the South Florida Water Management District. Staff Contributors: James Harmon, P.G, Brian Moore. January 2025.